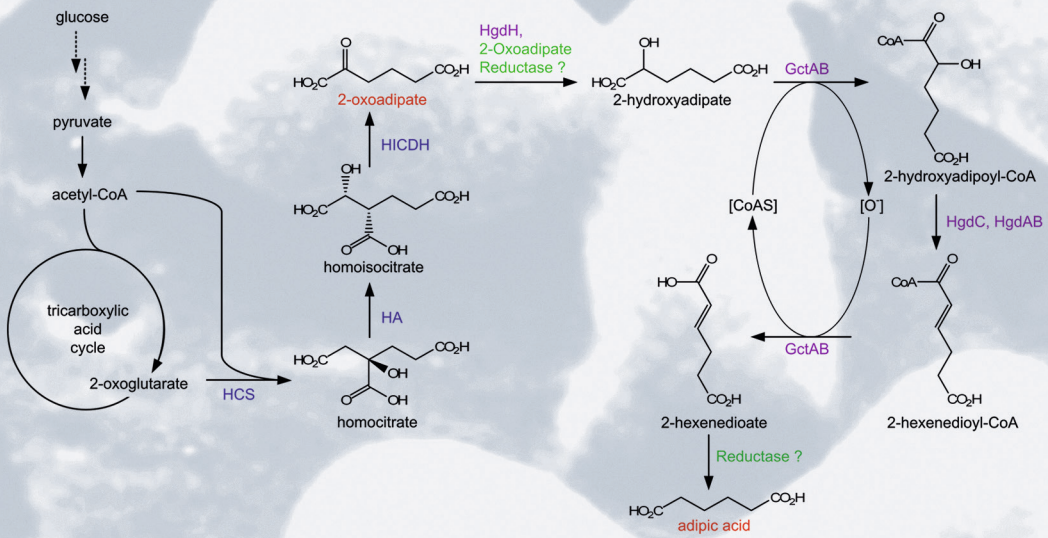

Metabolic engineering of *Corynebacterium glutamicum* for production of the adipate precursor 2-oxoadipate

Markus Sebastian Spelberg

Member of the Helmholtz Association

JÜLICH
FORSCHUNGSZENTRUM

Schriften des Forschungszentrums Jülich
Reihe Gesundheit / Health Band / Volume 70

Forschungszentrum Jülich GmbH
Institute of Bio- and Geosciences (IBG)
Biotechnology (IBG-1)

Metabolic engineering of *Corynebacterium glutamicum* for production of the adipate precursor 2-oxoadipate

Markus Sebastian Spelberg

Schriften des Forschungszentrums Jülich
Reihe Gesundheit / Health

Band / Volume 70

ISSN 1866-1785

ISBN 978-3-89336-954-6

Bibliographic information published by the Deutsche Nationalbibliothek.
The Deutsche Nationalbibliothek lists this publication in the Deutsche Nationalbibliografie; detailed bibliographic data are available in the Internet at http://dnb.d-nb.de.

Publisher and Distributor: Forschungszentrum Jülich GmbH
Zentralbibliothek
52425 Jülich
Tel: +49 2461 61-5368
Fax: +49 2461 61-6103
Email: zb-publikation@fz-juelich.de
www.fz-juelich.de/zb

Cover Design: Grafische Medien, Forschungszentrum Jülich GmbH

Printer: Grafische Medien, Forschungszentrum Jülich GmbH

Schriften des Forschungszentrums Jülich
Reihe Gesundheit / Health, Band / Volume 70

D 61 (Diss. Düsseldorf, Univ., 2013)

ISSN 1866-1785
ISBN 978-3-89336-954-6

The complete volume is freely available on the Internet on the Jülicher Open Access Server (JUWEL) at www.fz-juelich.de/zb/juwel

CONTENT

Abbreviations

2-OA	2-oxoadipate
AA	adipate
AAA	α-aminoadipate
Arg (R)	arginine
ATCC	American Type Culture Collection
BHI(S)	Brain Heart Infusion (+Sorbitol)
bp	base pair
cDNA	complementary DNA
cdw	cell dry weight
CoA	coenzyme A
CoB	coenzyme B
DCPIP	2,6-dichlorophenolindophenol
DNA	deoxyribonucleic acid
dNTP	deoxynucleoside triphosphate
DTT	dithiothreitol
EDTA	ethylenediaminetetraacetic acid
et al.	*et alii*
FA	formaldehyde
Fig	Figure
fw	forward
GC-ToF MS	gas chromatography time of flight mass spectrometer
HA	homoaconitase
HC	homocitrate
HCS	homocitrate synthase
HEPES	4-(2-hydroxyethyl)-1-piperazineethanesulfonic acid
HICDH	homoisocitrate dehydrogenase
His (H)	histidine
HPLC	high performance liquid chromatography
IPTG	Isopropyl β-D-1-thiogalactopyranoside
Kan^R	Kanamycin resistance
LB	Luria Bertani
Leu (L)	leucine
Lys (K)	lysine
MeOX	O-methylhydroxylamine
Met (M)	methionine
Mio	million
Mo	molybdenum
MOPS	3-(N-morpholino)propanesulfonic acid
mRNA	messenger ribonucleic acid
MSTFA	N-acetyl-N-(trimethylsilyl)-trifuoroacetamide
NADH	nicotinamide adenine dinucleotide
OD	optical density
ori	origin of replication

PAGE	polyacrylamide gel electrophoresis
PCA	protocatechuate
PCR	polymerase chain reaction
PEP	phosphoenolpyruvate
PMT	photomultiplier tube
Pro (P)	proline
PTS	phosphotransferase system
RNA	ribonucleic acid
rpm	revolutions per minute
rv	reverse
SD	synthetic defined
SDS	sodium dodecyl sulfate
Ser (S)	serine
Sp	Species
Tab	Table
TAE	tris-acetate-EDTA
Tet^R	Tetracycline resistance
Tris	tris(hydroxymethyl)-aminomethane
U	Unit (specific enzyme activity)
Ura	uracil
UTP	uridine-5'-triphosphate
v/v	volume per volume
w/v	weight per volume
ε	absorption coefficient

Discovery is seeing what everybody else has seen,
And thinking what nobody else has thought.

Albert Szent-Gyorgyi

1 Summary

1.1 Summary

The C6-dicarboxylic acid adipate is one of the most important building blocks in the chemical industry. The chemical syntheses of adipate are connected to insanitary and environmentally harmful reagents and catalysts. Therefore, the establishment of a biotechnological process for adipate production based on renewable carbon sources is of substantial interest. Thus, the main objective of this work was the metabolic engineering of *Corynebacterium glutamicum* for the production of the adipate precursor 2-oxoadipate. This organism is an industrially established producer of amino acids, but was also shown to possess a high capability for the production of organic acids, such as lactate or succinate.

Neither adipate nor 2-oxoadipate (solutions adjusted to pH 7) were metabolised by *C. glutamicum* wild type and they did not inhibit growth in glucose minimal medium in concentrations up to 50 mM ($\mu = 0.43\ h^{-1}$). Addition of 150 mM or 250 mM adipate resulted in a 37% decreased growth rate ($\mu = 0.29\ h^{-1}$), whereas a concentration of 500 mM adipate almost completely abolished growth. When adjusting the pH of the adipate solution with KOH to pH 7, the addition of 500 mM adipate still allowed a growth rate μ of 0.09 h^{-1}. Additional supplementation of 5 mM of the compatible solute L-proline further increased the growth rate to 0.16 h^{-1}. The latter result and DNA microarray experiments performed in the presence of 50 mM and 150 mM adipate indicated that the growth retardation might be caused to some extent by osmotic stress. Furthermore, the transcriptome data revealed high up-regulation of the transcriptional regulator PcaR and its target genes *pcaIJ* and *pcaFDO*, belonging to the PCA (protocatechuate) branch of the β-ketoadipate pathway. Thus, adipate probably acts as an activator molecule of PcaR in *C. glutamicum*.

The initial metabolic engineering studies focused on the introduction (plasmid-based or chromosomally) into *C. glutamicum* of the genes *lys20* (*Saccharomyces cerevisiae*) or *ttc1550* (*Thermus thermophilus*) encoding homocitrate synthase (HCS) for homocitrate production from 2-oxoglutarate. Under standard batch cultivation conditions with 222 mM (40 g l^{-1}) glucose, *C. glutamicum*/pEKEx2-*lys20* and *C. glutamicum* Δ*gdh*::P_{tuf}-*lys20* (strain MS-1) excreted up to 2.6 mM (0.54 g l^{-1}) and up to 4.1 mM (0.83 g l^{-1}) homocitrate, respectively, showing that the heterologous HCS was active.

Further studies focused on the enhancement of the titers of both products by metabolic engineering and by modified culture conditions. In a fed-batch cultivation with initially 222 mM glucose and addition of 222 mM glucose and 204 mM acetate at the beginning of the stationary phase, homocitrate production by strain MS-1 (*C. glutamicum* Δ*gdh*::P_{tuf}-*lys20*)

was increased up to 27.1 mM (5.5 g l^{-1}). Chromosomal integration of *pyc*^{P458S} coding for a pyruvate carboxylase into strain MS-1 and simultaneous deletion of *pta-ackA* in combination with an additional plasmid-based copy of *lys20* resulted in the most promising homocitrate producer MS-3-pHCS, which accumulated up to 52.1 mM (10.6 g l^{-1}) homocitrate in fed-batch cultivation with glucose and acetate as an additional carbon source. This titer represents a yield of 0.21 mol $C_{homocitrate}$/mol $C_{glucose+acetate}$.

2-Oxoadipate production in *C. glutamicum* was established by introducing (plasmid-based and chromosomally) a homoaconitase (HA, *lys4*) and a homoisocitrate dehydrogenase (HICDH, *lys12*) from *S. cerevisiae*. The resulting strains *C. glutamicum*/ pEKEx2-*lys20*/pVWEx2-*lys4-lys12* and *C. glutamicum* Δ*gdh*::P_{tuf}-*lys20*Δ*aceA*::P_{tuf}-*lys4-lys12* (strain MS-5) excreted 2.3 mM (0.37 g l^{-1}) and up to 3.5 mM (0.56 g l^{-1}) 2-oxoadipate, respectively, confirming the activity of the heterologous HA and HICDH. Moreover, these results showed that *C. glutamicum* has the capability to export both homocitrate and 2-oxoadipate.

Cultivation of *C. glutamicum*/pEKEx2-*ttc1550*/pVWEx2-*lys4-lys12* under nitrogen limitation increased 2-oxoadipate production up to 9.1 mM (1.5 g l^{-1}). The highest 2-oxoadipate titer of 27.1 mM (4.3 g l^{-1}) (0.13 mol $C_{2\text{-}oxoadipate}$/mol $C_{glucose+acetate}$) was produced by strain MS-5-pHCS, which differs from strain MS-5 by an additional plasmid-based copy of *lys20*. The results reported above demonstrate the capability of *C. glutamicum* for production of homocitrate and 2-oxoadipate and form the basis for further studies directed at conversion of 2-oxoadipate to adipate.

1.2 Zusammenfassung

Adipat ist eine C6-Dicarbonsäure und stellt als Vorstufe für Nylon-6,6 einen der wichtigsten Bausteine in der chemischen Industrie dar. Bisher wird Adipat durch chemische Syntheseverfahren unter Verwendung von gesundheitsschädlichen und umweltbelastenden Reagenzien hergestellt. Daher ist die biotechnologische Produktion von Adipat, basierend auf erneuerbaren Kohlenstoffquellen, von großem Interesse. Vor diesem Hintergrund war das Hauptziel dieser Arbeit die Etablierung der Produktion der Adipatvorstufe 2-Oxoadipat mittels *Metabolic Engineering* in *Corynebacterium glutamicum*. Neben der industriellen Verwendung als Produktionsorganismus für Aminosäuren, besitzt *C. glutamicum* ein hohes Potential für die Produktion von organischen Säuren wie Lactat oder Succinat.

Kultivierungsexperimenten ergaben, dass weder Adipat noch 2-Oxoadipat von *C. glutamicum* verstoffwechselt wird. Auf die Wachstumsrate von *C. glutamicum* hatte die Zugabe von pH-neutralisierten Adipat- (μ = 0.43 h^{-1}) und 2-Oxoadipat-Lösungen (μ = 0.43 h^{-1}) bis zu Konzentrationen von 50 mM keinen Einfluss. Die Zugabe von 150 mM oder 250 mM Adipat führte zu einer um 37% verminderten Wachstumsrate (μ=0.29 h^{-1}). In Gegenwart von 500 mM Adipat lag hingegen eine fast vollständige Wachstumshemmung von *C. glutamicum* vor. Eine mit KOH auf pH 7 eingestellte Adipatlösung steigerte die Wachstumsrate bei Zugabe von 500 mM auf μ = 0.09 h^{-1}. Die Zugabe von 5 mM der osmotisch wirksamen Substanz Prolin führte zu einer Wachstumsrate von μ = 0.16 h^{-1}.
Diese Ergebnisse sowie DNA-Chip Experimente in Anwesenheit von 50 mM und 150 mM Adipat zeigten, dass die Wachstumshemmung teilweise durch osmotischen Stress bedingt sein kann. Des Weiteren konnte anhand der Transkriptomdaten gezeigt werden, dass als Folge der Adipat-Zugabe der Transkriptionsregulator *pcaR* als auch dessen Zielgene *pcaIJ* und *pcaFDO*, die im β-Ketoadipat Stoffwechselweg vorkommen, stark hoch-reguliert waren. Adipat fungiert in *C. glutamicum* somit wahrscheinlich als Aktivatormolekül des Transkriptionsregulators PcaR.

Zur Etablierung der Homocitrat-Produktion ausgehend von 2-Oxoglutarat, wurden die Gene für die Homocitrat-Synthase (HCS) aus *Saccharomyces cerevisiae* (*lys20*) und *Thermus thermophilus* (*ttc1550*) in *C. glutamicum* (Plasmid-basiert und chromosomal) etabliert. Die Aktivität der heterologen HCS wurde durch die Produktion von Homocitrat in Standard-Kultivierungsexperimenten mit 222 mM (40 g l^{-1}) Glukose nachgewiesen. Dabei produzierte der Stamm *C. glutamicum*/pEKEx2-*lys20* bis zu 2,6 mM (0,54 g l^{-1}) und der Stamm *C. glutamicum* Δ*gdh*::P_{tuf}-*lys20* (Stamm MS-1) bis zu 4,1 mM (0,83 g l^{-1}) Homocitrat.

Zur Steigerung der Produkttiter wurden weitere genetische Modifikationen implementiert sowie die Kultivierungsbedingungen modifiziert. Die Homocitrat-Produktion mit dem Stamm MS-1 (*C. glutamicum* Δ*gdh*::P_{tuf}-*lys20*) konnte unter *fed-batch* Bedingungen mit anfänglich 222 mM Glukose und zusätzlicher Zugabe von 222 mM Glukose und 204 mM Acetat am Anfang der stationären Phase auf 27,1 mM (5,5 g l^{-1}) gesteigert werden. Die chromosomale Integration einer Pyruvat-Carboxylase (*pyc*^{P458S}), bei gleichzeitiger Deletion der *pta-ackA* Region, sowie die Expression einer weiteren Plasmid-basierten Genkopie von *lys20* (*C. glutamicum* MS-3-pHCS) führten unter *fed-batch* Bedingungen zur weiteren Erhöhung der Produktion auf 52,1 mM (10,6 g l^{-1}) Homocitrat. Dies entspricht einer Ausbeute von 0,21 mol $C_{Homocitrat}$/ mol $C_{Glukose+Acetat}$.

Zur Etablierung der 2-Oxoadipat-Produktion wurden Gene, die für die Homoaconitase (HA) aus *S. cerevisiae* (*lys4*) und die Homoisocitrat-Dehydrogenase (HICDH) aus *S. cerevisiae* (*lys12*) kodieren in *C. glutamicum* Plasmid-basiert und chromosomal integriert, eingefügt. Durch die Akkumulation von bis zu 2,3 mM (0,37 g l^{-1}) 2-Oxoadipat mit dem Stamm *C. glutamicum*/pEKEx2-*lys20*/pVWEx2-*lys4*-*lys12* und von bis zu 3,5 mM (0,56 g l^{-1}) mit dem Stamm *C. glutamicum* Δ*gdh*::P_{tuf}-*lys20*Δ*aceA*::P_{tuf}-*lys4*-*lys12* (MS-5) wurde die Aktivität der heterolog exprimierten HA und HICDH bestätigt. Weiterhin waren diese Ergebnisse ein Beleg für die Fähigkeit von *C. glutamicum* Homocitrat und 2-Oxoadipat zu exportieren.

Die Kultivierung des Stamms *C. glutamicum*/pEKEx2-*ttc1550*/pVWEx2-*lys4*-*lys12* führte unter Stickstofflimitierung zur Steigerung der 2-Oxoadipat-Produktion auf 9,1 mM (1,5 g l^{-1}). Mit dem aktuell besten 2-Oxoadipat-Produzenten MS-5-pHCS, welcher sich durch eine weitere Plasmid-basierte Genkopie von *lys20* von dem Stamm *C. glutamicum* MS-5 unterscheidet, wurde 27,1 mM (4,4 g l^{-1}) 2-Oxoadipat produziert. Das entspricht einer Ausbeute von 0,13 mol $C_{2\text{-}Oxoadipat}$/mol $C_{Glukose+Acetat}$.

Die hier präsentierten Ergebnisse zeigen somit zum einen das Potential von *C. glutamicum* zur Produktion von Homocitrat und 2-Oxoadipat und sind zum anderen die Basis für weitere Untersuchungen zur Umsetzung von 2-Oxoadipat zu Adipat.

2 Introduction

2.1 Significance and application of adipate

Adipate (alternative names are hexanedioic acid or 1,4-butanedicarboxylic acid) with a molecular mass of 146.14 g mol^{-1} and pK_a values of 4.43 and 5.41 is the most important commercial aliphatic, straight-chain dicarboxylic acid. It is isolated as colourless, odourless crystals having an acidic taste (Musser, 2005, Davis, 1985). The GRAS (generally recognised as safe) compound is soluble in acetone and alcohol and slightly soluble in water (14.2 g l^{-1} at 15°C) (van Kempen *et al.*, 2001, Davis, 1985). It occurs rarely in nature and was found in beet red and sugar beet. The global production of adipate has been estimated to be at 2.6 million tons/a in 2011 with 410,000 tons (16%) produced in Germany. The forecast of adipate production is an average growth of 4.1% annually, leading to a global production of 3.3 million tons in 2016 (Merchant Research & Consulting Ltd., 2011). The price of adipate in Europe was reported to be $2,900 per ton in April 2011 and is expected to be globally at $3,100 per ton in 2016. The global adipate market is tightly associated with the health of the economy (Global Industry Analysts Inc., 2012). The price of the key material cyclohexane, which is coupled to the oil price, significantly impacts the adipate market (Global Industry Analysts Inc., 2012).

Nearly 65% of the global adipate production is used for the manufacturing of nylon 6,6 fibres and resins (Merchant Research & Consulting Ltd., 2011). The primary application process leads to nylon 6,6 by condensation of adipate and hexamethylenediamine and subsequent elimination of water. This important process was established in the early 1930s by W. H. Carothers of DuPont (Luedeke, 1977). Further application areas are the production of polyurethanes and polyester polyols as well as the conversion to esters for the production of plasticizers and lubricants (Merchant Research & Consulting Ltd., 2011, Musser, 2005). Adipate is also used in the food industry as ingredient (E355, E356, E357) in gelatines, jams, desserts and other foods that require acidulation (Merchant Research & Consulting Ltd., 2011). Derivatives of adipate are used for target products such as fungicides, pesticides, pharmaceuticals and textile treatment (Merchant Research & Consulting Ltd., 2011).

2.2 Chemical production of petroleum-based adipate

Most of the commercially produced adipate in the chemical industry is synthesised from cyclohexane through a two-step oxidation process (Fig. 1). Starting material of this route is benzene, which is hydrogenated to cyclohexane.

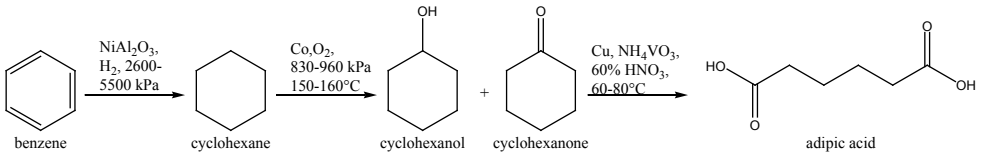

Fig. 1: Chemical synthesis of adipate via benzene route (Niu *et al.*, 2002).

Cyclohexane reacts in the first oxidation with oxygen in the presence of the catalysts cobalt or manganese at 150-160°C to produce KA oil, a mixture of cyclohexanol and cyclohexanone. The second oxidation step results in adipate by oxidising KA oil with nitric acid and air, using copper or vanadium as catalysts (Merchant Research & Consulting Ltd., 2011, Niu *et al.*, 2002). Two butadiene-based routes demonstrate further adipate production processes which are rarely used in the industry. The first route, developed by BASF in the early 1970s, involves the production of adipate by two carbomethoxylation steps of butadiene to dimethyl adipate, followed by hydrolysis to adipate (Musser, 2005). The second route was developed by DuPont in the mid-1980s, producing adipate by direct dihydrocarboxylation of butadiene (Musser, 2005). Adipate is also made by palladium halide-catalysed dicarbonylation of 1,4-disubstituted 2-butenes or by one-step-oxidation of cyclohexane with nitric acid, nitrogen dioxide or air (Musser, 2005).

Almost all of the chemical, large scale industrial processes for adipate production are based on environmentally harmful reagents. Benzene, the starting material of the most commonly used method, is a volatile carcinogen and linked to acute myeloid leukaemia (Galbraith *et al.*, 2010). During the oxidation process of KA oil to adipate, NO_2, NO, N_2O and N_2 are formed (Merchant Research & Consulting Ltd., 2011). The formation of NO_x emissions and especially the unavoidable formation of the main product nitrous oxide (1 mol per mol of adipate) represents a global environmental concern (Reimer *et al.*, 1994). Nitrous oxide is a chemical active greenhouse gas, which leads to ozone depletion and global warming. Today 80% of nitrous oxide produced in adipate plants is reduced with state of the art techniques, for example modern catalytic decomposition of N_2O and tail gas treatment to innocuous gases (O_2 and N_2) (Alini *et al.*, 2007, van Duuren *et al.*, 2011a, Matsuoka *et al.*, 2000). However, it is estimated that about 10% of N_2O released per year in the atmosphere

originates from production of adipate (Alini *et al.*, 2007). As an alternative "green" route Sato and co-workers described a direct organic-solvent and halide-free oxidation of cyclohexane to adipate using an aqueous 30% hydrogen peroxide solution. The efficiency of this route is based on many factors during the reaction steps and will only be attractive if the costs of hydrogen peroxide are clearly reduced (Sato *et al.*, 1998, Blach *et al.*, 2010).

2.3 Approaches for production of bio-based adipate

Adipate belongs to the high-volume bulk chemicals. Substances listed as high-volume bulk chemicals were classified according to their potential of chemical functionality and potential applications i.e. based on the number of new molecules which can be produced in biotechnological and chemical processes (Werpy & Petersen, 2004). To date, chemical production of adipate is linked to the damage of the environment. Its market price is tightly coupled to the oil price (Merchant Research & Consulting Ltd., 2011, Niu *et al.*, 2002). Therefore, the major long-term objective for the development of a sustainable industrial society is the shift from the dependence on petroleum to biotechnological processes based on renewable resources (Sauer *et al.*, 2008). This includes the production of bulk chemicals of high purity in an environmentally acceptable and energy-efficient manner (Cooke, 2008). In the case of adipate only few microbial approaches to produce this compound or its precursors by fermentation processes using selected or engineered organisms have been published.

2.3.1 Microbial cyclohexane oxidation to adipate

Adipate is naturally produced by animals through a combination of β-oxidation and ω-oxidation (van Kempen *et al.*, 2001, Mortensen, 1980). It has been hypothesised that it is important to detoxify excess fatty acids (Gregersen *et al.*, 1983). Furthermore, adipate occurs naturally as an intermediate in the degradation pathways of cyclohexane, cyclohexanone and ε-caprolactam and is further metabolised via β-oxidation to succinyl-CoA and acetyl-CoA (Cheng *et al.*, 2002, Steffensen & Alexander, 1995). Brzostowicz and co-workers used mRNA differential display to identify cyclohexane oxidation genes (Fig. 2, purple pathway) in a mixed microbial community originating from a wastewater bioreactor. The identified DNA fragments encode genes for cyclohexanone monooxygenase, caprolactone hydrolase, 6-hydroxyhexanoate dehydrogenase and 6-oxohexanoic dehydrogenase, derived from the bacteria *Arthrobacter* sp., and *Rhodococcus* sp. (Brzostowicz *et al.*, 2003). It was shown that traces of adipate could be detected in the presence of cyclohexanone in a culture of *E. coli* cells carrying cosmids encoding these genes (Brzostowicz *et al.*, 2003).

2.3.2 Microbial production of the adipate precursor *cis, cis*-muconate

Cis, cis-muconate is a dicarboxylic acid with conjugated double bonds, which can be reduced in a hydrogenation process using platinum on carbon as catalyst to form adipate (Niu *et al.*, 2002, van Duuren *et al.*, 2011b). In the past few years two different processes for the microbial production of *cis, cis*-muconate from renewable carbon sources have been established: (i) the degradation of benzoate and (ii) the biosynthesis based on glucose. The degradation of benzoate to *cis, cis*-muconate has been described for the bacteria *Pseudomonas* sp. B13, *P. putida* BM014, *P. putida* KT2440, *Acinetobacter* strain ADP1, *Arthrobacter* sp., and *Spingobacterium* strain GCG (Schmidt & Knackmuss, 1984, Bang & Choi, 1995, Choi *et al.*, 1997, van Duuren *et al.*, 2011b, van Duuren *et al.*, 2012, Collier *et al.*, 1998, Mizuno *et al.*, 1988, Wu *et al.*, 2004).

The degradation pathway of benzoate proceeds via the ortho-cleavage pathway of catechol to *cis, cis*-muconate and further to succinyl-CoA and acetyl-CoA in the β-ketoadipate pathway. The benzoate pathway in *P. putida* (and other organisms) is encoded by the genes that belong to the *ben*, *cat* and *pca* operons (Fig. 2, green pathway) (van Duuren *et al.*, 2011b). Benzoate is converted by a benzoate dioxygenase (*benABC*) to the corresponding 1,2-diol. The resulting 1,2-dihydroxybenzoate is dehydrogenated to catechol by a 1,2-dihydroxybenzoate dehydrogenase (*benD*). The cleavage of catechol is catalysed by two catechol-1,2-dioxygenases, encoded on the *cat* operon (*catA*) and the *ben* operon (*catA2*), respectively, to form *cis, cis*-muconate (van Duuren *et al.*, 2011b). The transcriptional regulators BenR and CatR were found to be involved in the regulation of the benzoate pathway in *P. putida*. In the presence of benzoate BenR activates transcription of the *benABCD* operon and CatR induces the transcription of the *catBCA* operon in response to *cis, cis*-muconate (Cowles *et al.*, 2000, McFall *et al.*, 1998). In the last two decades several attempts to increase *cis, cis*-muconate production were performed. A *Pseudomonas* sp. B13 strain lacking the gene of muconate cycloisomerase and grown in succinate mineral medium reached a *cis, cis*-muconate titer of 7.4 g l^{-1} (52 mM) (Schmidt & Knackmuss, 1984). The titer of *cis, cis*-muconate could be increased to 44.1 g l^{-1} (310 mM) using an *Arthrobacter* strain also lacking muconate cycloisomerase activity and additionally exposed to UV irradiation (Mizuno *et al.*, 1988). Recently, van Duuren and co-workers developed the strain *P. putida* KT2440-JD-1, which accumulates in a pH-controlled fed-batch process up to 18.5 g l^{-1} (130 mM) *cis, cis*-muconate with an overall product yield close to 100% (van Duuren *et al.*, 2012). This strain was derived from *P. putida* KT2440 by random mutagenesis with N-methyl-N´-nitro-N-nitrosoguanidine and exposure to 3-fluorobenzoate. It was shown that

this strain no longer grows on benzoate as sole carbon source, but co-metabolised benzoate during growth on glucose. Transcriptome analysis revealed that the *cat* operon was no longer induced in the presence of benzoate due to a single point mutation in the transcriptional regulator gene *catR*. Under these conditions the genes of the *ben* operon were highly induced and the strain *P. putida* KT2440 JD-1 was still able to convert catechol to *cis, cis*-muconate. The conversion is based on the presence of the second catechol 1,2-dioxygenase (*catA2*, PP_3166) encoded in the *ben* operon, as the *catA*-encoded enzyme was not induced due to the defective CatR regulator (van Duuren *et al.*, 2011b).

A second approach for the synthesis of adipate from renewable carbon sources like glucose was reported by Draths and co-workers. An artificial pathway was established in *E. coli* converting D-glucose to *cis, cis*-muconate followed by hydrogenation to adipate (Fig. 2, red pathway) (Draths & Frost, 1994). The conversion of D-glucose to 3-dehydroshikimate is catalysed by enzymes naturally present in *E. coli*. To prevent further conversion of 3-dehydroshikimate the strain lacks shikimate dehydrogenase. The synthesis of 3-dehydroshikimate to *cis, cis*-muconate is performed by introducing three heterologous, plasmid-encoded enzymes in the *E. coli* strain: 3-dehydroshikimate dehydratase of *Klebsiella pneumoniae* (*aroZ*) catalyses the dehydration to protocatechuate, protocatechuate decarboxylase (*aroY*) of *K. pneumoniae* decarboxylates protocatechuate to catechol, which is then cleaved to *cis, cis*-muconate by catechol 1,2-dioxygenase of *Acinetobacter calcoaceticus* (*catA*). Batch cultivation of this *E. coli* strain with glucose as sole carbon source lead to the accumulation of about 2.4 g l^{-1} (17 mM) *cis, cis*-muconate (Draths & Frost, 1994). Improvement of the synthesis by integration of two additional copies of the *aroZ* gene in the parental *E. coli* strain leads to 36.8 g l^{-1} (259 mM) of *cis, cis*-muconate, corresponding to a 24% (mol/mol) yield from glucose. The subsequent chemocatalytic hydrogenation of *cis, cis*-muconate results in 97% conversion to adipate (Niu *et al.*, 2002).

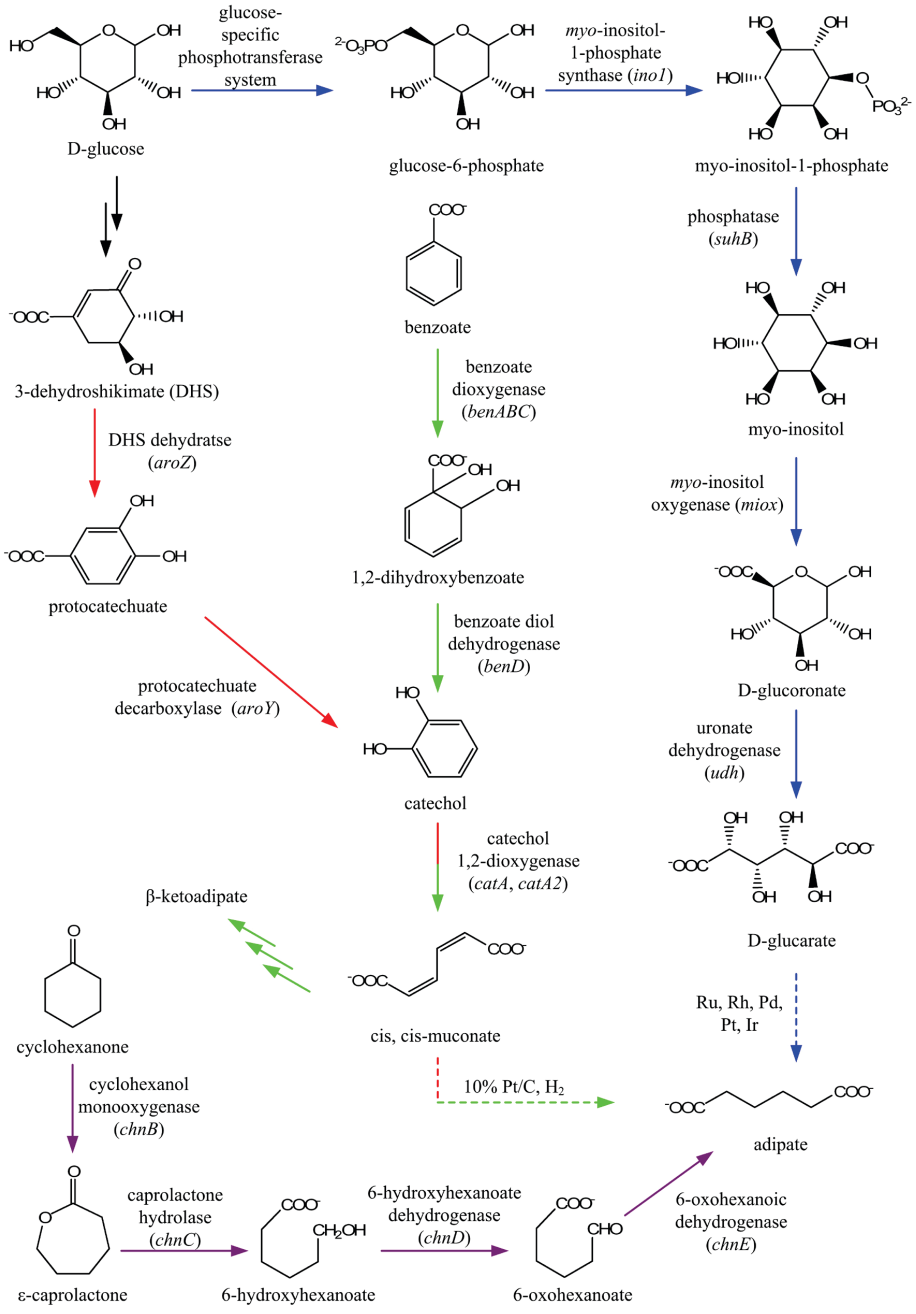

Fig. 2: Synthetic pathways for the bio-based production of adipate: The purple pathway shows cyclohexanone oxidation to adipate (Brzostowicz *et al.*, 2003). Synthesis of the adipate precursor *cis, cis*-muconate occurs via degradation of benzoate (green pathway, van Duuren *et al.*, 2011b) or via an artificial pathway from glucose (red pathway, Niu *et al.*, 2002). The blue pathway indicates the synthesis of the precursor D-glucaric acid from glucose (Moon *et al.*, 2009). Black arrows indicate the microbial conversion of D-glucose to 3-dehydroshikimic acid. Continuous lines indicate enzymatic reactions, dashed lines show chemocatalytic reactions. The gene names of enzymes involved are shown in brackets.

2.3.3 Microbial production of the adipate precursor glucarate

D-glucarate was identified as "top value-added chemical from biomass" with a high potential as building block for polymers (Werpy & Petersen, 2004). For the production of D-glucarate from glucose a synthetic pathway was established in *E. coli* (Fig. 2, blue pathway). Glucose is taken up into the cell and converted to glucose-6-phosphate via the PTS (phosphotransferase system). The coexpression of the gene for *myo*-inositol-1-phosphate synthase (*ino1*) of *Saccharomyces cerevisiae* and *myo*-inositol oxygenase (*miox*) of mice led to the formation of D-gluconate via the intermediate *myo*-inositol. *Myo*-inositol-1-phosphate is dephosphorylated by an endogenous phosphatase, likely SuhB of *E. coli*. The last step to D-glucarate is catalysed by an uronate dehydrogenase (*udh*) of *Pseudomonas syringae*. Cultivation of the *E. coli* strain carrying these three heterologous genes resulted in the accumulation of up to 1.1 g l^{-1} D-glucarate (Moon *et al.*, 2009). Subsequent chemocatalytical conversion of D-glucarate led to adipate. It was demonstrated that the MIOX activity is the rate limiting step in the pathway for glucarate production from glucose. To overcome this limitation, polypeptide scaffolds built from protein-protein interaction domains were implemented to co-localise all three heterologous enzymes. This increased the MIOX activity resulting in an approximately 5-fold increased product titer (2.5 g l^{-1}) of D-glucarate (Moon *et al.*, 2010).

2.4 A new synthetic pathway for the bio-based production of 2-oxoadipate and adipate

Metabolic engineering was defined as "the improvement of cellular activities by manipulations of enzymatic, transport and regulatory functions of the cell with the use of recombinant DNA technology" (Bailey, 1991). Since the last decade, the field of synthetic biology which aims at the design and construction of new biological components or the redesign of existing biological components, became more and more prominent (Keasling, 2008). The application of the tools of synthetic biology is a promising idea to significantly simplify metabolic engineering. For engineering an existing or for designing a new synthetic pathway there are some key points, which have to be considered: (i) The chassis (microbial host organism) should be genetically stable, should have the ability to grow with minimal requirements to the growth medium and should be able to switch on the entire biosynthetic pathway at the correct time point to avoid accumulation of toxic intermediates. (ii) It is important to coordinate the simultaneous expression of many genes carrying out multiple enzymatic reactions. (iii) The application of computer-aided design systems supports the

selection of biological components for the development of a new synthetic pathway. (iv) Finally, biological debugging routes help to identify and solve problems in the engineered pathways (Keasling, 2012).

2.4.1 Production of the intermediate 2-oxoadipate from glucose

The new synthetic bio-based pathway proposed in this work represents the conversion of glucose to adipate via the intermediate 2-oxoadipate, which occurs in the α-aminoadipate (AAA) pathway. The first three enzymatic steps of the AAA pathway convert 2-oxoglutarate and acetyl-CoA to 2-oxoadipate (Fig. 3). Besides the diaminopimelate pathway, which is found in most plants, bacteria and lower fungi, the AAA pathway is the second distinct pathway for the biosynthesis of L-lysine. The AAA pathway consists of eight enzymatic steps and was found in several yeasts and higher fungi (Vogel, 1964, Zabriskie & Jackson, 2000).

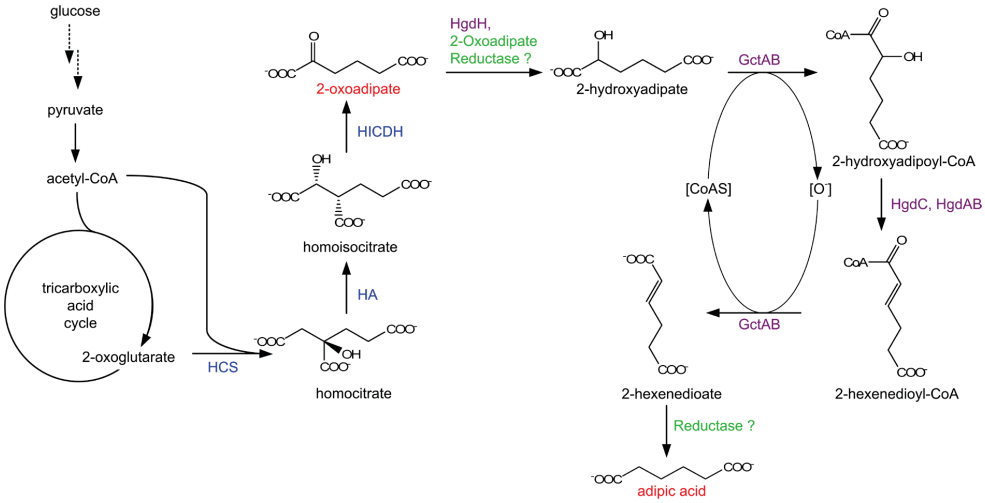

Fig. 3: Proposed synthetic pathway for the bio-based production of 2-oxoadipate and adipate from glucose. Enzymes marked in blue catalyse the first three reactions of the α-aminoadipate pathway for L-lysine biosynthesis to form 2-oxoadipate from 2-oxoglutarate and acetyl-CoA. Dashed lines indicate the enzymatic reactions of glycolysis, forming pyruvate from glucose. The proposed conversion of 2-oxoadipate to 2-hexendioate was recently reported (enzymes marked in purple, Parthasarathy *et al.*, 2011). Genes encoding a 2-oxoadipate reductase and an enzyme converting 2-hexendioate to adipate (green displayed enzymes) have not been described yet. Enzyme abbreviations: HCS = homocitrate synthase, HA = homoaconitase, HICDH = homoisocitrate dehydrogenase, HgdH = 2-hydroxyglutarate dehydrogenase, GctAB = glutaconate CoA-transferase, HgdC+HgdAB = 2-hydroxyglutaryl-CoA dehydratase.

An AAA-like pathway is also present in the thermophilic bacteria *Thermus thermophilus* and *Pyrococcus horikoshii*. The synthesis of the intermediate α-aminoadipate from 2-oxoglutarate and acetyl-CoA proceeds in the same way, but conversion of α-aminoadipate to L-lysine is different in the prokaryotic organisms (Kosuge & Hoshino, 1998, Nishida & Nishiyama, 2000). Most research for characterising the regulation and enzyme activities of the AAA pathway was performed using the baker's yeast *S. cerevisiae*. The first three enzymatic steps of the AAA pathway form 2-oxoadipate, a precursor of adipate. The first reaction is a condensation of 2-oxoglutarate and acetyl-CoA to form homocitrate, catalysed by homocitrate synthase (HCS). Homocitrate synthase is the rate limiting enzyme of the AAA pathway due to feedback inhibition by the end product L-lysine (Feller *et al.*, 1999, Andi *et al.*, 2005). It was possible to overcome the feedback inhibition by substitutions of particular amino acids resulting in L-lysine-insensitive variants (Feller *et al.*, 1999, Bulfer *et al.*, 2010). The two-step conversion of homocitrate to homoisocitrate via the intermediate homoaconitate is catalysed by homoaconitase (HA), also known as homoaconitate hydratase. This enzyme belongs to the aconitase superfamily and catalyses the dehydration of homocitrate to homoaconitate as well as the subsequent rehydration to homoisocitrate (Xu *et al.*, 2006). Homoisocitrate dehydrogenase (HICDH) catalyses the oxidative decarboxylation of homoisocitrate to 2-oxoadipate by a mechanism, which is proposed to be similar to that of isocitrate dehydrogenase (Grodsky *et al.*, 2000). The conversion of 2-oxoglutarate to 2-oxoadipate is also described for some archaea, including *Methanocaldococcus jannaschii*. In these strictly anaerobic methanogens the reactions are part of coenzyme B (CoB) biosynthesis, which is essential for methane formation. The reactions are catalysed by the same enzymes described for the AAA pathway, but in contrast the methanogenic pathway (called homocitrate pathway), recycles its products, extending 2-oxoadipate (C6) to 2-oxopimelate (C7) and 2-oxopimelate to 2-oxosuberate (C8). In each of the elongation pathways (condensation of acetyl-CoA with the 2-oxoacid, rearrangement of the hydroxy group, oxidative decarboxylation) the reactions are catalysed by the same enzymes, including homocitrate synthase, homoaconitase and homoisocitrate dehydrogenase (Graham, 2011). As consequence of a less polar binding site, the methanogen HCS is reported to be the only family member catalysing acetyl addition to 2-oxoacids of varying chain length (Howell *et al.*, 1998). The dicarboxylate elongation pathway provides not only precursors for CoB biosynthesis, but also demonstrates potential for the production of high-value polymer precursors (Graham, 2011).

2.4.2 A synthetic pathway for the conversion of 2-oxoadipate to adipate

Up to now the challenging task to develop a synthetic pathway for the enzymatic conversion of 2-oxoadipate to adipate was addressed only very recently. Buckel and co-workers demonstrated the conversion of 2-oxoadipate to 2-hexendioate, a direct precursor of adipate. The enzymes 2-hydroxyglutarate dehydrogenase (HgdH) and glutaconate CoA-transferase (GctAB) from *Acidaminococcus fermentans* as well as 2-hydroxyglutaryl-CoA dehydratase (HgdC + HgdAB) from *Clostridium symbiosium* catalyse the conversion of 2-oxoglutarate to glutaconate and side-activity is found for the conversion of 2-oxoadipate to 2-hexendioate (Fig. 3) (Djurdjevic *et al.*, 2011, Parthasarathy *et al.*, 2011). No enzyme activity catalysing the reduction of 2-hexendioate to adipate is described until now. Despite the successful conversion of the six carbon substrates by the three enzymes, several obstacles have to be solved before the production pathway of adipate can work. The main problem seems to be the 2-hydroxyglutarate dehydrogenase, which prefers 2-oxoglutarate over 2-oxoadipate. To solve this problem, the authors propose the construction of an enzyme, which does not accept 2-oxoglutarate as substrate (Parthasarathy *et al.*, 2011). However, a few decades ago, it was reported that 2-oxoadipate reductase, which is involved in mammalian lysine and tryptophan degradation, catalyses the formation of 2-hydroxyadipate from 2-oxoadipate (Suda *et al.*, 1976). Originally, this enzyme was isolated from human term placenta and was further characterised in rat, especially from heart muscle, but the gene encoding this enzyme has not yet been identified (Suda *et al.*, 1977). In addition it was recently reported that homoisocitrate dehydrogenase of *S. cerevisiae*, which naturally catalyses the oxidative decarboxylation of homoisocitrate to 2-oxoadipate (Fig. 3), was engineered to specifically catalyse the conversion of 2-oxoadipate to 2-hydroxyadipate (Reitman *et al.*, 2012). This enzyme engineering approach is based on cancer-associated mutations of isocitrate dehydrogenase found in human brain tumor cells. By these mutations the active site of the isocitrate dehydrogenase were altered to gain an oxidoreductase activity to convert 2-oxoglutarate to 2-hydroxyglutarate. In an enzyme re-engineering approach the mutations of isocitrate dehydrogenase were applied to homologous residues of homoisocitrate dehydrogenase of *S. cerevisiae*. The mutated enzyme specifically catalyse the conversion of 2-oxoadipate to 2-hydroxyadipate (Reitman *et al.*, 2012).

2.5 *Corynebacterium glutamicum* as host for 2-oxoadipate and adipate production

The Gram-positive, predominantly aerobic, non-pathogenic soil bacterium *Corynebacterium glutamicum* was first isolated by Kinoshita and co-workers as a result of its ability to excrete glutamate under biotin-limiting conditions (Kinoshita *et al.*, 1957). This biotin-auxotrophic species is non-motile, non spore-forming and rod-shaped with an irregular morphology (Abe *et al.*, 1967*).* It belongs to the class of *Actinobacteria* and has become a model organism for the order of *Actinomycetes* to study common features of corynebacteria and pathogenic mycobacteria, including the human-pathogens *Corynebacterium diphtheriae* and *Mycobacterium tuberculosis*. The 3.3 Mbp genome has been completely sequenced and revealed a high GC-content (53.8%) (Kalinowski *et al.*, 2003, Yukawa *et al.*, 2007). Since *C. glutamicum* is a firmly established industrial producer and since in the last decade many details regarding the metabolism and its regulation have been elucidated, this bacterium exhibits a high potential as host for the biotechnological production of various industrially relevant products (Eggeling & Bott, 2005). Today, it is used for the industrial production of amino acids, predominantly L-glutamate (2.2 mio t/a) and L-lysine (1.5 mio t/a) (Ajinomoto Co. Inc., 2010a, Ajinomoto Co. Inc., 2010b). Additionally, *C. glutamicum* has been engineered for the production of organic acids like pyruvate, 2-oxoglutarate or succinate (Wieschalka *et al.*, 2012, Jo *et al.*, 2012, Litsanov *et al.*, 2012a, Litsanov *et al.*, 2012b, Litsanov *et al.*, 2013). Besides its application in biotechnological processes, extensive research on the regulation and especially on the regulators of the citrate cycle genes has been performed (Bott, 2007).

Since 2-oxoglutarate serves as precursor for 2-oxoadipate production, regulation of the 2-oxoglutarate dehydrogenase complex (ODHC) is of strong interest for this study. With respect to the regulation mechanism, it was shown, that two proteins, OdhI and PknG, are involved: The serine/threonine protein kinase G (PknG) was shown to phosphorylate OdhI at threonine residue 14, which prohibits binding of OdhI to OdhA, the E1 subunit of ODHC. Unphosphorylated OdhI forms a complex with OdhA and causes inhibition of the ODHC activity (Niebisch *et al.*, 2006). A further study revealed that the lack of the OdhI protein leads to drastically diminished glutamate production, whereas a decreased ODHC activity is beneficial for glutamate production (Schultz *et al.*, 2007). Besides ODHC activity and its regulation, the recently reported development of a strain producing increased product titers of 2-oxoglutarate is of strong interest. For this purpose blockage of the pathways competing with the biosynthesis of 2-oxoglutarate resulted in elevated levels of 2-oxoglutarate (Jo *et al.*, 2012).

Based on this detailed knowledge and the proven capability to form dicarboxylic acids such as succinate in titers exceeding 130 g l^{-1}, *C. glutamicum* was considered as a promising host for the development of 2-oxoadipate and adipate producer strains (Litsanov *et al.*, 2012b).

2.6 Aim of this thesis

The overall goal of this project is the generation of a new synthetic pathway for the bio-based microbial production of adipate from glucose. In the study presented here, the primary aim was to test the potential of the model organism and biotechnologically important microbe *Corynebacterium glutamicum* to produce the adipate precursors homocitrate and 2-oxoadipate. To this end, enzymes of the α-aminoadipate pathway should be selected, cloned and heterologously expressed from plasmids and chromosomally integrated. First generation strains should be further improved by metabolic engineering strategies improving e.g. precursor supply. Furthermore, growth parameters and transcriptional responses of *C. glutamicum* wild-type cells in the presence of adipate and 2-oxoadipate should be analysed to study the possible consumption of these compounds and their influence on global gene expression.

3 Material and methods

3.1 Strains and plasmids

The strains used in this study are listed in Tab. 1 and the plasmids in Tab. 2.

Tab. 1: Strains used in this study and their relevant characteristics

Strain	Relevant characteristics	Reference
C. glutamicum ATCC 13032	wild-type strain, biotin-auxotrophic	Abe *et al.*, 1967
C. glutamicum Δ*pknG*	ATCC13032 derivative with in-frame deletion of *pknG* (cg3064), encoding serine/threonine protein kinase G	Niebisch *et al.*, 2006
C. glutamicum Δ*dctA* Δ*dccT*	ATCC13032 derivative with in-frame deletions of *dctA* (cg2870) encoding a Na^+/H^+ dicarboxylate symporter and *dccT* (cg0277) encoding another dicarboxylate uptake system	Youn *et al.*, 2009
E. coli DH5α	F^- Φ80*dlac*Δ (*lacZ*)M15 Δ (*lacZYA-argF*) U169 *endA1 recA1 hsdR17* (r_K^-, m_K^+) *deoR thi-1 phoA supE44* λ^- *gyrA96 relA1*	Invitrogen (Germany)
S. cerevisiae Y00000 (BY4741)	MAT**a**; *his3Δ1; leu2Δ0; met15Δ0; ura3Δ0*	EUROSCARF (Germany)
S. cerevisiae Δ*yer152c*	derivative of Y0000 with YER152c::kanMX4	EUROSCARF (Germany)
S. cerevisiae Δ*ygl202w*	derivative of Y0000 with YGL202w::kanMX4	EUROSCARF (Germany)
C. glutamicum MS-1	ATCC13032 derivative with an in-frame deletion of the *gdh* gene (glutamate dehydrogenase) and chromosomal integration of the *lys20* gene of *S. cerevisiae* encoding homocitrate synthase into the Δ*gdh* locus under control of the *tuf* promoter	This work
C. glutamicum MS-1-pHCS	MS-1 derivative containing pEKEx2-*lys20*, encoding homocitrate synthase (*lys20*) of *S. cerevisiae* under control of the *tac* promoter	This work

Strain	Relevant characteristics	Reference
C. glutamicum MS-2	MS-1 derivative containing pAN6-*pyc*^{P458S} encoding a modified pyruvate carboxylase (*pyc*^{P458S}) of *C. glutamicum* DM1727 under control of the *tac* promoter	This work
C. glutamicum MS-3	MS-1 derivative with an in-frame deletion of *pta-ackA* (phosphotransacetylase, acetate kinase) and chromosomal integration of the gene *pyc*^{P458S} of *C. glutamicum* DM1727 into the Δ*pta-ackA* locus under control of the *tac* promoter	This work
C. glutamicum MS-3-pHCS	MS-3 derivative containing pEKEx2-*lys20*, encoding homocitrate synthase (*lys20*) of *S. cerevisiae* under control of the *tac* promoter	This work
C. glutamicum MS-4	*C. glutamicum* Δ*pknG* derivative with an in-frame deletion of the *gdh* gene (glutamate dehydrogenase) and chromosomal integration of the *lys20* gene of *S. cerevisiae* encoding homocitrate synthase into the Δ*gdh* locus under control of the *tuf* promoter	This work
C. glutamicum MS-5	MS-1 derivative with an in-frame deletion of the *aceA* gene (isocitrate lyase) and chromosomal integration of the genes *lys4* and *lys12* of *S. cerevisiae* encoding homoaconitase and homoisocitrate dehydrogenase into the Δ*aceA* locus under control of the *tuf* promoter	This work
C. glutamicum MS-5-pHCS	MS-5 derivative containing pEKEx2-*lys20*, encoding homocitrate synthase (*lys20*) of *S. cerevisiae* under control of the *tac* promoter	This work

Tab. 2: Plasmids used in this study

Plasmid	Relevant characteristics	Reference
pEKEx2	Kan^{r}; *C. glutamicum/E. coli* shuttle vector for regulated gene expression (P_{tac}, *lacI*^{q}, pBL1 *ori*$V_{C.\,g.}$, pUC18 *ori*$V_{E.\,c.}$)	Eikmanns *et al.*, 1991
pEKEx2-*lys20*	Kan^{R}; pEKEx2 derivative containing the *lys20* gene encoding homocitrate synthase of *S. cerevisiae* under control of the *tac* promoter	This work
pEKEx2-*lys20*^{R276K}	Kan^{R}; pEKEx2 derivative containing the *lys20*^{R276K} gene encoding homocitrate synthase of *S. cerevisiae* under control of the *tac* promoter	This work
pEKEx2-*ttc1550*	Kan^{R}; pEKEx2 derivative containing the *ttc1550* gene encoding homocitrate synthase of *T. thermophilus* under control of the *tac* promoter	This work
pEKEx2-*nifV*	Kan^{R}; pEKEx2 derivative containing the *nifV* gene encoding homocitrate synthase of *A. vinelandii* under control of the *tac* promoter	This work
pVWEx2	Tet^{R}; *C. glutamicum/E. coli* shuttle vector for regulated gene expression; derived from pEKEx2	Peters-Wendisch *et al.*, 2001
pVWEx2-*lys4-lys12*	Tet^{R}, pVWEx2 derivative containing the genes *lys4* encoding homoaconitase and *lys12* encoding homoisocitrate dehydrogenase of *S. cerevisiae* under control of the *tac* promoter	This work
pAN6	Kan^{R}; *C. glutamicum*/*E. coli* shuttle vector for regulated gene expression; derivative of pEKEx2 (P_{tac}, *lacI*^{q}, pBL1 *ori*$V_{C.g.}$, pUC18 *ori*$V_{E.c.}$);	Frunzke *et al.*, 2008
pAN6-*pyc*^{P458S}	Kan^{R}; pAN6 derivative containing the *pyc*^{P458S} gene encoding pyruvate carboxylase of *C. glutamicum* DM1727 under control of the *tac* promoter	Litsanov *et al.*, 2012a
pK19*mobsacB*	Kan^{R}.; vector for allelic exchange in *C. glutamicum*; (pK18 *ori*$V_{E.c.}$, *sacB*, *lacZ*α)	Schäfer *et al.*, 1994

Plasmids	Relevant characteristics	Reference
pK19*mobsacB*-Δ*pta*-Δ*ackA*	Kan^R, pK19*mobsacB* derivative containing an overlap extension PCR product covering the flanking regions of the *pta-ackA* genes from *C. glutamicum*	Litsanov *et al.*, 2012a
pK19*mobsacB*-Δ*pta*-Δ*ackA*::P_{tuf}-*pyc*^{P458S}	Kan^R, pK19*mobsacB* derivative containing a double overlap PCR product which carries the *tuf* promoter of *C. glutamicum* fused to the *pyc*^{P458S} gene encoding pyruvate carboxylase of *C. glutamicum* DM1727 within the flanking regions of the *pta-ackA* genes *from C. glutamicum*	Litsanov *et al.*, 2012b
pK19*mobsacB*-Δ*gdh*	Kan^R, pK19*mobsacB* derivative containing an overlap extension product covering the flanking regions of the *gdh* gene from *C. glutamicum*	This work
pK19*mobsacB*-Δ*gdh*::P_{tuf}-*lys20*	Kan^R, pK19*mobsacB* derivative containing the *lys20* gene encoding homocitrate synthase of *S. cerevisiae* fused to the *tuf* promoter of *C. glutamicum* within the flanking region of the *gdh* gene of *C. glutamicum*	This work
pK19*mobsacB*-Δ*gdh*::P_{tuf}-*lys20*^{R276K}	Kan^R, pK19*mobsacB* derivative containing the *lys20*^{R276K} gene encoding homocitrate synthase of *S. cerevisiae* fused to the *tuf* promoter of *C. glutamicum* within the flanking region of the *gdh* gene of *C. glutamicum*	This work
pK19*mobsacB*-Δ*gdh*::P_{gap}-*lys20*	Kan^R, pK19*mobsacB* derivative containing the *lys20* gene encoding homocitrate synthase of *S. cerevisiae* fused to the *gap* promoter of *C. glutamicum* within the flanking region of the *gdh* gene of *C. glutamicum*	This work
pK19*mobsacB*-Δ*gdh*::P_{tac}-*lys20*	Kan^R, pK19*mobsacB* derivative containing the *lys20* gene encoding homocitrate synthase of *S. cerevisiae* fused to the *tac* promoter within the flanking region of the *gdh* gene of *C. glutamicum*	This work

Plasmids	Relevant characteristics	Reference
pK19*mobsacB*-Δ*aceA*	Kan^R, pK19*mobsacB* derivative containing a crossover product covering the flanking regions of the *aceA* gene of *C. glutamicum*	This work
pK19*mobsacB*-Δ*aceA*::P_{tuf}-*lys4*-*lys12*	Kan^R, pK19*mobsacB* derivative containing the genes *lys4* encoding homoaconitase and *lys12* encoding homoisocitrate dehydrogenase of *S. cerevisiae* fused to the *tuf* promoter of *C. glutamicum* within the flanking region of the *gdh* gene of *C. glutamicum*	This work

Tab. 3: Oligonucleotides used in this study. In some cases oligonucleotides were designed to introduce sites for restriction endonucleases (recognition sites underlined, restriction endonucleases in parenthesis) or to introduce codon exchanges (printed in italics). For gene replacement the overlapping sequences are highlighted in bold.

Name	5'-3' sequence and properties	Application
ttc1550-fw	CTAGTCGACGAAAGGAGGATATAGATATGCGGGAGTGGAAGATTATTG (SalI)	Amplification of the homocitrate synthase gene *ttc1550* of *T. thermophilus*
ttc1550-rv	AGAGGTACCTCACGCCGTGATCCACTCCCG (KpnI)	
nifV-fw	CTAGGATCCGAAAGGAGGATATAGATATGGCTAGCGTGATCATCGAC (BamHI)	Amplification of the homocitrate synthase gene *nifV* of *A. vinelandii*
nifV-rv	CTAGGTACCTCATGCCATTCCTCCTGCGG (KpnI)	
lys20-fw	CTACTGCAGGAAAGGAGGATATAGATATGACTGCTGCTAAACC (PstI)	Amplification of the homocitrate synthase gene *lys20* of *S. cerevisiae*
lys20-rv	AGAGGTACCTTAGGCGGATGGCTTAG (KpnI)	
lys4-fw	CTAGTCGACGAAAGGAGGATATAGATATGCTACGATCAACCAC (SalI)	Amplification of the homoaconitase gene *lys4* of *S. cerevisiae*
lys4-rv	**ATCTATATCCTCCTTTCTAG**TTATAGTTGGGATTTGACC	
lys12-fw	**CTAGAAAGGAGGATATAGAT**ATGTTTAGATCTGTTGCTACT	Amplification of the homoisocitrate dehydrogenase gene *lys12* of *S. cerevisiae*
lys12-rv	AGATCTAGACTATAATCTCGACAAAACGTC (XbaI)	

Name	5'-3' sequence and properties	Application
lys20^{R276K}-fw	GTTGCACAAGATCA*A*AGACATTGAAA ACCTGG	Introduction of amino acid exchange R276K within the homocitrate synthase *lys20* of *S. cerevisiae*
lys20^{R276K}-rv	CCAGGTTTTCAATGTCT*T*TGATCTTGT GCAAC	
M13-control-fw	CGCCAGGGTTTTCCCAGTCAC	pEKEx2-specific oligonucleotides for checking transformed plasmids
M13-control-rv	AGCGGATAACAATTTCACACAGGA	
lys20 integration		
Δgdh-1	CTAAAGCTTATCGGCGGAGCTTCGCA AAT (HindIII)	Amplification of overlapping fragment *gdh*-1 for in-frame deletion of the *gdh* gene (glutamate dehydrogenase) in *C. glutamicum*
Δgdh-2	**TGCGGCCGCTCACTTAAGATCCCGG GA**GCTGGCTTCAAGAAGGTAGC (NotI, AflII, XmaI)	
Δgdh-3	**TCCCGGGATCTTAAGTGAGCGGCCG CA**TTATTATTATTAGACCTGCTCATCA ACTGTCAT (XmaI, AflII, NotI)	Amplification of overlapping fragment *gdh*-2 for in-frame deletion of the *gdh* (glutamate dehydrogenase) in *C. glutamicum*
Δgdh-4	AGAGAATTCTCAGTCAACTGGTCTCAT TCG (EcoRI)	
Δgdh-control-fw	CAAGCTGGCGCAACTACGGT	Checking of in-frame deletion of the *gdh* gene and chromosomal integration of *lys20*-variants
Δgdh-control-rv	TAGCGCCTATAAAAGTCGTAC	
P_{tuf}-fw	CTAGCGGCCGCCCACAGGGTAGCTGG TAGT (NotI)	Amplification of the *tuf* promoter fragment of *C. glutamicum* for chromosomal integration into the Δ*gdh* locus
P_{tuf}-rv	CTACTTAAGTCCTCCTGGACTTCGTGG T (AflII)	
P_{gapA}-fw	**CTA**GCGGCCGCATGTGTCTGTATGATT TTGC (NotI)	Amplification of the *gapA* promoter fragment of *C. glutamicum* for chromosomal integration into the Δ*gdh* locus
P_{gapA}-rv	CTACTTAAGTCTCCTCTAAAGATTGTA GGA (AflII)	
P_{tac}-fw	CTAGCGGCCGCGAGCTGTTGACAATT AATCATC (NotI)	Amplification of the *tac* promoter fragment from the plasmid pEKEx2 for chromosomal integration into the Δ*gdh* locus
P_{tac}-rv	CTACTTAAGATCTATATCCTCCTTTCTC TAG (AflII)	
lys20-gdh-fw	CTACTTAAGATGACTGCTGCTAAACC (AflII)	Amplification of the homocitrate synthase gene *lys20* of *S. cerevisiae* for chromosomal integration into the Δ*gdh* locus
lys20-gdh-rv	AGACCCGGGTTAGGCGGATGGCTTAG TC (XmaI)	

Name	5'-3' sequence and properties	Application
lys4, *lys12* integration		
ΔaceA-1	CTAAAGCTTCTACCTCTGGAATCTAGG TG (HindIII)	Amplification of overlapping fragment *aceA*-1 for in-frame deletion of the *aceA* gene (isocitrate lyase) in *C. glutamicum*
ΔaceA-2	**TCCCGGGATCCTAGGTGAGCGGCCG CATTATTATTATTATGGCTTTCCAAC GTTTGACAT (XmaI, AvrII, NotI)**	
ΔaceA-3	**TGCGGCCGCTCACCTAGGATCCCGG GA**TCTACCACCGCTTTGAAGGG (NotI, AvrII, XmaI)	Amplification of overlapping fragment *aceA*-2 for in-frame deletion of the *aceA* gene (isocitrate lyase) in *C. glutamicum*
ΔaceA-4	AGAGAATTCCAACGCTGCTGGTGAAA CAA (EcoRI)	
ΔaceA-control-fw	GCCTAAACCAGAAGAATGCG	Checking of in-frame deletion of the *aceA* gene and chromosomal integration of *lys4-lys12*
ΔaceA-control-rv	CGCTACGGAATCGCAGATC	
P_{tuf}-aceA-rv	CTACCTAGGTGTATGTCCTCCTGGACT TC (AvrII)	Amplification of the *tuf* promoter fragment of *C. glutamicum* for chromosomal integration into the Δ*aceA* locus
lys4-aceA-fw	CTACCTAGGATGCTACGATCAACCAC ATTTA (AvrII)	Amplification of the homoaconitase gene *lys4* of *S. cerevisiae* for chromosomal integration into the Δ*aceA* locus
lys12-aceA-rv	AGACCCGGGCTATAATCTCGACAAAA CGTCG (XmaI)	Amplification of the homoisocitrate dehydrogenase gene *lys12* of *S. cerevisiae* for chromosomal integration into the Δ*aceA* locus

3.2 Chemicals and culture media

All chemicals used in the course of this work were obtained by Merck AG (Darmstadt, Germany), Fluka (Steinheim, Germany), Sigma-Aldrich (Taufkirchen, Germany), Roth GmbH & Co. (Karlsruhe, Germany) and Roche Diagnostics GmbH (Mannheim, Germany). The components of complex media were used from Difco Laboratories (Detroit, USA).

The following media were used for cultivation

LB medium: yeast extract (5 g l^{-1}), tryptone (10 g l^{-1}), NaCl (10 g l^{-1})

BHI medium: brain heart infusion (37 g l^{-1})

BHIS medium: brain heart infusion (37 g l^{-1}), sorbitol (91 g l^{-1})

CGXII medium: MOPS (42 g l^{-1}), $(NH_4)_2SO_4$ (20 g l^{-1}), urea (5 g l^{-1}), KH_2PO_4 (1 g l^{-1}), K_2HPO_4 (1 g l^{-1}), $MgSO_4$ x 7 H_2O (0.25 g l^{-1}), $CaCl_2$ (10 mg l^{-1}), the pH was adjusted to 7 with KOH. After autoclaving, biotin (0.2 mg l^{-1}), protocatechuate (30 mg l^{-1}), glucose (4 g l^{-1}) and supplementary salts containing $FeSO_4$ x 7 H_2O (10 mg l^{-1}), $MnSO_4$ x H_2O (0.1 mg l^{-1}), $ZnSO_4$ x 7 H_2O (1 mg l^{-1}), $CuSO_4$ x 5 H_2O (0.2 mg l^{-1}) $NiCl_2$ x 6 H_2O (20 µg l^{-1}) were added to the medium

SD medium: YNB (yeast nitrogen base) supplemented with NH_4^+ (6.7 g l^{-1}), glucose (20 g l^{-1}) and 10 ml l^{-1} 100x amino acid solution (4 g l^{-1} tryptophan, 4 g l^{-1} alanine, 2 g l^{-1} histidine, 2 g l^{-1} methionine, 6 g l^{-1} leucine, 3 g l^{-1} lysine, 2 g l^{-1} uracil); before autoclaving the pH was adjusted to 6 with KOH

M63 medium: KH_2PO_4 (3 g l^{-1}), K_2HPO_4 (7 g l^{-1}), $(NH_4)_2SO_4$ (2 g l^{-1}), $FeSO_4$ (0.5 mg l^{-1}); pH adjusted to 7 with KOH. After autoclaving thiamine (100 mg l^{-1}), $MgSO_4$ x 7 H_2O (0.16 g l^{-1}) and glucose (2 g l^{-1}) were added to the media.

For agar plates, 18 g l^{-1} agar was added to the media. When appropriate, kanamycin (25 µg ml^{-1} for *C. glutamicum* or 50 µg ml^{-1} for *E. coli*) or tetracycline (5 µg ml^{-1} for *C. glutamicum*) were added to the culture medium or the agar plates.

3.3 Cultivation and conservation of bacteria

3.3.1 Cultivation of *E. coli* for plasmid isolation

For plasmid isolation *E. coli* DH5α was routinely cultivated in 5 ml LB medium, supplemented with the appropriate antibiotics (kanamycin or tetracycline), for 12-24 h at 37°C and 170 rpm.

3.3.2 Cultivation of *C. glutamicum* in shake flaks

C. glutamicum was routinely cultivated at 30°C. For cultivation of *C. glutamicum* strains 5 ml BHIS medium was inoculated with a single colony from a fresh BHIS agar plate and incubated for 8 h. 100 µl of the first preculture were used to inoculate a 100 ml baffled shake flask containing 20 ml BHIS medium and cultivated overnight at 30°C. The cells were washed with 0.9% NaCl. The 60 ml main culture (500 ml shake flask) was inoculated to an OD_{600} of 1 and cultivated on a rotary shaker (120 rpm). For all main cultures of *C. glutamicum* CGXII medium containing glucose (111 mM or 222 mM) as carbon and energy source was used. Strains harbouring an expression plasmid with a *tac* promoter were induced with 0.7 mM IPTG at an OD_{600} of 1. For modified CGXII medium with nitrogen limitation, urea (1.67 g l^{-1}, 6.4%) was used as sole nitrogen source. Phosphate limitation was performed by reducing the phosphate concentration in the medium from 2 g l^{-1} to 0.15 g l^{-1}, using KH_2PO_4. Cultivation with additional feeding in the stationary phase was performed by adding 222 mM glucose and 204 mM potassium acetate dissolved in standard CGXII medium. To test whether *C. glutamicum* was able to consume adipate, 2-oxoadipate or homocitrate, growth experiments were performed by adding various concentrations (50 mM to 500 mM) of these compounds to the glucose minimal medium of the main culture. The pH value of the various organic acid solutions was adjusted with NaOH or KOH to pH 7 before addition to the culture media.

For DNA microarray analysis of the transcriptional response to the presence of adipate and 2-oxoadipate, *C. glutamicum* cells were pregrown in CGXII minimal medium with 222 mM glucose and 50 mM of the respective dicarboxylate and then used to inoculate the main culture with the same medium composition to an OD_{600} of 1. Cells of the main culture were harvested in the exponential phase at an OD_{600} of 6 for RNA preparation.

3.3.3 Conservation of bacteria

For long-term conservation of *E. coli* and *C. glutamicum* strains, 2 ml of an overnight culture (12-15 h) were centrifuged at room temperature for 2 min at 5,000 x *g*. The cell pellet was resuspended in 0.75 ml of appropriate media (LB or BHIS) and mixed with 0.75 ml of sterile glycerol. The strains were stored in cryovials at -70°C.

3.3.4 Cultivation of *C. glutamicum* in a bioreactor

For cultivating *C. glutamicum* strains in a bioreactor, a starter culture with 5 ml BHIS medium in a test tube was inoculated with a single colony of a fresh BHIS agar plate and incubated for 10-12 h on a rotary shaker a 30°C. A second preculture in a 100 ml baffled shake flask containing 60 ml CGXII minimal medium with 4% (222 mM) glucose as sole carbon source was inoculated to an OD_{600} of 0.25. After overnight cultivation at 30°C and 120 rpm a 1.4 l bioreactor (Multifors multi fermenter system with six independent controllable bioreactors, Infors, Einsbach, Germany) was inoculated with cells of the preculture to an OD_{600} of 1. Each bioreactor contained 500 ml of modified CGXII minimal medium with 4% (222 mM) glucose as sole carbon source omitting the buffer substance MOPS. If required 25 µg ml^{-1} kanamycin and 0.7 mM IPTG were added. The bioreactor was fumigated with 0.9 l min^{-1} air. The flow rate was controlled by a mass flow regulator. Oxygen saturation during the experiment was measured online using a polarimetric oxygen electrode (Mettler Toledo, Giessen, Germany). To prevent dropping of oxygen saturation below 30%, oxygen was permanently held above 30% by stepwise increasing stirrer speed from 500 rpm to 800 rpm and increasing molecular oxygen in the inflow gas mix by 5% to a maximal value of 30%. The pH was also measured online using a standard electrode (Mettler Toledo) and automatically adjusted to pH 7 with 3 M sodium hydroxide and 3 M hydrochloric acid. Foam formation was prevented by automatic addition of 25% (v/v) Antifoam 204 suspension in water (Sigma Aldrich, Steinheim, Germany). Carbon dioxide and oxygen was measured in a partial flow of exhaust air with an Off-gas analyser (Infors). Determination of CO_2 and O_2 concentration was performed via near-infrared absorption. Feeding of additional carbon sources (glucose and acetate) was automatically performed by either continuous feeding a solution of 25% (w/v) glucose and 12.5% (w/v) acetate in modified CGXII medium or by feeding the solution in dependency of oxygen saturation. When oxygen saturation was above 80%, indicating that the cells did not further consume oxygen and thus were limited by carbon supply, glucose and potassium acetate were added to final concentrations of 20 mM and 10 mM, respectively. Another strategy was to add manually one pulse of a 25% glucose and 12.5% acetate solution to final concentrations of 222 mM glucose and 204 mM potassium acetate.

3.3.5 Cultivation of *S. cerevisiae*

For cultivation of *S. cerevisiae* strains a 5 ml culture in a test tube containing SD minimal medium was inoculated with a single colony from a fresh SD agar plate. This starter culture was incubated over night at 30°C and 170 rpm. Main cultures of *S. cerevisiae* were performed in shake flasks in 60 ml SD minimal medium at 30°C and 120 rpm, inoculated to an OD_{600} of 0.25 with cells from the starter culture.

3.4 Determination of growth parameters

Cell growth in liquid culture was followed by measuring the optical density at 600 nm against a blank sample with an UV-1800 spectrophotometer (Shimadzu, Duisburg, Germany). For measuring in the linear detection range (OD_{600} 0.05-0.75), the samples were diluted in water. The *C. glutamicum* biomass was calculated from the OD_{600} values using an experimentally determined correlation factor of 0.25 g (cell dry weight) l^{-1} for an OD_{600} of 1 (Kabus *et al.*, 2007).

3.5 Molecular biology methods

3.5.1 Isolation of nucleic acid

3.5.1.1 Isolation of plasmid DNA

E. coli or *C. glutamicum* strains harbouring a plasmid were cultivated overnight in 5 ml LB or BHIS media containing the appropriate antibiotics at 37°C or 30°C, respectively. The cells were harvested at room temperature by centrifugation at 5,000 x *g* for 2 min. For isolation of plasmid DNA of *E. coli* or *C. glutamicum* the QIAprep Spin Miniprep Kit (Qiagen, Hilden, Germany) or GeneJET Plasmid Miniprep Kit (Fermentas) were used according to the corresponding manual. The isolation procedure is based on alkaline cell lysis (Bimboim & Doly, 1979). Membrane-bound DNA was eluted with sterile water. The complex cell wall of *C. glutamicum* requires cell disruption for isolation of plasmid DNA, either by beat-beating three to four times for 20 s with silica beats (300 mg Ø 0.1 mm, Roth) using the Silamat® S5 (Ivoclar Vivadent) or by shaking the cell suspension for 2 hours at 37°C in buffer P1 (Qiagen) or Resuspension solution (Fermentas) with 15 mg lysozyme (Schwarzer & Puhler, 1991).

3.5.1.2 Isolation of total RNA

To isolate total RNA of *C. glutamicum* the strains were cultivated as described above (3.2 and 3.3). 25 ml of the cultures were harvested by centrifugation at 5,000 x *g* and 4°C for 5 min in prechilled falcon tubes, filled with 15 g of ice. The collected cells were either frozen in liquid nitrogen and stored at –20°C or directly used for RNA isolation. The cell pellets were resuspended in 700 µl RLT buffer supplemented with 10 mM dithiothreitol and transferred to a 1.5 ml reaction tube, loaded with ~300 mg silica beats (Ø 0.1 mm, Roth). The cells were disrupted by beat-beating three to four times for 20 s using the Silamat® S5 (Ivoclar Vivadent). The isolation of total RNA of *C. glutamicum* was performed using the RNeasy Mini Kit (Qiagen) with on-column digestion of DNA. This method is based on cell lysis in the presence of dithiothreitol and guanidine isothiocyanate, which leads to inactivation of RNAses and allows the isolation of intact RNA. Afterwards the RNA was absorbed in the presence of ethanol and a specific salt solution (RNeasy Kit) to a silica-gel membrane which binds selectively single-stranded RNA molecules. Isolation steps were carried out according to the RNeasy Kit manual. The membrane-bound RNA was eluted with sterile water and stored at -20°C.

3.5.1.3 Isolation of genomic DNA of *S. cerevisiae*

Isolation of genomic DNA of the baker's yeast *S. cerevisiae* was performed using the DNeasy Kit (Qiagen). 5 ml LB medium supplemented with glucose (20 g l^{-1}) and casein (10 g l^{-1}) was inoculated with 10 µl *S. cerevisiae* cell suspension to and incubated for 24 h at 30°C. 3 ml of the culture was centrifuged at 6,000 x g for 2 min at room temperature. The cell pellet was resuspended in 180 µl ATL (DNeasy Kit, Qiagen) and transferred to a 1.5 ml reaction tube containing 200 mg silica beats (∅ 0.5 mm, ROTH). The cells were disrupted by beat-beating two times for 30 s using the Silamat® S5 (Ivoclar Vivadent). The cell debris were separated by centrifugation at 6,000 x *g* for 2 min at room temperature. The supernatant was used for the isolation of genomic DNA according to the DNeasy Kit manual. The genomic DNA was eluted with sterile water and stored at 4°C.

3.5.1.4 Purification of DNA fragments

Purification of DNA fragments to remove residual nucleotides and enzymes after PCR and restriction digestion was performed using the PCR Purification Kit (Qiagen) according to the manual. The DNA was eluted with sterile water and stored at -20°C.

3.5.1.5 Isolation of DNA fragments from agarose gels

To separate DNA fragments of PCR or restriction digests, agarose gel electrophoresis was performed. After electrophoresis the DNA fragment of interest was carefully excised. Extraction of the DNA fragments was done with the QIAquick Gel Extraction Kit (Qiagen) or Omnipure-OLS®-Kit (OMNI Life Sciences) according to the respective manual. The DNA fragments were eluted with sterile water and stored at -20°C.

3.5.2 DNA gel electrophoresis

Separation of DNA fragments by size in an electric field is based on the negatively charged DNA molecules. Electrophoresis was performed using 0.7% - 2% (w/v) agarose gels depending on the size of the fragment of interest in 1x TAE buffer. The samples were mixed with 6x loading buffer and loaded onto the gel, which contained one lane with GeneRuler™ (Thermo Scientific) 1 kb DNA marker. Electrophoresis was carried out in 1x TAE buffer at 80-100 V for 1 hour. After electrophoresis the gel was stained with an ethidium bromide solution (2 µg/mL) for 10 min. Before gel documentation was done with an Image Master VDS System (Amersham Biosciences) the gel was destained for 10 min in a water bath.

6x DNA loading buffer	4 M urea, 1 mM EDTA, 50% (w/v) sucrose, 0.1% (w/v) bromophenol blue
50x TAE buffer	242 g Tris, 57.1 ml acetic acid, 14.7 g EDTA

3.5.3 RNA gel electrophoresis

RNA gel electrophoresis was used to check the quality and purity of isolated total RNA. Therefore 1.2% (w/v) formaldehyde gels were prepared adding 0.6 g agarose to 5 ml 10x FA buffer and 45 ml double autoclaved water. After heating in the microwave to dissolve the agarose 4 µl GelRed® solution was added. The solution was cooled to 60°C before 900 µl 37% formaldehyde was added. The gel was polymerised and equilibrated for 30 min in 1x FA running buffer. The RNA samples were mixed with 5x RNA loading buffer and incubated for 5 min at 65°C. The samples were chilled on ice and loaded onto the gel. RNA was separated by electrophoresis at 70-80 V for 75-90 min. Gel documentation was done with an Image Master VDS System (Amersham Biosciences).

FA buffer (10x)	200 mM MOPS, 50 mM sodium acetate, 20 mM EDTA, pH 7.0 (NaOH)
FA running buffer (1x)	100 ml FA buffer (10x), 20 ml formaldehyde (37%), 880 ml H_2O, pH 7.0
RNA loading buffer (5x)	60 µl saturated bromophenol blue solution, 80 µl 0.5 M EDTA (pH 8.0), 720 µl formaldehyde (37%), 2 ml glycerol (100%), 4 ml FA buffer (10 x), 3 ml formamide

3.5.4 Determination of nucleic acid concentrations

The concentration of nucleic acids was determined by measuring the extinction at 260 nm with a spectrophotometer (Nanodrop® ND-1000, PeqLab Biotechnologie GmbH, Erlangen). The following conversion factors were used to calculate the DNA or RNA concentration (Sambrook *et al.*, 2001):

Single-strand RNA: OD_{260} = 1 corresponds to a concentration of 40 µg/ml

Double-strand DNA: OD_{260} = 1 corresponds to a concentration of 50 µg/ml

The purity of DNA and RNA was determined by the ratio of OD_{260}/OD_{280}, which should be between 1.8 and 2.0 for DNA and at 2.0 for RNA.

3.5.5 Recombinant DNA work

3.5.5.1 Restriction of DNA

Restriction of DNA fragments was performed using type II restriction endonucleases at 37°C. The enzymes were obtained from Fermentas or New England Biolabs. Restriction with the "Fast Digest Enzymes" of Fermentas was performed for 45 min using the "Fast Digest buffer". When using the enzymes of New England Biolabs the recommended "NEBuffer" was used and digestion was performed for 2 h. Restriction of PCR products or plasmids was performed in a total volume of 100 µl, containing 1-2 U of the enzymes per µg of DNA and 1-2 µg of digested DNA. The buffer for double digests with enzymes of New England Biolabs was chosen according to the recommendations of the manufacturer.

3.5.5.2 Dephosphorylation of restricted plasmid DNA

Alkaline phosphatase catalyses hydrolytic elimination of a phosphate group at the 5'-end of DNA and was used to prevent recircularisation of plasmid DNA during ligation. For dephosphorylation of restricted plasmid DNA the "shrimp alkaline phosphatase" from Roche

Diagnostics was used. The plasmid was incubated with 1 U of the phosphatase for 1 h at 37°C. Afterwards the phosphatase was inactivated by heating to 65°C for 15 min.

3.5.5.3 Ligation

The T4 DNA ligase catalyses the formation of a phosphodiester bond between 5'-phosphate and 3'-hydroxy groups in double-stranded DNA. For ligation of PCR products with appropriate plasmids the "DNA Rapid Ligation" Kit of Fermentas was used. The ligase catalyses both, ligation of sticky- and blunt-ended DNA fragments. Ligation was carried out in 20 µl mixtures containing 100 ng plasmid DNA and a 2-3 times molar excess of the PCR product. The reaction was incubated for 1 h at room temperature or overnight at 4°C.

3.5.6 Generation and transformation of competent *E. coli* cells

Generation of competent, logarithmic grown *E. coli* cells were performed by $RbCl_2$ treatment to introduce free DNA into the cell. The preparation of competent cells was performed according to Hanahan (Hanahan, 1985). 5 ml LB medium in a test tube was inoculated with a single colony from a fresh agar plate and cultivated overnight at 37°C and 170 rpm. 200 µl of this culture was inoculated into 70 ml LB medium and cultivated to an OD_{600} of 0.6 at 37°C and 120 rpm. The culture was transferred to a precooled 50 ml falcon tube and chilled on ice for 15 min. The cells were harvested by centrifugation for 10 min at 4°C and 5,000 x *g*. Afterwards the cell pellet was resuspended in 25 ml RF1 solution and incubated on ice for 10 min, followed by centrifugation for 10 min at 4°C and 5,000 x *g*. The pellet was resuspended in 2 ml RF2 solution and dispensed in 150 µl aliquots, which were frozen in liquid nitrogen and stored at -70°C.

RF1 solution	100 mM RbCl, 50 mM $MnCl_2$, 30 mM potassium acetate, 10 mM $CaCl_2$, pH 5.8 (acetic acid) The solution was filter-sterilized before use.
RF2 solution	10 mM RbCl, 10 mM MOPS, 75 mM $CaCl_2$ x 6 H_2O, 15% (v/v) glycerol, pH 5.8 (NaOH) The solution was autoclaved before use.

Transformation of chemically competent *E. coli* cells was carried out by a heat shock protocol. 10-100 ng of plasmid DNA or 10 µl of ligation mixture was mixed with 150 µl of

competent cells and incubated for 20 min on ice. To transfer the DNA into the cells a heat shock at 42°C for 1 min was performed. Subsequently, the cells were regenerated by adding 500 µl of LB medium to the cells and by incubation for 1 h at 37°C and 300 rpm. The cell suspension was plated on LB agar plates containing the appropriate antibiotics and incubated overnight at 37°C.

3.5.7 Generation and transformation of competent *C. glutamicum* cells

Generation of electro-competent *C. glutamicum* cells was performed according to the protocol of Tauch *et al.*, 2002. A 20 ml BHIS starter culture (100 ml shake flask) was inoculated with a single colony from a fresh BHIS agar plate and incubated overnight at 30°C and 120 rpm. The 50 ml BHIS main culture (500 ml shake flask) was inoculated to an OD_{600} of 0.5 and cultivated at 30°C and 120 rpm to an OD_{600} of 1.75. The cells were transferred to a 50 ml falcon tube and harvested by centrifugation at 4°C and 5,000 x *g* for 20 min. After the supernatant had been completely removed, the pellet was resuspended in 8 ml ice-cold TG buffer and centrifuged for 10 min at 4°C and 5,000 x *g*. This washing step was repeated two times. Afterwards the cell pellet was resuspended in 8 ml ice-cold 10% (v/v) glycerol and centrifuged for 10 min at 4°C and 5,000 x *g*. This washing step was repeated two times. Then the supernatant was completely removed, the cell pellet was resuspended in 2 ml ice-cold 10% glycerol and dispensed in 150 µl aliquots. The aliquots were frozen in liquid nitrogen and stored at -70°C.

TG buffer	1 mM Tris-HCl pH 7.5, 10% (v/v) glycerol

The transformation of *C. glutamicum* was performed by electroporation. Initially, 4 ml BHIS medium was pre-warmed to 46°C in a water bath. Competent *C. glutamicum* cells were gently thawed on ice and mixed with 0.1-2 µg plasmid DNA. The mixture was transferred to a 0.2 cm Gene Pulser cuvette (BioRad) and carefully covered with 0.8 ml 10% (v/v) glycerol. Electroporation was performed at 2.5 kV, 25 µF and 200 Ω, at which the time constant should be between 3.5 ms and 4 ms. Subsequently, the cell suspension was transferred into a 15 ml falcon tube containing pre-warmed BHIS medium for heat-shocking the cells at 46°C for 6 min. Then the cells were regenerated for 50 min at 30°C and 170 rpm. The cell suspension was plated onto BHIS agar plates containing the appropriate antibiotics and incubated over night at 30°C.

3.5.8 Polymerase chain reaction (PCR)

The polymerase chain reaction is a method for amplification of DNA fragments (Mullis *et al.*, 1986). PCR was performed either in a PCR Gene Amp PCR System 9700 (Applied Biosystems) or in a Mastercycler Personal (Eppendorf) according to standard set up (see below). Amplification for preparative procedures was done with KOD Hot Start Polymerase (Novagen, Darmstadt, Germany), Advantage HD Polymerase (Clontech) or Phusion® High-Fidelity DNA Polymerase (New England Biolabs, Frankfurt am Main, Germany). For analytical procedures or checking transformed cells *Taq* DNA polymerase from Fermentas was used. Colony PCR was performed by transferring cell material of a colony to the PCR reaction tube. An initial denaturation step for 10 min at 95°C was used to disrupt the cells. The annealing temperature was chosen 2-4°C below the melting temperature of the oligonucleotides. The melting temperature was calculated using the formula T_M [°C] = [(G + C) x 4] + [(A + T) x 2]. The extension time of the PCR was chosen according to the size of the DNA fragment to be amplified (1 min for 1,000 bp). Amplification using the Advantage HD Polymerase (Clontech) was performed lacking the annealing step. For overlap extension PCR both preliminary amplified PCR products were used in equal molar ratio. This method is based on identical 15-30 bp at the 3'-end of the first DNA fragment and the 5'-end of the second fragment. In contrast to the standard PCR set up, the overlap extension PCR set up contained 20-50 ng of each DNA fragment, the forward primer of the first fragment and the reverse primer of the second fragment. The oligonucleotides used in the course of this work are listed in Tab. 3.

<u>50 µl standard PCR set up</u>

PCR buffer	according to manufacture manual
dNTP mix (10 mM each, Roche Diagnostics)	1 µl
$MgSO_4$ (25 mM) (only in case of KOD)	3 µl
forward (5') primer (10 µM)	2 µl
reverse (3') primer (10 µM)	2 µl
Template DNA	0.5-50 ng
DNA polymerase	0.02 U
Sterile water	to 50 µl total volume

3.5.9 Construction of expression plasmids

For expression of heterologous genes in *E. coli* and *C. glutamicum* the plasmids pEKEx2 and pVWEx2 were used (Tab. 2). The genes were amplified from chromosomal DNA of *S. cerevisiae* (provided by Prof. Hegemann, Heinrich Heine University Duesseldorf, Germany), *T. thermophilus* (DSMZ, Braunschweig, Germany) or *A. vinelandii* (DSMZ, Braunschweig, Germany) using the oligonucleotides listed in Tab. 3. In front of each gene an artificial ribosomal binding site (GAAAGGAGG) was cloned, with the last "G" located 9 bp in front of the start codon. After amplification the DNA fragments were purified and restricted with appropriate enzymes (Tab. 3). The restricted DNA fragments were purified and ligated with the appropriately restricted vector DNA, followed by transformation of *E. coli* DH5α cells. *E. coli* colonies grown on the selective agar plates were chosen to test for the desired recombinant plasmid by colony PCR with plasmid or target gene specific oligonucleotides (Tab. 3).

3.5.10 Construction of chromosomal gene replacements using the pK19*mobsabB* system

The *gdh* gene was replaced by the HCS gene lys20. Three different promoters (P_{tuf}, P_{gapA}, P_{tac}) have been fused to lys20 to test their ability for HCS expression. For this purpose the three plasmids pK19*mobsacB*-Δ*gdh*::P_{tuf}-*lys20*, pK19*mobsacB*-Δ*gdh*::P_{gapA}-*lys20*, pK19*mobsacB*-Δ*gdh*::P_{tac}-*lys20* were constructed. Therefore, the up- and downstream regions (approximately 500 bp each) of the *gdh* gene, containing codons for the first 7 and the last 17 amino acids of the *gdh* sequence, were amplified from chromosomal DNA of *C. glutamicum* using the oligonucleotides pairs designated Δ*gdh*-1/Δ*gdh*-2 and Δ*gdh*-3/Δ*gdh*-4 (Tab. 3). The resulting PCR products served as templates for an overlap extension PCR using the oligonucleotides Δ*gdh*-1 and Δ*gdh*-4. This overlap PCR product, named Δ*gdh*-olf (overlapping fragment), contained a multiple cloning site harbouring the restriction sites NotI, AflII and XmaI as well as seven in-frame stop codons terminating the translation of Gdh. The overlap PCR product Δ*gdh*-olf (approximately 1,000 bp) was digested with the enzymes HindIII and EcoRI and cloned into the vector pK19*mobsacB*, designated pK19*mobsacB*-Δ*gdh*. The promoters P_{tuf} and P_{gapA} were amplified from chromosomal DNA of *C. glutamicum* using the oligonucleotides P_{tuf}-fw/P_{tuf}-rv and P_{gapA}-fw/P_{gapA}-rv, respectively (Tab. 3). The plasmid pVWEx1 served as template for the amplification of the promoter P_{tac} with the oligonucleotides P_{tac}-fw and P_{tac}-rv (Tab. 3). The PCR products of the three different promoters were digested with the enzymes NotI and AflII and cloned into the plasmid pK19*mobsacB*-Δ*gdh*. The resulting plasmids were named pK19*mobsacB*-Δ*gdh*::$P_{promoter\ name}$.

For the cloning of the homocitrate synthase the gene *lys20* was amplified from chromosomal DNA of *S. cerevisiae* using the oligonucleotides *lys20*-Δ*gdh*-fw and *lys20*-Δ*gdh*-rv (Tab. 3), digested with the enzymes AflII and XmaI and cloned into the plasmid pK19*mobsacB*-Δ*gdh*::$P_{promoter\ name}$, designated pK19*mobsacB*-Δ*gdh*::$P_{promoter\ name}$-*lys20*. For gene expression an artificial ribosomal binding site (AGGAGGA) was cloned in front of the *lys20* gene, with the last "A" located 7 bp in front of the start codon.

The construction of the plasmid for the gene replacement of the gene *aceA* by the fused genes *lys4*-*lys12* was performed as described above. The oligonucleotides used for the Δ*aceA* overlap fragment were named Δ*aceA*-1/Δ*aceA*-2 and Δ*aceA*-3/Δ*aceA*-4 (Tab. 3). The multiple cloning site within the Δ*aceA*-olf contained the restriction sites for the enzymes NotI, AvrII and XmaI as well as seven in-frame stop codons terminating the translation of *aceA*. Amplification of the P_{tuf}-promoter was performed using the oligonucleotides P_{tuf}-fw and P_{tuf}-*aceA*-rv. The genes *lys4* and *lys12* were amplified from plasmid pVWEx2-*lys4*-*lys12* using the oligonucleotide *lys4*-*aceA*-fw/*lys12*-*aceA*-rv (Tab. 3). The PCR product was digested with the enzymes AvrII and XmaI and cloned into the vector pK19*mobsacB*-Δ*ace*::P_{tuf} resulting in the plasmid pK19*mobsacB*-Δ*aceA*::P_{tuf}-*lys4*-*lys12*. The deletion/ integration of the genes was performed with a two-step homologous recombination technique as described by Niebisch & Bott, 2001. Kanamycin-sensitive and sucrose-resistant clones were analysed via colony PCR with the corresponding oligonucleotides Δ*gene*-control-fw and Δ*gene*-control-rv (Tab. 3).

3.5.11 Site-directed mutagenesis

Site-directed mutagenesis of the homocitrate synthase of *S. cerevisiae* was performed using the QuikChange XL Site-Directed Mutagenesis Kit (Agilent Technologies, Waldbronn, Germany). Replacement of a single base from G to A caused a change in the amino acid sequence from L-arginine to L-lysine (Feller *et al.*, 1999). The plasmid pEKEx2-*lys20* served as template for the amplification with the oligonucleotides *lys20*^{R276K}-fw and *lys20*^{R276K}-rv (Tab. 3) which were used to incorporate the point mutation. Further steps were carried out according to the manufacturer's manual with the exception that *E. coli* DH5α was used for transformation. The obtained point mutation was checked via DNA sequencing.

3.5.12 DNA sequencing

DNA sequencing was performed using the single read sequencing service of Eurofins MWG Operon. The samples were premixed with gene-specific primers or primers binding to the plasmid backbone according to the sequencing guidelines of the company. The received sequences were compared to the *in-silico* sequences using the freeware tool BioEdit (Ibis Biosciences, Carlsbad, USA).

3.6 Quantification of glucose and organic acids in the cell culture supernatant

For the quantification of substrate consumption and product formation, 1 ml samples were taken from cultures and centrifuged at room temperature at 6,000 x *g* for 5 min. The supernatant was transferred to a new 1.5 ml reaction tube and centrifuged at room temperature at 15,000 x *g* for 10 min. The supernatant was diluted 4 times in pure water and analysed via HPLC. Determination of glucose and organic acids in the cell-free culture supernatant was performed using an Agilent 1100 LC-system (Agilent Technologies, Waldbronn, Germany). Organic acids were detected with an Agilent 1100 Diode Array Detector and glucose with an Agilent 1100 Refractive Index Detector. Separation was carried out on a 300 x 8 mm organic acid column (polystyrol-divinylbenzol resin) and a guard column loaded with the same material (CS Chromatographie Service GmbH, Langerwehe, Germany). Isocratic elution was performed for 38 min at 40°C with 100 mM sulphuric acid as mobile phase at a flow rate of 0.4 ml/min. Quantification was done using calibration curves obtained from external standards dissolved in pure water.

3.7 GC-ToF-MS analysis of metabolites in the cell culture supernatant

For detection and analysis of metabolites in cell culture supernatants by GC-coupled mass spectrometry, 500 µl samples were taken from the culture at various time points during cultivation and centrifuged for 5 min at 13,000 x *g* and room temperature. 130 µl of the supernatant were shock-frozen in liquid nitrogen, lyophilised overnight in a Christ LT-105 freeze drier and then stored at -20 °C. The dried samples were consecutively derivatised with 50 µL MeOX (20 mg/mL O-methylhydroxylamine in pyridine) for 90 min at 30 °C and 600 rpm in a Thermomixer followed by an incubation with additionally 80 µL of MSTFA (N-acetyl-N-(trimethylsilyl)-trifuoroacetamide) for 90 min at 40 °C and 600 rpm. 1 µl of the samples was used for analyses. For the determination of the derivatised metabolites an Agilent 6890N gas chromatograph, equipped with a 30 m Varian FactorFour Vf-5ms column and a 10 m guard column was used coupled to a Waters Micromass GCT Premier high

resolution time of flight mass spectrometer. The system was controlled with the software Waters MassLynx 4.1. Under constant helium flux of 1 ml min^{-1} a temperature of 60°C was hold for 2 min and then increased gradually by 12°C min^{-1} to 300°C, which was hold for 8 min. The ToF-MS was performed in $[EI]^+$ modus with an energy of 70 eV and an ionisation temperature of 180°C. The MS was calibrated by the fragmentation pattern of Heptacosafluoro-tributylamin and the obtained masses were adjusted by Chloropentafluoro-benzene as an external standard. To identify the metabolites, masses were compared to the databases JuPoD (in-house database), NIST (National Institute of Standards and Technology) and GMD (Golm Metabolome Database). The GC-ToF-MS measurements and subsequent data analysis were performed by Jochem Gätgens (IBG-1: Biotechnology, Systems Biotechnology, Forschungszentrum Jülich GmbH, Germany).

3.8 Protein analysis

3.8.1 Determination of protein concentration

Protein concentrations of crude extracts were measured using the Bradford assay. This method is based on the formation of a complex between the dye Coomassie brilliant blue G and proteins. The unbound dye shows peak absorption at 465 nm, whereas the absorption shifts to 595 nm when a dye-protein complex is formed. 100 µl of appropriately diluted protein samples were mixed with 900 µl Bradford reagent (Sigma-Aldrich, Taufkirchen, Germany) and incubated for 10 min at room temperature in the dark. After incubation the absorption was measured at 595 nm. The calculation of the protein concentration was based on a calibration curve with bovine serum albumin (BSA) in the range of 20-100 µg/ml.

3.8.2 Homocitrate synthase enzyme assay

C. glutamicum strains containing either plasmid- or chromosomal-encoded homocitrate synthase were grown on BHIS agar plate and 5 ml BHIS liquid medium containing kanamycin if necessary were inoculated with a single colony. After cultivation for 9 h at 30°C 100 µl of the preculture were inoculated into 20 ml BHIS medium and cultivated overnight at 30°C. This preculture was then used to inoculate the main culture containing 60 ml CGXII minimal medium with 222 mM glucose to an OD_{600} of 1. Heterologous gene expression of plasmid-containing strains was induced with 1 mM IPTG at an OD_{600} of 1. Cells were harvested by centrifugation (15 min, 4,000 x *g*, 4°C) during the exponential phase after 6 h of growth and in the stationary phase after 24 h of cultivation, respectively. The supernatant was

completely removed and the cell pellet was either immediately used for the enzyme assay or frozen in liquid nitrogen. The enzyme activity assay was performed using the photo-colorimetric DCPIP (dichlorophenol indophenol) method as described previously (Quezada *et al.*, 2011). In the oxidised state DCPIP is blue and colourless when it is reduced. In this assay, homocitrate synthase activity was determined by measuring the reduction of DCPIP at 600 nm (ε_{600nm} = 20,600 cm^{-1} M^{-1}), which oxidise free CoASH that is released during the condensation of acetyl-CoA and 2-oxoglutarate (Armstrong, 1964, Schöbel *et al.*, 2010). Calculation of homocitrate synthase activity is based on a stoichiometry of 1:1 between CoASH and DCPIP (Andi *et al.*, 2004). For the enzyme assay the cells were washed with 50 mM MOPS pH 7.0 and 0.1% Triton X-100. The crude extract was obtained by disrupting the cells by bead-beating with silica beads (Ø 0.1 mm, Roth) three to four times for 20 s using the Silamat® S5 (Ivoclar Vivadent). The crude extract was separated from the cell debris by centrifugation (25 min, 13,000 x *g*, 4°C) and used for the enzyme assay. The assay was performed in a 1 ml mixture containing 50 mM HEPES pH 7.2, 100 mM 2-oxoglutarate, 0.1 mM DCPIP and 0.25 mM acetyl-CoA. After equilibration (5 min, 30°C) the assay was started by adding variable amounts of the crude extract. The decreasing absorption was measured for 10 min at 600 nm.

3.9 Global gene expression analysis using DNA microarrays

DNA microarray technology permits the comparison of genome-wide mRNA concentration of two independent samples, by using two differently fluorescence-labelled cDNA samples (Frunzke *et al.*, 2008). The used arrays were glass slides spotted with synthetic oligonucleotides. Analysis of global gene expression of *C. glutamicum* was performed with custom-made whole genome DNA microarrays (Operon Biotechnologies, Cologne, Germany) containing sequence-specific 70mer oligonucleotides of the *C. glutamicum* genome (Kalinowski *et al.*, 2003). The spotted oligonucleotides represented 3057 protein coding genes, 1294 intergenic regions, 50 tRNA genes, 15 rRNA genes and 140 oligonucleotides for positive and negative controls.

3.9.1 cDNA synthesis

For DNA microarray analysis of *C. glutamicum*, fluorescently labelled cDNA was synthesised from RNA isolated from cells harvested in the exponential growth phase. Fluorescence labelling was performed by using the dUTP analogues Cy3-dUTP ($\lambda_{absorption\ max}$ 550 nm, $\lambda_{fluorescence\ max}$ 570 nm, green, Amersham Biosciences) and Cy5-dUTP ($\lambda_{absorption\ max}$ 649 nm, $\lambda_{fluorescence\ max}$ 670 nm, red, Amersham Biosciences). For cDNA synthesis equal

amounts of isolated RNA samples (20-25 µg) were mixed with 1 µl (500 ng) of pdND6 random hexamer primer (Amersham Biosciences) and filled up to 15 µl with RNase free water. The mixtures were incubated for 10 min at 65°C followed by incubation on ice for 2 min. Afterwards 3 µl of the 1 mM dUTP analogues were added and the reverse transcription of the RNA was performed by adding the following reaction mixture (components obtained from Life Technologies GmbH, Darmstadt, Germany):

First Strand buffer (5x)	6 µl
DTT (0.1 M)	3 µl
dNTPs (25 mM dATP, dCTP, dGTP and 10 mM dTTP)	0.6 µl
Superscript® II (200 U/ml)	2 µl

Reverse transcription was performed at room temperature for 10 min and afterwards for 110 min at 42°C. The cDNA reaction was stopped by adding 10 µl 0.1 N NaOH and incubation for 10 min at 70°C. 10 µl of 0.1 N HCl was added to neutralise the mixture. To remove oligonucleotides and enzyme components and to concentrate the cDNA, ultrafiltration using Microcon YM-30 (Millipore) was performed. The reaction mixtures were transferred to Microcons containing 450 µl RNase-free water and centrifuged for 10 min at room temperature and 16,100 x *g*. The cDNA samples were pooled and the washing step (480 µl RNase-free water) was repeated two times. The concentrated cDNA (10 µl) was directly used for DNA microarray hybridisation.

3.9.2 *C. glutamicum* DNA microarray hybridisation

3.9.2.1 Array pre-hybridisation

To check the spotting and the background the DNA microarray was pre-scanned at wavelengths of 532 nm and 635 nm at 600 PMT with a Genepix^{TM} 4000B Laser Scanner (Axon Instruments). Pre-hybridisation was performed to saturate unspecific binding sites. The SDS-containing OpArray Pre-Hyb solution (Operon Biotechnologies) was heated to 42°C and 50 ml were filtrated with a 0.2 µm syringe filter (Sarstedt) into a 50 ml falcon tube to remove undissolved SDS. The DNA microarray was gently slewed in this solution at 42°C for 1 h. Afterwards the microarray was slewed for 5 min at 37°C in Wash A solution (1.25 ml Wash B, Operon Biotechnologies, 48.75 ml H_2O_{bidest}) and washed twice with water. Subsequently, the slide was transferred to a new falcon tube and dried by centrifugation at

1,300 x *g* for 5 min. To determine the background after pre-hybridisation the slide was scanned at 532 nm and 635 nm at 600 PMT.

3.9.2.2 DNA microarray hybridisation

The concentrated Cy3- and Cy5-labeled cDNA samples (5 µl) were mixed with 50 µl OpArray Hyb Solution (Operon Biotechnologies), denatured at 95°C for 3 min and cooled to 42°C. For hybridisation, a mixer (MAUI®Mixer AO, BioMicro® Systems) was fixed via adhesive strips at the frame to the slide which generates a space between mixer and slide. The denatured cDNA samples were transferred into the fillport of the DNA microarray. To avoid evaporation during the hybridisation the fillports were sealed with adhesive strips. Hybridisation was performed using the pre-heated MAUI® hybridisation system (BioMicro® Systems) for 14-16 h at 42°C.

3.9.2.3 Post-hybridisation

Before starting post-hybridisation of the DNA microarray, Wash 2, 3, and 4 solutions had to be prepared in 50 ml falcon tubes. All washing steps were performed in the dark to avoid damage of the fluorescent dyes. Initially, Wash 2 solution was filtered and heated to 42°C. In Wash 2 solution the DNA microarray was quickly removed from the mixer to avoid drying. The slide was gently slewed in Wash 2 solution for 10 min at 42°C. Afterwards the microarray was slewed in Wash 3 solution for 10 min at 37°C and in Wash 4 solution for 5 min at room temperature. Subsequently, the microarray was quickly transferred to a 50 ml falcon tube and dried by centrifugation at 1,300 x *g* for 5 min. After post-hybridisation, scanning of the DNA microarray was performed using the Genepix™ 4000B Laser Scanner.

Wash 2	5 ml Wash A, 2.5 ml Wash B, 42.5 ml H_2O
Wash 3	5 ml Wash A, 45 ml H_2O
Wash 4	1 ml Wash A, 49 ml H_2O

Wash A and Wash B were ordered from Operon Biotechnologies.

3.9.3 Measurement and analysis of the fluorescence signals

For determination of the relative mRNA level of the samples to be compared, the surface of the DNA microarrays was irradiated with monochromatic light at wavelengths of 532 nm and 635 nm to stimulate the fluorescent dyes Cy3-dUTP and Cy5-dUTP, respectively. The ratio of Cy3- and Cy5- fluorescence correlates to the relative number of mRNA molecules in

the samples and therefore it is a dimension for the relative mRNA level. The emitted fluorescence was registered by light sensitive cathodes at 570 nm (Cy3 fluorescence) and at 670 nm (Cy5 fluorescence) that convert the emitted fluorescence into electrical current, which was further amplified. The determined electric current correlates directly with the Cy3 and Cy5 fluorescence. The fluorescence of each spot was converted to a numerical value and assigned to the appropriate genes of *C. glutamicum* (gene array lists) using the Genepix Pro 6.0 software. The calculation of signal to noise ratios of Cy3- and Cy5-fluorescent signals resulted from the quotient signal intensity$_{spot}$/signal intensity$_{background}$. Fluorescent signals exhibiting a signal to noise ratio less than 3 were not included in the further analysis. The numerical values of the fluorescent signals were normalised by using R-packages limma and marray (http://www.bioconductor.org/). Normalised data were uploaded to an in-house database for further analyses. Genes showing up- or down-regulation (ratio of Cy3/Cy5) less than 2-fold were not considered as “regulated” in the further analysis.

4 Results

4.1 Influence of 2-oxoadipate and adipate on growth parameters of *C. glutamicum*

For an industrial scale production process of 2-oxoadipate and later on of adipate the impact of the intermediates, occurring during the production process, on the host organism is of great interest. In case of *C. glutamicum* adipate is no biological intermediate of the metabolism and thus not characterised concerning toxicity or inhibitory effects. In contrast, 2-oxoadipate occurred naturally in *C. glutamicum* as an intermediate of the tryptophan degradation pathway (Kegg Map 00380). The tricarboxylate homocitrate is structurally related to citrate and occurs naturally not only as an intermediate of the α-aminoadipate pathway but also as a component (organic ligand) of the iron-molybdenum cofactor of nitrogenases in nitrogen fixing bacteria (Durrant *et al.*, 2006). Cultivation experiments to analyse the influence of the available α-aminoadipate pathway intermediates homocitrate and 2-oxoadipate as well as of adipate on growth parameters of *C. glutamicum* were performed. Furthermore, it was investigated whether *C. glutamicum* possesses the ability to metabolise these substances. The remaining intermediates of the AAA pathway were not commercially available and were not tested.

To analyse the growth behaviour of *C. glutamicum* in response to adipate, 2-oxoadipate and homocitrate, the wild-type strain was cultivated in the presence of various concentrations of these substances. The cultivations were performed in medium-scale shake flasks (60 ml medium) and in the micro-scale BioLector cultivation system (750 µl medium). The CGXII minimal medium contained 2% (111 mM) glucose as carbon source and were supplemented with adipate in concentrations of 0 mM (control), 50 mM (7.3 g l^{-1}), 150 mM (21.9 g l^{-1}), 250 mM (36.5 g l^{-1}) and 500 mM (73.1 g l^{-1}) or with 50 mM (8 g l^{-1}) 2-oxoadipate. The pH value of the adipate and 2-oxoadipate solutions was adjusted with NaOH to pH 7 before added to the cultivation media. The main culture was inoculated with *C. glutamicum* wild-type cells to an OD_{600} of 0.5. Growth was observed for 30 h (Fig. 4A). Concentrations of up to 50 mM adipate did not significantly affect the growth of *C. glutamicum* wild-type cells, as similar growth rates of 0.41 ± 0.03 h^{-1} and 0.4 ± 0.02 h^{-1} were observed in the absence and presence of 50 mM adipate. Cultivation in the presence of 250 mM adipate caused a 37% decrease of the growth rate ($\mu = 0.29 \pm 0.002\ h^{-1}$), compared to the control culture, whereas the final OD_{600} was only slightly decreased from 30.1 ± 1.6 to 28.6 ± 2.0. *C. glutamicum* cells cultivated in the presence of 500 mM adipate showed a strong growth defect with a growth rate of 0.08 ± 0.01 $h^{-1}$and reached only 10% of the maximal OD_{600} of the control culture (OD_{600} = 2.96 after 30 h). Cells growing in the presence of 50 mM 2-oxoadipate showed a

similar growth rate ($\mu = 0.37 \pm 0.04\ h^{-1}$) and maximal OD_{600} (32.5 ± 5.8) as the control culture ($\mu = 0.37 \pm 0.03\ h^{-1}$, maximal $OD_{600} = 34.1 \pm 0.7$).

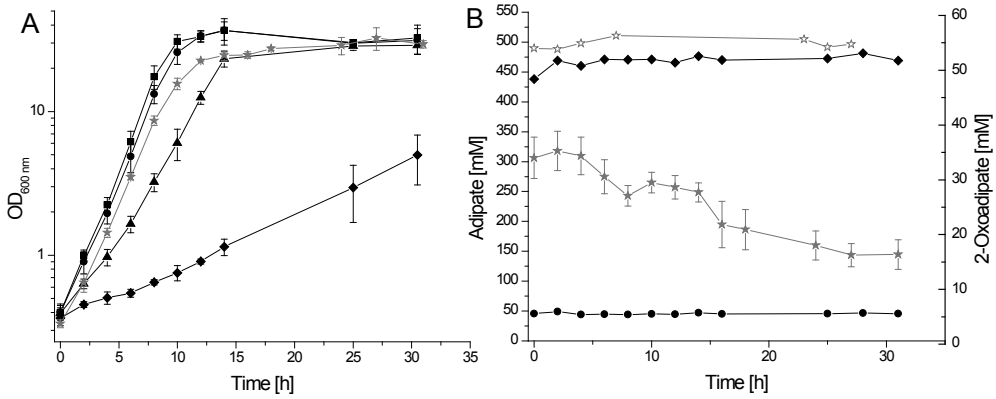

Fig. 4: Growth and concentrations of organic acids during shake flask cultivations in the presence of adipate and 2-oxoadipate. (A) Growth of *C. glutamicum* wild type in CGXII minimal medium with 2% (w/v) glucose and either no supplement (–■–) or supplemented with 50 mM (–●–), 250 mM (–▲–) or 500 mM (–◆–) adipate or with 50 mM 2-oxoadipate (–★–). (B) Concentrations in the supernatant of adipate and 2-oxoadipate in cultures supplemented with either 50 mM (–●–) or 500 mM (–◆–) adipate or with 50 mM 2-oxoadipate (50 mM (–★–). Medium supplemented with 50 mM 2-oxoadipate but without cells was used as a control to check for chemical degradation of this compound (–☆–). Mean values from three independent experiments were shown. HPLC measurements of adipate and 2-oxoadipate in the control culture were performed only in single analyses.

Besides the growth of *C. glutamicum* in the presence of 2-oxoadipate and adipate, the metabolisation of the substances by *C. glutamicum* was tested (Fig. 4B). The quantification of the organic acids was performed by HPLC analysis of the cell-free supernatant of samples taken during the cultivation. No significant concentration changes were detected over 30 h in the cultures containing 50 mM and 500 mM adipate. The determined average of 45.7 mM and 467.9 mM showed a variation of 8.6% and 6.6%, respectively. In contrast 2-oxoadipate continuously decreased over 30 h from 34 ± 3.7 mM to 16 ± 2.7 mM. Surprisingly, only 34 mM 2-oxoadiapte was found at the beginning of the cultivation instead of the expected 50 mM. In the control culture without cells an initial concentration of 54 mM was found, in good agreement with the expectation. An explanation for this could be the immediate binding of 2-oxoadipate to the cells directly after inoculation leading to extraction of 2-oxoadipate from the media. Further it is possible that 2-oxoadipate enters the cell and *C. glutamicum* can metabolise 2-oxoadipate via the tryptophan metabolism to some extent. Since it is reported that 2-oxoadipate can be converted to glutaryl-CoA by 2-oxoglutarate dehydrogenase within the tryptophan metabolism (http://www.genome.jp/kegg-bin/show_pathway?org_name=cgb&

mapno=00380&mapscale=&show_description=hide) this might be a reason for the continuous decrease during cultivation.

Further, the impact of homocitrate, the first intermediate of the AAA pathway, on *C. glutamicum* wild-type cells was tested. Since homocitrate is an expensive substance, cultivation experiments were performed in 750-µl-scale using the BioLector system. In addition, 2-oxoadipate and adipate growth experiments were performed under these conditions. The experiments were done in 48-well plates at 30°C and 1200 rpm. The main culture containing 750 µl CGXII minimal medium with 4% glucose (222 mM) was supplemented with 50 mM of either homocitrate, 2-oxoadipate or adipate and inoculated to an OD_{600} of 1. As controls, cultures containing *C. glutamicum* cells without supplements and media with supplements but without cells were used. Growth was automatically monitored by the BioLector System over 47 h (Fig. 5), measuring the absorption seven times per hour.

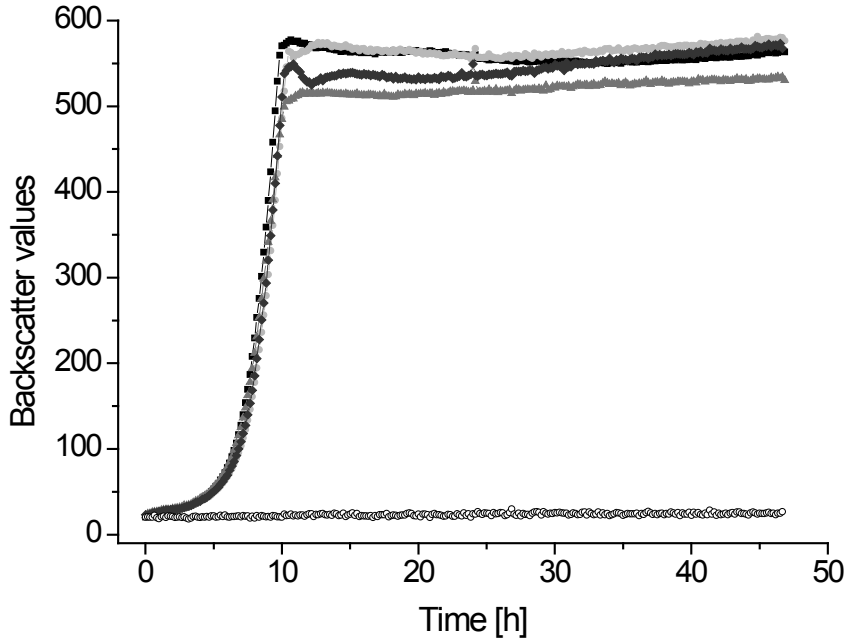

Fig. 5: Growth of *C. glutamicum* wild type in the presence of adipate, 2-oxoadipate and homocitrate in a micro-scale BioLector system. *C. glutamicum* wild type was cultivated in CGXII minimal medium with 4% (w/v) glucose and either no supplement (–■–) or supplemented with 50 mM homocitrate (–●–), 50 mM 2-oxoadipate (–▲–), or 50 mM adipate (–◆–). The control culture containing 50 mM 2-oxoadipate without cells is indicated by (–○–). Data of representative experiments are shown and two independent replicates gave comparable results.

After 0 h, 24 h and 47 h samples were taken to determine the concentrations of the organic acid in the supernatant. The cultivation of *C. glutamicum* in the presence of 2-oxoadipate and adipate under these conditions showed similar results to the experiments in shake flasks: In comparison to the control culture without additives, no growth retardation was observed. The addition of 50 mM homocitrate also revealed no growth inhibition. In contrast to the similar growth rates observed for all tested conditions, a difference in the maximal OD_{600} was observed for the culture supplemented with 50 mM 2-oxoadipate. The cells reached 94% of the maximal OD_{600} compared to supplementation with adipate or homocitrate. The results of the organic acid quantifications in the cell-free culture supernatants revealed constant concentration over 47 h for all three tested metabolites, with and without cells (control) in the culture (Tab. 4), indicating that none of the substances was metabolised by *C. glutamicum* or degraded in the media.

Tab. 4: Concentrations of adipate, 2-oxoadipate and homocitrate during the cultivation of *C. glutamicum* in 750 µl micro scale. Concentrations of homocitrate (HC), 2-oxoadipate (2-OA) and adipate (AA) in the cell free supernatant of the cultivation with and without *C. glutamicum* cells using the BioLector system were determined via HPLC measurements after 0 h, 24 h and 47 h.

	CGXII + additives + *C. glutamicum*			CGXII + additives		
Time	HC [mM]	2-OA [mM]	AA [mM]	HC [mM]	2-OA [mM]	AA [mM]
0	43.0	67.6	48.1	43.6	68.1	49.0
24	44.9	65.9	49.6	44.9	70.6	50.5
47	49.4	66.9	52.7	49.8	71.1	52.2

In the case of 2-oxoadipate this result was unexpected, since the data of the shake flask experiments revealed a continuous decrease to about the half of the initial 2-oxoadipate concentration during growth (Fig. 4). The reason for this difference is not clear yet, however, as all these experiments were performed in triplicate, an experimental error seems unlikely. Possibly, the difference is related to the different cultivation condition. For example, it is know that cultivation in shake flasks leads to oxygen limitation at higher cell densities (Koch-Koerfges *et al.*, 2012), which is probably not the case in the BioLector cultivations.

4.2 Improved growth in the presence of growth-inhibiting adipate concentrations

As shown before, no relevant growth of *C. glutamicum* occurred in the presence of 500 mM adipate when using NaOH to adjust adipate solution to pH 7 (Fig. 6A). To examine a possible inhibitory effect of Na^+ ions, *C. glutamicum* wild-type cells were cultivated in CGXII minimal medium with 4% glucose supplemented with 500 mM adipate, adjusted to pH 7 using KOH instead of NaOH. This condition allowed slow growth of the cells ($\mu = 0.09\ h^{-1}$) and the culture finally reached a similar maximal OD_{600nm} as the control culture ($\mu = 0.41\ h^{-1}$) after 50 h of cultivation (Fig. 6A). In a further control experiment, cells were cultivated in the presence of 500 mM KCl to test adipate-independent osmotic stress. Under these conditions, cells grew with a rate of $0.27\ h^{-1}$, corresponding to a 34% decrease compared to the control culture (Fig. 6A). This result indicates that growth retardation in the presence of 500 mM adipate, neutralised with KOH, is due to the high concentrations of both, adipate and potassium ions.

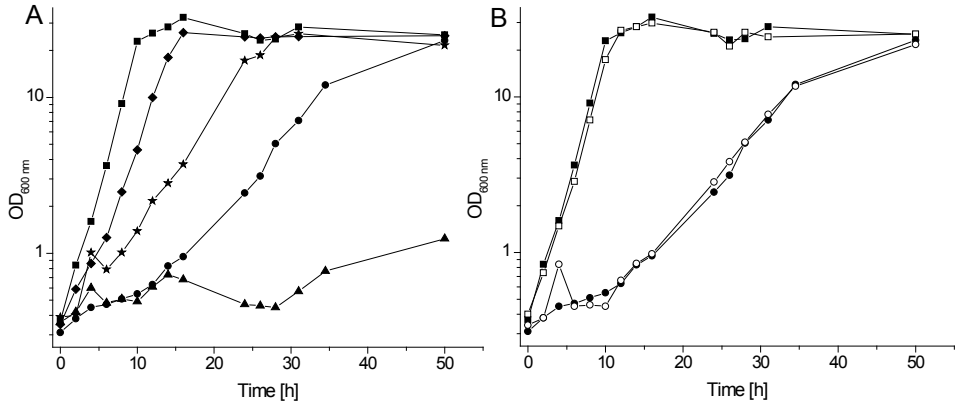

Fig. 6: Studies to test the influence of modified cultivation conditions (A) and the impact of the chromosomal deletions of *dctA* and *dccT* (B) on growth in the presence of adipate. *C. glutamicum* wild type was cultivated in standard CGXII medium without supplements (–■–),with 500 mM KCl (–◆–), with 500 mM adipate adjusted to pH 7 with KOH (–●–), with 500 mM adipate adjusted to pH 7 with NaOH (–▲–), and with 500 mM adipate adjusted to pH 7 with KOH and 5 mM L-proline and 5 mM L-glutamate (–★–). Furthermore, the strain *C. glutamicum* Δ*dctA*Δ*dccT* was cultivated under standard CGXII conditions (–□–) or supplemented with 500 mM adipate adjusted to pH 7 with KOH (–○–). Data were obtained from a single experiment.

Regarding the influence of osmotic stress, it has been previously described that the accumulation of osmoprotective solutes such as betaine, ectoine or proline reduces hyperosmotic stress (Peter *et al.*, 1998). Thus, *C. glutamicum* was cultivated in the presence of 500 mM adipate (pH adjusted with KOH) supplemented with 5 mM proline. Besides proline, 5 mM glutamate was added to analyse a possible inhibitory effect of adipate towards citrate synthase, which is based on the structural similarity of adipate to citrate. Addition of

glutamate prevent a limitation of amino acid supply, which could be caused by inhibition of the citrate synthase (Van Ooyen, 2011). The cultivation in the presence of proline and glutamate resulted in a growth rate of $\mu = 0.16\ h^{-1}$ and thus 44% increase in comparison to the experiment without proline and glutamate supplementation (Fig. 6A).

It was shown above that adipate is not consumed in measurable amounts by *C. glutamicum* during cultivation (Fig. 4B). However, it might be possible that some adipate enters the cell via transport systems and, as it cannot be degraded, it could act inhibitory. Two known possible candidates for adipate import in *C. glutamicum* are the dicarboxylate transporters DctA and DccT. To analyse the influence of the dicarboxylate transporters in adipate uptake, growth of a double deletion mutant of *dctA* and *dccT* (provided by Volker F. Wendisch, University of Muenster) was analysed in the presence of adipate (Youn *et al.*, 2008, Youn *et al.*, 2009). Cultivation of *C. glutamicum* Δ*dctA*Δ*dccT* in CGXII medium with 4% glucose and 500 mM adipate revealed a similar growth rate ($\mu = 0.08\ h^{-1}$) compared to wild type ($\mu = 0.08\ h^{-1}$) cultivated under the same conditions (Fig. 6B). The deletion of both dicarboxylate transporters did not affect growth in the presence of 500 mM adipate.

4.3 Impact of 2-oxoadipate and adipate on global gene expression of *C. glutamicum*

Since it was shown that adipate causes growth retardation of *C. glutamicum*, DNA microarray analyses were performed to determine global gene expression changes in response to the presence of adipate. Furthermore, global gene expression experiments were also carried out in the presence of 2-oxoadipate. To investigate the specific impact of adipate on *C. glutamicum* gene expression, secondary effects such as a reduced growth rate, should be avoided. Therefore, a concentration of 50 mM adipate was selected for the DNA microarray experiments, as this concentration had no significant effect on growth in glucose minimal medium (section 4.1). On the other hand global gene expression in the presence of 150 mM adipate was investigated to gain information about the mechanism how adipate impacts growth (performed by Olga Valdau during her internship in May 2010).

The gene expression in the presence of either adipate or 2-oxoadipate was compared to that of cells grown without these supplements. In contrast to standard cultivation conditions, precultures in CGXII medium with 2% glucose (111 mM) as carbon source and supplemented with either 50 mM adipate or 50 mM 2-oxoadipate were performed to adapt the cells to these conditions. The main culture was carried out under the same conditions and inoculated to an OD_{600} of 0.5 with cells of the preculture at the end of the exponential growth phase. For DNA microarray analyses the cells were harvested in the mid-exponential phase (OD_{600} = 5-6). After RNA isolation, the RNA of both samples was transcribed into fluorescently labelled cDNA, which were then mixed in a 1:1 ratio and hybridised to the DNA microarray. The data of at least two independent replicate experiments were filtered for evaluation. Only genes exhibiting an average mRNA level change of more than two-fold (red fluorescence signal divided by green fluorescence signal) and a signal-to-noise ratio >3 for the red and the green fluorescence signal were considered in the further analysis.

In the presence of 50 mM adipate, the mRNA levels of 23 genes were more than two-fold increased and that of 4 genes were more than two-fold decreased. DNA microarray experiments with cells exposed to 150 mM adipate resulted in 41 genes with increased and 22 genes with decreased mRNA levels. The genes regulated under both conditions are listed in Tables 5 and 6.

Tab. 5: Overview of genes, which showed an increased mRNA level in the presence of adipate. Transcriptome comparison of *C. glutamicum* wild type grown in glucose minimal medium either in the absence or in the presence of 50 mM or 150 mM adipate (AA). Cells were harvested during the mid-exponential growth phase. Genes which fulfil the criteria of an average mRNA ratio (+ adipate/- adipate) of ≥2 in at least two independent experiments, a signal-to-noise ratio >3 for Cy3 or Cy5, and a p-value ≤0.05 in one or both of the comparisons are listed. Genes changed in both comparisons are shaded in grey. Genome annotation, literature and database searches (http://www.coryneregnet.de/ and http://www.genome.jp/kegg/kegg2.html) were performed to assign the function of the corresponding proteins.

Gene	Annotation	mRNA ratio (150 mM AA)	mRNA ratio (50 mM AA)
cg0005	*recF*, recombination protein F	2.01	1.1
cg0340	putative integral membrane transport protein	17.19	13.38
cg0341	*fadD1*, putative fatty-acid-CoA ligase transmembrane protein	38.13	15.91
cg0344	*fabG1*, 3-oxoacyl-(acyl-carrier protein) reductase	27.72	12.61
cg0345	metal-dependent hydrolase of the TIM-barrel fold	19.69	11.62
cg0346	*fadE*, glutaryl-CoA dehydrogenase	16.64	10.49
cg0347	*hdtZ*, 3-hydroxyacyl-thioester dehydratase	18.04	11.64
cg0444	*ramB*, transcriptional regulator, involved in acetate metabolism	3.11	0.92
cg0645	*cytP*, cytochrome P450	3.38	1.22
cg0759	*prpD2*, propionate catabolism protein PRPD	4.20	2.13
cg0760	*prpB2*, probable methylisocitric acid lyase	3.19	2.19
cg0762	*prpC2*, 2-methylcitrate synthase	3.37	2.35
cg0998	trypsin-like serine protease	2.40	1.11
cg1016	*betP*, glycine betaine transporter	2.31	1.4
cg1129	*aroF*, 3-deoxy-7-phosphoheptulonate synthase	2.34	1.14
cg1214	cysteine sulfinate desulfinase/cysteine desulfurase or related enzyme	2.46	1.27
cg1215	*nadC*, nicotinate-nucleotide pyrophosphorylase	2.85	1.43
cg1216	*nadA*, quinolinate synthetase	4.32	1.46
cg1218	ADP-ribose pyrophosphatase	3.52	1.35
cg1224	*phnB2*, similarity to alkylphosphonate uptake operon protein PhnB of *Escherichia coli*	2.24	1.05
cg1226	*pobB*, 4-hydroxybenzoate 3-monooxygenase	3.22	1.07
cg1292	flavin-containing monooxygenase 3	2.70	1.29
cg1616	*cmk*, cytidylate kinase	2.37	1.03
cg2234	ABC-type cobalamin/Fe^{3+}-siderophores transport system, secreted component	2.73	1.09
cg2622	*pcaJ*, β-ketoadipate succinyl-CoA transferase subunit	48.28	10.55
cg2623	*pcaI*, β-ketoadipate succinyl-CoA transferase subunit	85.59	11.96

Gene	Annotation	mRNA ratio (150 mM AA)	mRNA ratio (50 mM AA)
cg2624	*pcaR*, transcriptional regulator of 4-hydroxybenzoate, protocatechuate, p-cresol pathway	33.45	7.82
cg2625	*pcaF*, β-ketoadipyl CoA thiolase	26.59	8.15
cg2626	*pcaD*, β-ketoadipate enol-lactone hydrolase	23.14	7.51
cg2627	*pcaO*, transcriptional regulator of 4-hydroxybenzoate, protocatechuate, p-cresol pathway	4.75	2.39
cg2634	*catC*, muconolactone isomerase	3.82	3.5
cg2635	*catB*, chloromuconate cycloismerase	4.57	3.86
cg2636	*catA1*, catechol 1,2-dioxygenase	15.30	5.70
cg2637	*benA*, benzoate 1,2-dioxygenase alpha subunit (aromatic ring hydroxylation dioxygenase A)	22.22	13.43
cg2638	*benB*, benzoate dioxygenase small subunit	15.08	13.42
cg2642	*benK1*, putative benzoate transport protein	5.87	3.72
cg2888	*phoR*, two component response regulator	2.89	0.98
cg3240	permease of the major facilitator superfamily	6.69	3.80
cg3335	*malE*, malic enzyme	3.01	2.40
cg3389	*oxiC*, myo-inositol dehydrogenase	3.24	1.10
cg3395	*proP*, proline/ectoine carrier	2.72	1.38

Tab. 5 shows several genes with increased mRNA level regulated under both, 50 mM and 150 mM adipate. The data of the global gene expression experiments revealed increased mRNA levels for several genes involved in the metabolism of the aromatic compounds benzoate and protocatechuate. Changes of mRNA levels of genes belonging to the *ben* operon (*benA*, *benB*, *benK1*) or to the *cat* operon (*catA1*, *catB*, *catC*) were observed. With exception of *catA1* and *benB* (15-fold increased mRNA levels), the other genes showed only slightly changed mRNA levels (3-5-fold). Enzymes of the *ben* operon are involved in benzoate degradation to catechol, whereas enzymes of the *cat* operon are part of the catechol branch of the β-ketoadipate pathway (Brinkrolf *et al.*, 2006). The highest mRNA level change (up to 85-fold) was observed for genes (*pcaIJFDO*) of the *pca* operon, which is part of the protocatechuate branch of the β-ketoadipate pathway in *C. glutamicum* (Brinkrolf *et al.*, 2006). Interestingly, mRNA levels of both regulator genes of the *pca* gene cluster were also increased, namely *pcaR* (33-fold) and *pcaO* (5-fold). Adipate might act as an activator molecule of PcaR and PcaO.

Further, several genes belonging to the fatty acid metabolism were highly up-regulated in the presence of adipate: the four genes *fabG1*, cg0345, *fadE*, *hdtZ* of the predicted operon

OP_cg0344 as well as cg0340 and *fadD1* revealed elevated mRNA levels of 10-fold and 20-fold due to the addition of 50 mM and 150 mM adipate, respectively (Tab. 5). These results indicate that adipate is involved in gene regulation of fatty acid metabolism, maybe by its structural similarity to fatty acids. The mRNA levels of genes of the *prp2* operon (*prpB2*, *prpC2*, *prpD2*), which are involved in the propionate catabolism, were two-fold increased in the presence of 50 mM and three to four-fold increased in the presence of 150 mM adipate. Further, in response to 150 mM adipate genes involved in the stress response of *C. glutamicum* displayed increased mRNA levels: The genes *proP* (2.7-fold) and *betP* (2.3-fold), which encode osmoregulatory proteins (ProP and BetP), obtained slightly elevated mRNA levels in the presence of 150 mM adipate. Both proteins function as osmoregulated secondary transporter systems for compatible solutes and were described to be beneficial for *C. glutamicum* to cope with hyperosmotic stress conditions (Peter *et al.*, 1998).

Table 6 shows the genes with decreased mRNA levels in the presence of 50 mM and 150 mM adipate. Only two genes were found to have a decreased mRNA level at both, 50 mM and 150 mM adipate (Tab. 6), which are cg1384 coding for putative NUDIX hydrolase and cg3405 coding for an NADPH quinone reductase or Zn-dependent oxidoreductase. The latter one seems to be down regulated as a stress response of *C. glutamicum* in the presence of adipate, since it is associated in the global stress response of *C. glutamicum* (Busche *et al.*, 2012). In the presence of 150 mM adipate several genes of central metabolism enzymes showed decreased mRNA levels: the mRNA levels of *pyk* (8.9-fold) and *ldh* (7.7-fold), coding for pyruvate kinase and lactate dehydrogenase, respectively, were strongly decreased. Furthermore, the genes *mdh* (2.9-fold) coding for malate dehydrogenase and *ackA* (2.4-fold) coding for acetate kinase showed a reduced expression level. A 2.3-fold reduced mRNA level was observed for *ramA*, coding for global regulator of metabolism in *C. glutamicum* (Auchter *et al.*, 2011). Since down-regulation of these genes occurred only in the presence of 150 mM adipate, a stress-related response seems to be the most likely explanation for these results.

In the presence of 50 mM adipate, the mRNA level of the gene *dctA* coding for a Na^+/H^+ dicarboxylate symporter (Youn *et al.*, 2009), was 2.1-fold decreased. Besides *dctA*, the mRNA level of the second dicarboxylate uptake system in *C. glutamicum* (DccT) was also decreased (1.9-fold). Both, DctA and DccT are known to enable *C. glutamicum* to grow on the TCA cycle intermediates succinate, fumarate and malate as sole carbon source. Since the native expression levels of *dctA* or *dccT* are not sufficient to allow growth on these dicarboxylates as sole carbon source in minimal medium, (high) plasmid-borne expression

levels of *dctA* or *dccT* or promoter up-mutations are required (Youn *et al.*, 2008, Youn *et al.*, 2009).

Tab. 6: Overview of genes exhibiting decreased mRNA levels in the presence of adipate. Transcriptome comparison of *C. glutamicum* wild type grown in glucose minimal medium either in the absence or in the presence of 50 mM or 150 mM adipate (AA). Cells were harvested during the mid-exponential growth phase. Genes which fulfil the criteria of an average mRNA ratio (+ adipate/- adipate) of ≤ 2 in at least two independent experiments, a signal-to-noise ratio >3 for Cy3 or Cy5, and a p-value ≤0.05 in one or both of the comparisons are listed. The genes showing altered expression in both comparisons are shaded in grey. Genome annotation, literature and database searches (http://www.coryneregnet.de/ and http://www.genome.jp/kegg/kegg2.html) were performed to assign the function of the corresponding proteins.

Gene	Annotation	Average ratio (150 mM AA)	Average ratio (50 mM AA)
cg0238	L-gulonolactone oxidase	0.46	1.03
cg0260	*moaC*, molybdenum cofactor biosynthesis protein C	0.44	0.97
cg0277	*dccT*, dicarboxylate uptake system (succinate, fumarate or L-malate)	0.52	0.51
cg1384	putative NUDIX hydrolase	0.35	0.49
cg1647	ABC-type multidrug transport system, permease component	0.30	0.96
cg1744	*pacL*, cation-transporting ATPase	0.28	0.85
cg1769	*ctaA*, cytochrome oxidase assembly protein	0.31	1.05
cg2030	hypothetical protein predicted by Glimmer	0.63	0.45
cg2114	*lexA*, LexA repressor	0.39	0.97
cg2613	*mdh*, malate dehydrogenase	0.34	0.99
cg2831	*ramA*, transcriptional regulator, acetate metabolism	0.44	0.91
cg2845	*pstC*, ABC-type phosphate transport system, permease component	0.26	1.06
cg2846	*pstS*, ABC-type phosphate transport system, secreted component	0.10	1.02
cg2870	*dctA*, Na+/H+-dicarboxylate symporter	0.78	0.47
cg3047	*ackA*, acetate/propionate kinase	0.40	0.62
cg3099	*grpE*, molecular chaperone GrpE (heat shock protein)	0.31	0.8
cg3100	*dnaK*, molecular chaperone DnaK	0.39	1.02
cg3107	*adhA*, Zn-dependent alcohol dehydrogenase	0.39	0.75
cg3218	*pyk*, pyruvate kinase	0.11	0.87
cg3219	*ldh*, L-lactate dehydrogenase	0.13	1.23
cg3227	*lldD*, quinone-dependent L-lactate dehydrogenase LldD	0.21	0.88
cg3255	*uspA3*, universal stress protein family	0.35	1.03
cg3367	ABC-type multidrug transport system, ATPase component	0.28	0.86
cg3368	ABC-transporter permease protein	0.28	0.93
cg3405	NADPH quinone reductase or Zn-dependent oxidoreductase	0.09	0.08

As mentioned above, transcriptome analyses of *C. glutamicum* wild type were also performed with RNA from cells grown in the presence and absence of 50 mM 2-oxoadipate (Tab. 7). With such RNA samples also one experiment was performed by Nadine Dobler using an Agilent tiling array to test something else, however, the results can be additionally used here. The results of the data analyses showed up to 5-fold increased mRNA levels of the genes *hemL*, cg0519, cg0520, *ccsA*, cg0523 and *ccsB* belonging to the predicted operon OP_cg0516. This operon is described to be involved in metal homeostasis. Further, mRNA level changes (up to 10-fold increased) of genes, which are part of the metal homeostasis in *C. glutamicum*, were observed for components of an ABC-type cobalamin/Fe^{3+}-siderophore transport system. In only one of the experiments the genes *benA* (2.8-fold) and *benB* (3.8-fold) coding for subunits of benzoate 1,2-dioxygenase showed elevated mRNA levels (Tab. 7). Both genes showed also increased mRNA levels in the presence of adipate (Tab. 5). Among the regulated genes in response to 50 mM 2-oxoadipate, no one was identified, which could be directly linked to the possible metabolisation of 2-oxoadipate observed in the cultivation experiments described above.

Tab. 7: Overview of genes exhibiting altered mRNA levels in the presence of 2-oxoadipate. Transcriptome comparison of *C. glutamicum* wild type grown in glucose minimal medium either in the absence or in the presence of 50 mM 2-oxoadipate. Cells were harvested during the mid-exponential growth phase. Genes which fulfil the criteria of an mRNA ratio (+ 2-oxoadipate/- 2-oxoadipate) of ≤ 2 or ≥2 in at least one of three independent experiments, a signal-to-noise ratio >3 for Cy3 or Cy5, and a p-value ≤0.05 are listed. Two experiments (Array I and II) were performed using a standard microarray (Operon Biotechnology) and one experiment was performed with a tilling array (TA). Genome annotation, literature and database searches (http://www.coryneregnet.de/ and http://www.genome.jp/kegg/kegg2.html) were performed to assign the function of the corresponding proteins.

Gene	Annotation	mRNA ratio Array I	mRNA ratio Array II	mRNA ratio TA	Average
cg0518	*hemL*, glutamate-1-semialdehyde aminotransferase	3.76	1.84	4.45	3.35
cg0519	putative phosphoglycerate mutase	2.97	1.80	3.90	2.89
cg0520	secreted thiol-disulfide isomerase or thioredoxin	n.d	1.59	4.00	2.79
cg0522	*ccsA*, cytochrome *c* biogenesis protein transmembrane protein	4.61	2.03	4.37	3.67
cg0523	membrane protein required for cytochrome *c* biosynthesis	5.05	2.42	4.09	3.85
cg0524	*ccsB*, cytochrome *c* assembly membrane protein	n.d	1.56	4.25	2.91
cg0569	cation-transporting ATPase	0.68	0.40	0.63	0.57

Gene	Annotation	mRNA ratio Array I	mRNA ratio Array II	mRNA ratio TA	Average
cg1494	putative secreted protein	0.50	0.49	n.d	0.49
cg1551	*uspA1*, universal stress protein UspA and related nucleotide-binding proteins	0.67	0.44	0.88	0.66
cg1832	ABC-type cobalamin/Fe3+-siderophores transport system, permease component	11.50	3.32	9.77	8.20
cg1833	ABC-type cobalamin/Fe3+-siderophores transport system, secreted component	12.98	4.31	12.93	10.07
cg2637	*benA*, benzoate 1,2-dioxygenase alpha subunit (aromatic ring hydroxylation dioxygenase A)	n.d	2.77	n.d	2.77
cg2638	*benB*, benzoate dioxygenase small subunit	n.d	3.79	n.d	3.79
cg3240	permease of the major facilitator superfamily	2.65	2.68	1.88	2.40

4.4 Selection of enzymes for the conversion of 2-oxoglutarate to 2-oxoadipate

The main focus of this work was to introduce the enzymes of the α-aminoadipate (AAA) pathway necessary for 2-oxoadipate production into *C. glutamicum* in order to produce 2-oxoadipate as precursor of adipate. In a first step, enzyme characteristics were analysed based on literature and databases (http://www.brenda-enzymes.info) especially regarding their substrate affinity and turnover number (Tab. 8). Additional selection criteria were the knowledge of the corresponding gene sequences as well as experimental experience in expressing the homocitrate synthase (HCS) gene in a heterologous host organism. The HCS enzymes of *Thermus thermophilus* (Wulandari *et al.*, 2002), *Azotobacter vinelandii* (Zheng *et al.*, 1997) and *S. cerevisiae* (Andi *et al.*, 2004) with the corresponding genes *ttc1550*, *nifV*, *lys20* were selected for heterologous expression in *C. glutamicum*. *T. thermophilus* is an extremely thermophilic, Gram-negative bacterium containing as an interesting feature an AAA-like pathway for the biosynthesis of L-lysine (Andi *et al.*, 2004). The Gram-negative bacterium *A. vinelandii* is an aerobic model organism, which is capable of fixing molecular nitrogen and thus playing an important role in the nitrogen cycle of the nature (Hamilton *et al.*, 2011). HCS of *A. vinelandii* is not required for lysine formation, but for synthesis of homocitrate, which is required as organic constituent of the FeMo cofactor (Zheng *et al.*, 1997). The gene *lys20* coding for HCS of *S. cerevisiae* was the only one selected from a

eukaryotic organism, as it represent the best characterised enzyme among the homocitrate synthases.

The gene *lys4* coding for homoaconitase (HA), also known as homoaconitate hydratase, was selected from *S. cerevisiae*. At the beginning of this project little was known about enzyme characteristics and mechanism, except its membership to the aconitase superfamily. Recently it was reported that the homoaconitase of *S. cerevisiae* only catalyses the hydration of homoaconitate to homoisocitrate, but not the dehydration of homocitrate to homoaconitate (Fazius *et al.*, 2012). For the conversion of homoisocitrate to 2-oxoadipate the homoisocitrate dehydrogenase (HICDH) with the corresponding gene *lys12* was used from *S. cerevisiae*.

Tab. 8: Characteristics of the enzymes selected for establishment of 2-oxoadipate production in *C. glutamicum*. Homocitrate synthase (HCS) was chosen from *T. thermophilus* (Okada *et al.*, 2010), *A. vinelandii* (Zheng *et al.*, 1997) and *S. cerevisiae* (Andi *et al.*, 2004). Homoaconitase (HA) and homoisocitrate dehydrogenase (HICDH) were selected from *S. cerevisiae* (Yamamoto *et al.*, 2007). N.a., value was not available in literature.

Enzyme (gene)	Organism	Substrate 1 (S1)	Substrate 2 or cofactor	Spec. activity (mU/mg)	K_M (mM) (S1)	k_{cat} (s^{-1}) (S1)
HCS (*ttc1550*)	*T. thermophilus*	2-Oxoglutarate	Acetyl-CoA	41 (50°C)	0.0054 (50°C)	0.18 (50°C)
HCS (*nifV*)	*A. vinelandii*	2-Oxoglutarate	Acetyl-CoA	657	2.24	n.a
HCS (*lys20*)	*S. cerevisiae*	2-Oxoglutarate	Acetyl-CoA	730	4.6	0.62
HA (*lys4*)	*S. cerevisiae*	Homocitrate	n.a	n.a	n.a	n.a
HICDH (*lys12*)	*S. cerevisiae*	Homoisocitrate	NAD^+	n.a	0.018	17

4.5 Homocitrate production with *C. glutamicum*

The aim of this project was to show the feasibility of *C. glutamicum* for the production of homocitrate and 2-oxoadipate with the use of the selected enzymes (Tab. 8). For homocitrate production, HCS activity was introduced into *C. glutamicum* by plasmid-based expression as well as chromosomal integration of the HCS genes. To establish HCS activity in *C. glutamicum*, each of the genes *ttc1550*, *nifV* and *lys20* were cloned into the vector pEKEx2 with the ribosomal binding site GAAAGGAGG for *C. glutamicum* located 8 bp in front of the start codon. Gene expression was controlled by the P_{tac} promoter already present in pEKEx2. *C. glutamicum* wild-type cells were transformed with one of the constructs, resulting in the strains *C. glutamicum*/pEKEx2-*ttc1550*, *C. glutamicum*/pEKEx2-*nifV* and *C. glutamicum*/pEKEx2-*lys20* (Fig. 7).

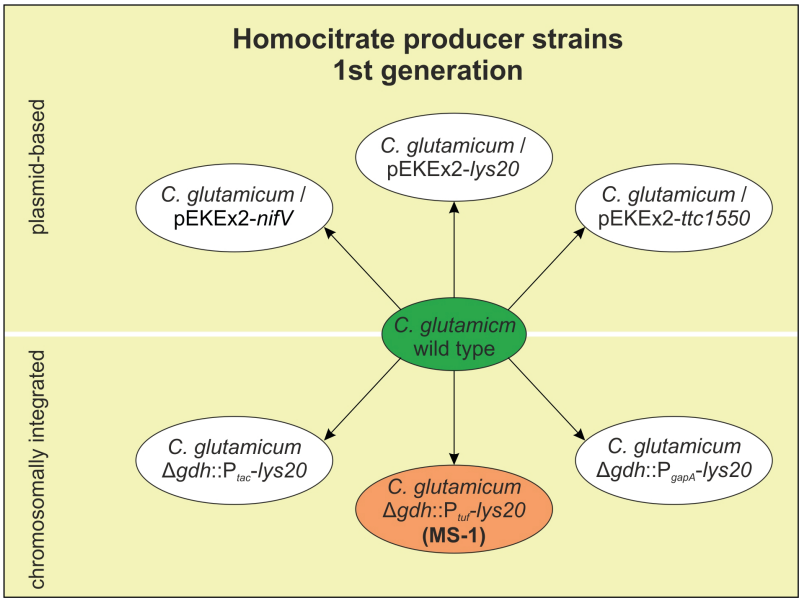

Fig. 7: Schematic overview of first generation homocitrate producer strains originating from the *C. glutamicum* wild-type strain. For plasmid-based expression of the homocitrate synthases the genes *lys20* (*S. cerevisiae*), *ttc1550* (*T. thermophilus*) and *nifV* (*A. vinelandii*) were cloned into the vector pEKEx2. Plasmid-free expression was established by in-frame deletion of *gdh* encoding glutamate dehydrogenase and simultaneous integration of *lys20* either under control of the promoter P_{tuf}, P_{gapA} or P_{tac}.

Besides the plasmid-based introduction of the HCS genes, chromosomal integration of *lys20* was also tested. The benefits of plasmid-free production are the avoidance of selection markers, e.g. antibiotics, plasmid-borne expression stress and plasmid instability. Thus, for the chromosomal establishment of the relevant genes, suitable integration loci were selected and tested. Recently it was shown, that the disruption of the genes *gdh* and *aceA*, coding for glutamate dehydrogenase and isocitrate lyase in *C. glutamicum*, enhance the production of

2-oxoglutarate up to 12 g l^{-1} by directing the carbon flux from isocitrate to 2-oxoglutarate (Jo *et al.*, 2012). Both enzymes are involved in pathways competing with 2-oxoglutarate (Fig. 11): *gdh* represents the key enzyme in the conversion of 2-oxoglutarate to L-glutamate and the deletion of *aceA* leads to the blocking of the glyoxylate cycle. In case of *aceA* it has to be mentioned that the glyoxylate shunt is only active under acetate overflow metabolism, but not under aerobic growth on glucose (Wendisch *et al.*, 1997). Since 2-oxoglutarate is the direct precursor for homocitrate, deletion of both genes should promote enhanced precursor supply for homocitrate and later on for 2-oxoadipate production.

The gene *lys20* of *S. cerevisiae* was selected to establish plasmid-free HCS activity. In-frame deletion of *gdh* with simultaneous integration of *lys20* under the control of either the P_{tac}, P_{gapA} or P_{tuf} promoter was tested. P_{gapA} and P_{tuf} are native promoters of *C. glutamicum* controlling the expression of the genes for glyceraldehyde-3-phosphate dehydrogenase and of the elongation factor TU, respectively. The synthetic promoter P_{tac} is derived from sequences of the *lac* and *trp* promoter of *E. coli* (de Boer *et al.*, 1983). Deletion of *gdh* and simultaneous integration of *lys20* in *C. glutamicum* wild type was performed via homologous recombination using the suicide vector pK19*mobsacB* (section 3.5.10). All three variants were successfully constructed, resulting in the strains *C. glutamicum* Δ*gdh*::P_{tuf}-*lys20*, *C. glutamicum* Δ*gdh*::P_{gapA}-*lys20* and *C. glutamicum* Δ*gdh*::P_{tac}-*lys20* (Fig. 7). To characterise the strains with respect to homocitrate production, cultivation experiments in standard CGXII minimal medium with 4% (w/v) glucose as sole carbon source were carried out. Samples of the cultures were taken over 72 h. The identification and quantification of extracellular metabolites was performed via HPLC measurements. The HPLC method for quantification was established by using external standards of the substances. In addition to the HPLC measurements, qualitative analyses using GC-ToF-MS measurements were performed to verify the identity of homocitrate and 2-oxoadipate as well as to identify accumulated by-products.

Growth of the homocitrate producer strains was compared to a control culture of *C. glutamicum* wild-type cells (Fig. 8A, B). The growth rate of *C. glutamicum*/pEKEx2-*ttc1550* ($\mu = 0.37 \pm 0.01$ h^{-1}) was very similar to that of the control culture (0.39 ± 0.01 h^{-1}), whereas the growth rate of *C. glutamicum*/pEKEx2-*lys20* ($\mu=0.30 \pm 0.01$ h^{-1}) revealed a 30% decreased growth rate. Further, it was noticed that the maximum OD_{600} of the producer strains (OD_{600} = 40) was about 23% lowered in comparison to the wild-type strain (OD_{600} = 52), indicating that available carbon is not completely utilised for cell growth. In accordance with the results of the growth, the strain *C. glutamicum*/pEKEx2-*lys20* showed a slightly slower

glucose uptake (consumption within 14 h), compared to the strains *C. glutamicum* wild type and *C. glutamicum*/pEKEx2-*ttc1550* (consumption within 12 h) (Fig. 8C). In comparison to the wild-type strain ($\mu = 0.39 \pm 0.01$ h^{-1}) and also to the plasmid-based strain *C. glutamicum*/pEKEx2-*lys20* ($\mu = 0.3 \pm 0.01$ h^{-1}), the three plasmid-free strains showed a strong growth retardation (Fig. 8B), most likely in consequence of the *gdh*-knock out.

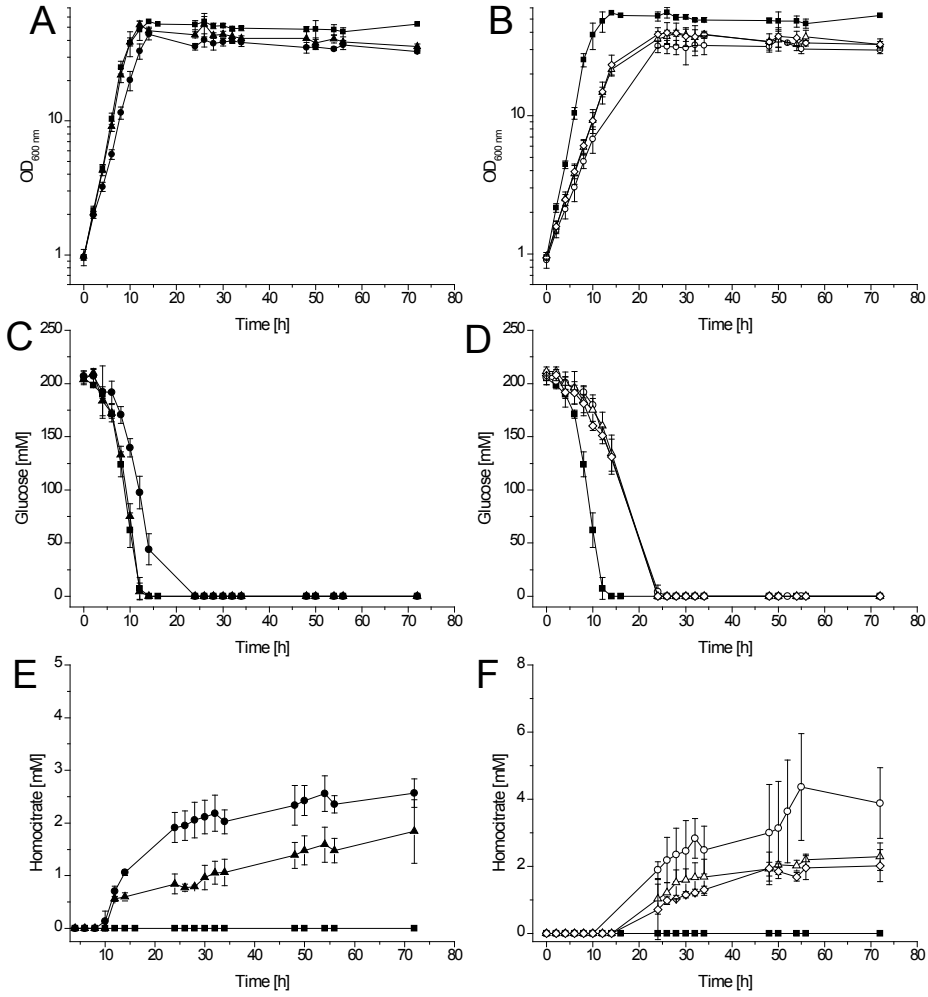

Fig. 8: Analyses of homocitrate production by plasmid-based (A, C, E) and chromosomal (B, D, F) expression of HCS genes under standard conditions. Growth (A, B), glucose consumption (C, D), and accumulation of homocitrate (E, F) of the strains *C. glutamicum* wild type (–■–), *C. glutamicum* pEKEx2-*lys20* (–●–), *C. glutamicum* pEKEx2-*ttc1550* (–▲–), *C. glutamicum* Δ*gdh*::P_{tuf}-*lys20* (–○–), *C. glutamicum* Δ*gdh*::P_{gapA}-*lys20* (–△–) and *C. glutamicum* Δ*gdh*::P_{tac}-*lys20* (–◇–). The curves shown here are mean values including standard deviation of three independent cultivation experiments.

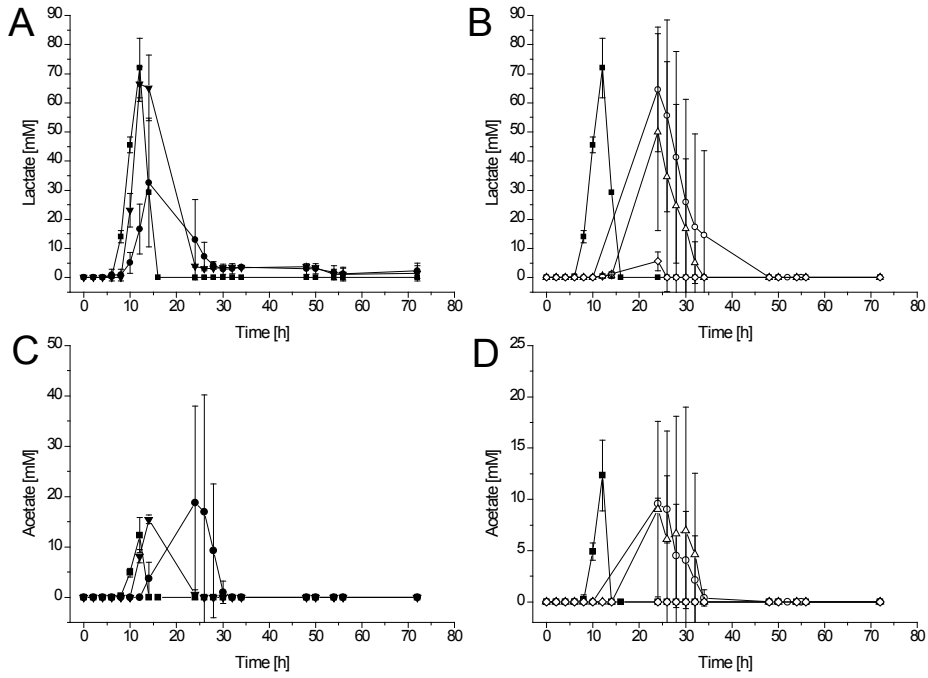

Fig. 9: Analyses of lactate (A, B) and acetate (C, D) formation during cultivation of homocitrate producer strains. Lactate and acetate accumulation of the strains *C. glutamicum* wild type (–■–), *C. glutamicum* pEKEx2-*lys20* (–●–), *C. glutamicum* pEKEx2-*ttc1550* (–▲–), *C. glutamicum* Δ*gdh*::P_{tuf}-*lys20* (–○–), *C. glutamicum* Δ*gdh*::P_{gapA}-*lys20* (–△–) and *C. glutamicum* Δ*gdh*::P_{tac}-*lys20* (–◇–) was observed under standard conditions. The curves shown here are mean values including standard deviation of three independent cultivation experiments.

The growth rates of the plasmid-free strains were determined to be 0.22 h^{-1} for *C. glutamicum* Δ*gdh*::P_{gapA}-*lys20* as well as *C. glutamicum* Δ*gdh*::P_{tac}-*lys20*, and 0.18 ± 0.02 h^{-1} for *C. glutamicum* Δ*gdh*::P_{tuf}-*lys20*, which represents a decrease of about 30% compared to *C. glutamicum*/pEKEx2-*lys20* . Also, decelerated glucose consumption was observed (Fig. 8D). The glucose uptake rates of the two faster growing strains were 6.0 mmol g_{cdw}^{-1} h^{-1}, whereas 4.84 ± 0.4 mmol g_{cdw}^{-1} $h^{-1}$was calculated for *C. glutamicum* Δ*gdh*::P_{tuf}-lys20, compared to 8.1 mmol g_{cdw}^{-1} $h^{-1}$for *C. glutamicum*/pEKEx-*lys20*.

Besides glucose, the cell culture supernatant was analysed towards accumulated metabolites, especially towards homocitrate. After 72 h the strains *C. glutamicum* pEKEx2-*lys20* and *C. glutamicum*/pEKEx2-*ttc1550* accumulated up to 2.6 mM homocitrate (HC) with a yield of 0.009 mol C_{HC}/mol $C_{glucose}$ and 1.8 mM homocitrate corresponding to 0.006 mol C_{HC}/mol $C_{glucose}$, respectively (Fig. 8E), whereas no homocitrate could be detected at all by the strain containing the HCS of *A. vinelandii* (data not shown). The carbon yield was calculated based on the amount of glucose consumed during the cultivation. Cultivation of the

negative controls *C. glutamicum* wild type and *C. glutamicum*/pEKEx2 (data not shown) exhibited no homocitrate accumulation. Homocitrate accumulation was also observed for all three strains harbouring a chromosomally integrated gene of the HCS (Fig. 8F, Tab. 9). After 72 h, the strain containing the *lys20* gene controlled by the P_{tuf} promoter showed the highest accumulation with a final titer of 4.1 mM, corresponding to a yield of 0.014 mol C_{HC}/ mol $C_{glucose}$. This corresponds to a doubled production yield compared to the plasmid-based strain cultivated under the same conditions. At the same time, the strains *C. glutamicum* Δ*gdh*::P_{gapA}-*lys20* and *C. glutamicum* Δ*gdh*::P_{tac}-*lys20* produced up to 2.3 mM and 2 mM homocitrate (0.007 mol C_{HC}/ mol $C_{glucose}$), respectively. The most promising strain *C. glutamicum* Δ*gdh*::P_{tuf}-*lys20* was chosen for further experiments and renamed *C. glutamicum* MS-1 (Fig. 7). It is worthwhile to notice that extracellular accumulation of homocitrate was first detectable after about 10-12 h. At this time point glucose as required carbon source was almost completely consumed indicating that homocitrate production seems to be somehow coupled to the stationary growth phase or the metabolic state of growth-limited cells.

Further analyses of the cell culture supernatant revealed accumulation of the homocitrate precursor 2-oxoglutarate. Surprisingly, also 2-hydroxyglutarate was accumulated in the cell culture supernatant of the homocitrate producers (Tab. 9). Both metabolites were not detected in the control culture. Since no enzyme reaction for the formation of 2-hydroxyglutarate is described in *C. glutamicum*, it seems feasible that 2-oxoglutarate serves as substrate for an uncharacterised dehydrogenase activity. Due to extensive overlapping of HPLC signals of 2-hydroxyglutarate and 2-oxoglutarate an appropriate quantification was not possible (section 4.6.3). At the beginning of the stationary growth phase when glucose was almost completely consumed, accumulation of lactate (Fig. 9G, H) and acetate (Fig. 9I, J) was observed. All tested strains showed high accumulation of lactate (30 – 70 mM), whereas acetate was accumulated up to 12 mM during the cultivation. An exception was *C. glutamicum* Δ*gdh*::P_{tac}-*lys20* which accumulated only 5 mM lactate and no acetate. In further course of the cultivation acetate and lactate were completely consumed again. In summary, this was the first time homocitrate production was demonstrated with *C. glutamicum*. This formed the basis for the improvement of homocitrate production as well as the establishment of 2-oxoadipate production in *C. glutamicum*.

Tab. 9: Growth parameters and product formation of plasmid-based and plasmid-free homocitrate production with *C. glutamicum*. The *C. glutamicum* strains were cultivated in standard CGXII minimal medium with 4% (w/v) glucose. The final titers of the products were determined after 72 h. Product concentrations were determined via HPLC measurements of the cell-free supernatants. Product titers of 2-oxoglutarate and 2-hydroxyglutarate could not be determined (n.d.) via the HPLC measurements.

C. glutamicum strains	Growth rate [h^{-1}]	Biomass [g_{cdw}^{-1} h^{-1}]	Glucose uptake rate [mmol g_{cdw}^{-1} h^{-1}]	Final homocitrate titer [mM]	2-OG + 2-HG [mAU*s]
pEKEx2-*lys20*	0.30 ± 0.01	8.2 ± 0.2	8.1 ± 0.1	2.6 ± 0.3	2,801
pEKEx2-*ttc1550*	0.37 ± 0.01	9.0 ± 0.4	9.1 ± 0.6	1.8 ± 0.6	715
Δ*gdh*::P_{tuf}-*lys20*	0.18 ± 0.02	7.4 ± 0.4	4.8 ± 0.5	4.1 ± 1.4	2,134
Δ*gdh*::P_{gapA}-*lys20*	0.22 ± 0.003	8.1 ± 0.4	6.0 ± 0.4	2.3 ± 0.4	1,277
Δ*gdh*::P_{tac}-*lys20*	0.22 ± 0.009	8.2 ± 0.8	6.0 ± 0.7	2.0 ± 0.5	730

4.6 Enhancement of homocitrate production

4.6.1 Influence of modified cultivation conditions

Recently, it was shown that limitation of the nitrogen supply during the cultivation of *C. glutamicum* is also beneficial for succinate production. This limitation bypasses a part of the carbon from biomass production to product formation and results in a lower OD (Litsanov *et al.*, 2012a). To test the effect of nitrogen limitation on homocitrate production, the corresponding *C. glutamicum* strains were cultivated in CGXII minimal medium with 222 mM glucose as sole carbon source and under limited nitrogen conditions (Tab. 9). Nitrogen supply was limited by omitting ammonium sulfate from the standard medium and reducing urea from 5 g l^{-1} to 1.67 g l^{-1}. The applied amount of nitrogen (59.6 mM corresponding to 6.7% of standard nitrogen amount) was calculated to limit the cell growth at an OD of 30. The homocitrate producer strains *C. glutamicum*/pEKEx2-*ttc1550* (μ = 0.27 ± 0.005 h^{-1}) and *C. glutamicum*/ pEKEx2-*lys20* (μ = 0.24 ± 0.01 h^{-1}) as well as the wild-type strain (μ = 0.3 ± 0.03 h^{-1}) showed reduced growth rates of 20-27% under nitrogen limitation (Fig. 10A). In addition, decelerated glucose consumption was observed for all strains (Fig. 10C). Glucose was consumed within 26 h by the wild-type strain, whereas the homocitrate producers depleted the glucose within 34 h. Determination of homocitrate production under nitrogen limitation revealed a positive effect of the final product titers (Fig. 10E). The homocitrate production was increased up to 8.2 mM with *C. glutamicum*/pEKEx2-*lys20* and up to 7 mM with *C. glutamicum*/pEKEx2-*ttc1550*, corresponding to yields of 0.03 and 0.02 mol C_{HC}/mol $C_{glucose}$, respectively. The homocitrate production under nitrogen limitation

was also detectable only after 10 h as under nitrogen excess conditions, but homocitrate accumulates constantly for 50 h instead of 30 h. This effect can be explained by glucose availability over a longer period of time in consequence of limited and slowed growth.

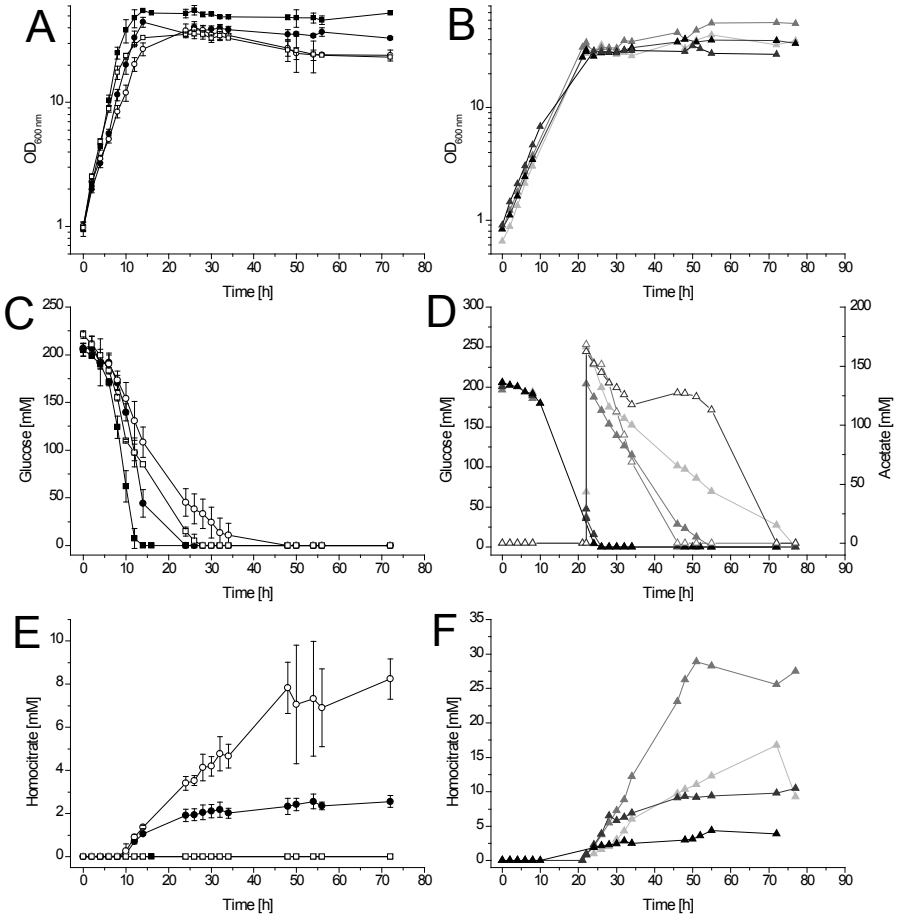

Fig. 10: Homocitrate production with *C. glutamicum* under standard and modified cultivation conditions. Growth (A), glucose consumption (C), and formation of homocitrate (E) of the strains *C. glutamicum* wild type (–■–/–□–) and *C. glutamicum*/pEKEx2-*lys20* (–●–/–○–) were tested in CGXII medium with 222 mM glucose under nitrogen excess (892 mM N, filled symbols) and nitrogen limitation (59.6 mM N, open symbols). Mean values and standard deviations of three independent experiments are shown. Further growth (B), glucose (D, filled symbols) and acetate consumption (D, open symbols), and formation of homocitrate (F) of the strain *C. glutamicum* MS-1 was analysed in "fed-batch" cultivation experiments. Cultivation was performed in GCXII medium with 222 mM glucose as starting carbon source (–▲–/–△–), at the beginning of the stationary growth phase 222 mM glucose (–▲–), 204 mM potassium acetate (–▲–) and 222 mM glucose + 204 mM potassium acetate (–▲–) were added. Data represent a single experiment.

Tab. 10: Growth parameters and product formation of plasmid-based and plasmid-free homocitrate production with *C. glutamicum* under nitrogen excess and nitrogen limitation. The *C. glutamicum* homocitrate producer strains were cultivated in standard CGXII medium with 4% (w/v) glucose under nitrogen excess (892 mM N) and nitrogen limitation (59.6 mM N). The final titer of homocitrate was determined after 72 h. Product concentrations were determined via HPLC measurements of the cell free supernatant. Product titers of 2-oxoglutarate and 2-hydroxyglutarate could not be determined from the HPLC measurements and are given as sum of the peak area

C. glutamicum strains	Condition	Growth rate [h^{-1}]	Biomass [g_{cdw}^{-1} h^{-1}]	Glucose uptake rate [mmol g_{cdw}^{-1} h^{-1}]	Final homo-citrate titer [mM]	2-OG + 2-HG [mAU*s]
pEKEx2-*lys20*	892 mM nitrogen	0.30 ± 0.01	8.2 ± 0.2	8.1 ± 0.1	2.6 ± 0.3	2,801
pEKEx2-*lys20*	59.6 mM nitrogen	0.24 ± 0.0	6.0 ± 0.6	8.8 ± 1.1	8.2 ± 0.9	5,966
pEKEx2-*ttc1550*	892 mM nitrogen	0.37 ± 0.01	9.0 ± 0.4	9.1 ± 0.6	1.8 ± 0.6	715
pEKEx2-*ttc1550*	59.6 mM nitrogen	0.27 ± 0.01	7.1 ± 0.4	8.3 ± 0.6	7.0 ± 1.06	9,558
Δ*gdh*::P_{tuf}-*lys20* (MS-1)	892 mM nitrogen	0.18 ± 0.02	7.4 ± 0.4	4.8 ± 0.5	4.1 ± 1.4	2,134
Δ*gdh*::P_{tuf}-*lys20* (MS-1)	59.6 mM nitrogen	0.14	6.0	5.2	3.1	4,935

Interestingly, cultivation of *C. glutamicum* MS-1 revealed decreased homocitrate accumulation (3.1 mM, data not shown) under same conditions, indicating that the inactivation of the Gdh negatively influence homocitrate production under nitrogen limitation. Furthermore, nitrogen limitation increased by-product formation of 2-hydroxyglutarate and 2-oxoglutarate by a factor of 2 or more (Tab. 10). The excess of the precursor 2-oxoglutarate indicates that homocitrate production is either limited by acetyl-CoA supply or by HCS activity.

Further experiments were performed to overcome a possible precursor limitation of 2-oxoglutarate and/or acetyl-CoA towards homocitrate production. Therefore, the strain *C. glutamicum* MS-1 (*C. glutamicum* Δ*gdh*::P_{tuf}-*lys20*) was tested under standard conditions with additional feeding of several carbon sources at the beginning of the stationary growth phase. The additional carbon sources (222 mM glucose, 204 mM potassium acetate, 222 mM glucose + 204 mM potassium acetate and 222 mM glucose + 20 mM 2-oxoglutarate (data of the cultivation experiments not shown)) were dissolved in standard CGXII medium without carbon source and added to the cultures after 22 h. The additional carbon supply led to

increased maximal OD, compared to standard conditions (Fig. 10B). In case of separately added glucose and acetate a maximal OD of 40 represents an increase of 12.5%, whereas the addition of glucose plus acetate revealed an increased OD of 56 (37.5%). The consumption of the additional carbon source was slight different (Fig. 10D): Acetate was consumed within 24 h within addition, whereas glucose was depleted within 72 h. Simultaneous metabolisation was observed when glucose and acetate were added together and completely consumed within 72 h. Concerning homocitrate production, every tested condition resulted in increased homocitrate titers (Fig. 10F). Before addition of the carbon sources, homocitrate concentration was about 1 mM. Feeding of additional glucose at the beginning of the stationary growth phase yielded 13 mM homocitrate, which represents an increase of 9 mM or about 225% (compared to 4 mM under standard conditions) with a corresponding yield of 0.03 mol C_{HC}/mol $C_{glucose}$. The carbon yield of the second production phase (after addition of carbon supply) was calculated on the basis of additionally added and consumed amount of substances (glucose, acetate, 2-oxoglutarate). The addition of acetate resulted in the accumulation of 9.8 mM homocitrate, whereas a combination of glucose and acetate increased the homocitrate titer to 27.5 mM, representing yields of 0.04 mol C_{HC}/mol $C_{acetate}$ and 0.06 mol C_{HC}/mol $C_{glucose+acetate}$, respectively. Additional glucose in combination with 2-oxoglutarate was also tested and yielded 12.2 mM homocitrate (0.026 mol C_{HC}/ mol $C_{glucose+2\text{-}oxoglutarate}$), which was very similar to the results obtained for additional glucose alone. In summary, the combination of glucose and acetate showed the strongest positive effect on homocitrate production. This clearly shows that homocitrate production is limited by precursor supply at the early stationary growth phase. However, the concentration of homocitrate reached about 1 mM before adding the additional carbon supply, giving further evidence for a coupling of production to the stationary growth phase or the metabolic status of the cells.

4.6.2 Characterisation of the homocitrate synthase mutein Lys20^{R276K}

Several working groups have reported that homocitrate synthase is subject to complex regulation by different components and mechanisms (Andi *et al.*, 2005). One of them is the feedback inhibition by L-lysine, the end product of the AAA pathway, representing the key point for limiting the metabolic flux through the AAA pathway in *S. cerevisiae* (Bulfer *et al.*, 2010). From previous studies it is known that the native Lys20 enzyme is 50% inhibited in the presence of 1 mM L-lysine. An amino acid exchange of arginine to lysine at position 276 (R276K) led to a decrease of sensitivity towards L-lysine up to 100 mM (Feller *et al.*, 1999). Since it is known that the intracellular concentration of L-lysine in the mid-exponential growth phase of *C. glutamicum* wild-type cells is about 5 mM (Binder *et al.*, 2012), inhibition of HCS activity might be a limiting factor for homocitrate production in *C. glutamicum*. In order to circumvent this possible limitation the R276K amino acid exchange of the HCS might be beneficial for homocitrate production in *C. glutamicum*. Thus, the base pair mutation AGA → AAA which leads to the amino acid exchange R276K was inserted into the *lys20* sequence (section 3.5.11). The effect of the mutein Lys20^{R276K} on homocitrate production was tested in strains containing the gene chromosomally integrated as well as plasmid-based. The strains were cultivated in CGXII minimal media with glucose as sole carbon source. Homocitrate accumulation was analysed after 6 h, 24 h and 52 h (Tab. 11). In case of the plasmid-based strains, up to 2.5 mM homocitrate was produced after 52 h with Lys20 and Lys20^{R276K}. A slight difference was observed for the strains containing the chromosomally integrated genes: The strain expressing the native enzyme accumulated up to 4.1 mM compared to 3.6 mM homocitrate produced by the strain with the mutein described to be L-lysine-insensitive.

Additionally, the HCS enzyme activities of the mutein and the native enzyme were measured at various time points (Tab. 11). HCS activity was determined in crude extracts using the DCPIP method. At the time points, at which homocitrate was already present in the supernatant (24 h, 52 h), the amino acid exchange in Lys20 led to lower enzyme activity for both, the chromosomally encoded variant and the plasmid-encoded variant, compared to the wild-type Lys20 (Tab. 11).

Moreover, the enzyme assay was performed with addition of 10 mM L-lysine to test the feedback inhibition. In case of both plasmid-encoded variants, the enzyme activity was 2-4 fold decreased in the presence of the inhibitor L-lysine, but the native enzyme showed a 3-fold higher activity compared to the claimed L-lysine insensitive variant (Tab. 11). For the

two chromosomally encoded Lys20 variants no HCS activity was detectable in the presence of the inhibitor.

Tab. 11: Homocitrate accumulation and homocitrate synthase activities of Lys20 and Lys20^{R276K}. The native enzyme Lys20 was compared to the L-lysine insensitive variant Lys20^{R276K} after 6 h, 24 h and 52 h cultivation in standard CGXII minimal medium. Both, the plasmid-based as well as the chromosomally integrated variants were tested in *C. glutamicum* wild type. The enzyme assay was performed with crude extracts with and without addition of 10 mM L-lysine.

Time	Strains							
	C. glutamicum pEKEx2-*lys20*		*C. glutamicum* pEKEx2-*lys20*^{R276K}		*C. glutamicum* Δ*gdh*::P$_{tuf}$-*lys20*		*C. glutamicum* Δ*gdh*::P$_{tuf}$-*lys20*^{R276K}	
	Spec. activity [mU/mg]	HC [mM]	Spec. activity [mU/mg]	HC [mM]	Spec. activity [mU/mg]	HC [mM]	Spec. activity [mU/mg]	HC [mM]
6 h	5	0	17	0	14	0	0	0
24 h	53	1.9	8	1.9	21	2.1	11	1.8
24 h + 10 mM Lys	12	1.9	4	1.9	0	2.1	0	1.8
52 h	36	2.5	9	2.4	29	4.1	2	3.6

These results indicate that the amino acid exchange R276K is not beneficial for HCS enzyme activity in the presence of L-lysine and HCS^{R276K} appears to be still sensitive to L-lysine. In addition, it was observed that on the one hand the strains containing the plasmid pEKEx2-*lys20* exhibited a higher HCS enzyme activity, but on the other hand accumulated only about one half of homocitrate in comparison to the strain harbouring the HCS gene within the genome. In summary, intracellular L-lysine levels could be a limiting factor for homocitrate production as HCS is inhibited and homocitrate titers could not be increased by using the mutein Lys20^{R276K}.

4.6.3 Metabolic engineering to improve precursor supply

The previous results showed that homocitrate production in *C. glutamicum* under standard conditions is relatively low and coupled to the stationary growth phase. To improve homocitrate production the best producer strain *C. glutamicum* MS-1 was selected for further genetic modifications, which increase the supply of the homocitrate precursors 2-oxoglutarate and acetyl-CoA (Fig. 11). In previous studies it has been reported for strain *C. glutamicum* R that overexpression of the native pyruvate carboxylase gene (*pyc*), catalysing the carboxylation of pyruvate to oxaloacetate, enhanced the rate of succinate production (Okino *et al.*, 2008). In this context it was further demonstrated that the amino acid exchange P458S in pyruvate carboxylase (*pyc*^{P458S}) is beneficial for the formation of oxaloacetate (Ikeda *et al.*, 2006).

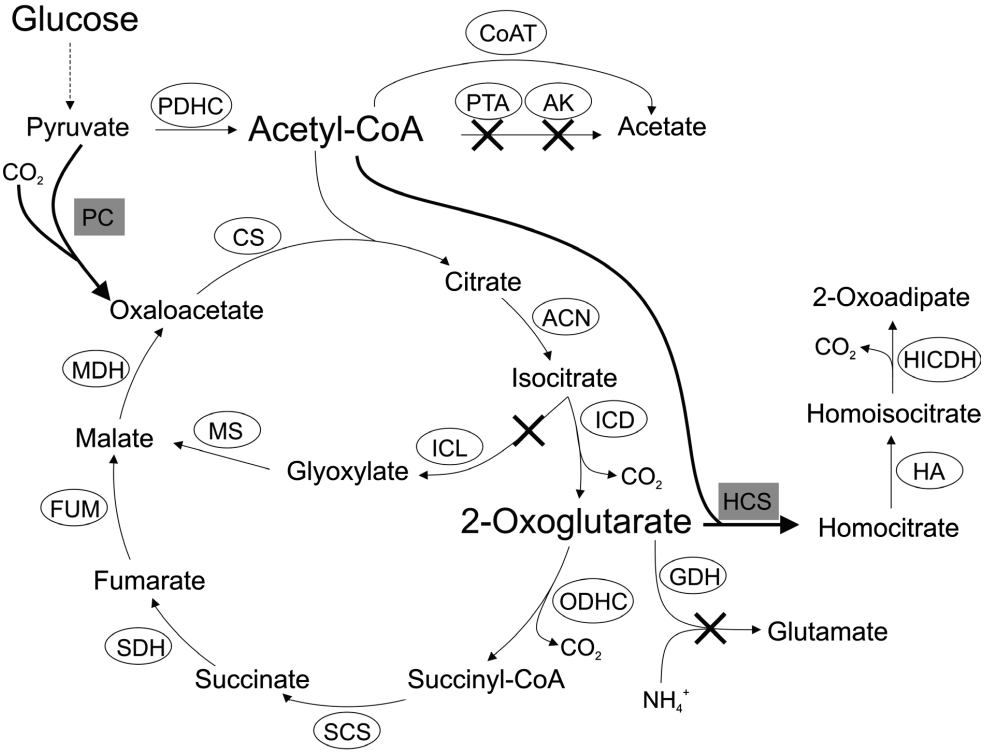

Fig. 11: Schematic overview of the central carbon metabolism of *C. glutamicum* and the genetic modifications applied to enhance the production of homocitrate and 2-oxoadipate. An enzymatic reaction (arrow) marked with an "X" indicates the deletion of the corresponding gene. Enzymes whose genes were overexpressed are displayed in grey boxes and their corresponding reactions are highlighted in bold arrows. Abbreviations: PDHC, pyruvate dehydrogenase; PC, pyruvate carboxylase; CoAT, CoA transferase; PTA, phosphotransacetylase; AK, acetate kinase; CS, citrate synthase; ACN, aconitase; ICD, isocitrate dehydrogenase; ODHC, 2-oxoglutarate dehydrogenase; SCS, succinyl-CoA synthetase; SDH, succinate dehydrogenase; FUM, fumarase; MDH, malate dehydrogenase; ICL, isocitrate lyase; MS, malate synthase; GDH, glutamate dehydrogenase; HCS, homocitrate synthase; HA, homoaconitase; HICDH, homoisocitrate dehydrogenase

To test the influence of Pyc^{P458S} on homocitrate production, C. *glutamicum* MS-1 was transformed with plasmid pAN6-*pyc*^{P458S}. In addition, *pyc*^{P458S} controlled by the P_{tuf} promoter was chromosomally integrated into the *pta-ackA* locus in *C. glutamicum* MS-1, thereby simultaneously inactivating *pta-ackA* by deletion. Deletion of the acetate activating genes *pta* and *ackA*, coding for phosphotransacetylase and acetate kinase was described to prevent acetate formation from acetyl-CoA (Reinscheid *et al.*, 1999). The emerging strains (Fig. 12) were named *C. glutamicum* MS-2 (*C. glutamicum* MS-1 pAN6-*pyc*^{P458S}) and *C. glutamicum* MS-3 (*C. glutamicum* MS-1 Δ*pta-ackA*::P_{tuf}-*pyc*^{P458S}).

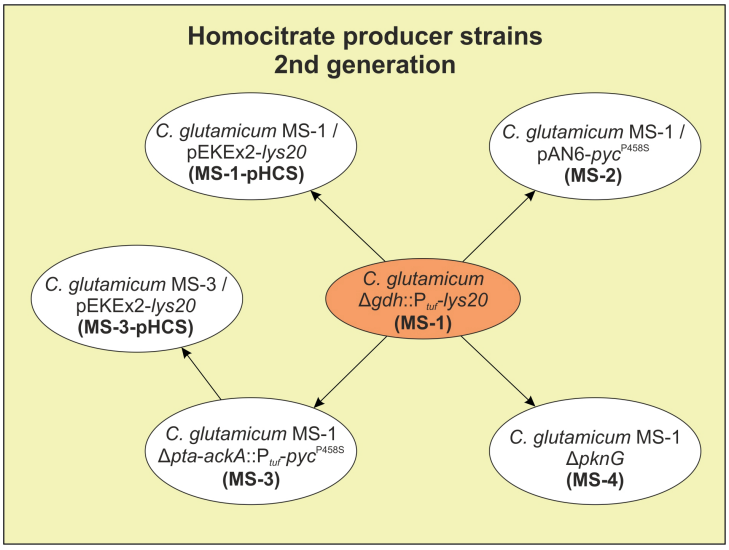

Fig. 12: Overview of second generation homocitrate producer strains derived from *C. glutamicum* MS-1. *C. glutamicum* MS-1 was transformed with the plasmids pEKEx2-*lys20*, encoding HCS of *S. cerevisiae* and pAN6-*pyc*^{P458S}, encoding a pyruvate carboxylase variant of *C. glutamicum* R, resulting in the strains *C. glutamicum* MS-1-pHCS and *C. glutamicum* MS-2, respectively. To generate *C. glutamicum* MS-3 gene deletions of *pta-ackA* (encoding phosphotransacetylase and acetate kinase) and simultaneous integration of *pyc*^{P458S}, controlled by the promoter P_{tuf}, was performed. *C. glutamicum* MS-3 was transformed with the plasmid pEKEx2-*lys20* to generate *C. glutamicum* MS-pHCS. Gene deletion of *pknG* (encoding serine/threonine protein kinase) in *C. glutamicum* MS-1 leads the strain *C. glutamicum* MS-4

A further strategy tested to increase the product titer of homocitrate was the enhancement of the gene dosage of the homocitrate synthase. Therefore the strains *C. glutamicum* MS-1 and *C. glutamicum* MS-3 were transformed with the plasmid pEKEx2-*lys20*, resulting in the strains *C. glutamicum* MS-1-pHCS (*C. glutamicum* MS-1/pEKEx2-*lys20*) and *C. glutamicum* MS-3-pHCS (*C. glutamicum* MS-3/pEKEx2-*lys20*). By this, both strains contained a plasmid-encoded Lys20 in addition to the chromosomally integrated one. In a further approach the P_{tuf}-*lys20* fragment was integrated in the *gdh* locus of the strain *C. glutamicum* Δ*pknG* (Niebisch et al., 2006), resulting in *C. glutamicum* MS-4. Deletion of the serine/threonine protein kinase

(PknG) prevents phosphorylation of OdhI. Unphosphorylated OdhI binds with high affinity to OdhA, the E1-component of the 2-oxoglutarate dehydrogenase complex (ODH) in *C. glutamicum*, and leads to inhibition of OdhA (Schultz *et al.*, 2007). In consequence of the OdhA inhibition, the homocitrate precursor 2-oxoglutarate accumulates, which should be beneficial for homocitrate formation.

To evaluate whether the genetically modified strains show increased product formation, cultivation experiments in shake flasks in CGXII medium was performed. Standard conditions with 4% glucose as starting carbon source as well as "fed-batch" conditions with addition of 4% glucose and 2% acetate at the beginning of the stationary growth phase were tested. Growth and product formation was observed over 72 h (Fig. 13).

In comparison to the parental strain *C. glutamicum* MS-1 ($\mu = 0.18 \pm 0.02\ h^{-1}$), the plasmid-based expression stress further reduced the growth rate of strain MS-1-pHCS to $0.07 \pm 0.007\ h^{-1}$, which means a decrease of about 53%. The slowed growth correlates with decelerated glucose consumption of MS-1-pHCS, showing complete consumption within 60 h to 72 h. Analyses of homocitrate concentration revealed up to 2.5 mM after 72 h, corresponding to a yield of 0.009 mol C_{HC}/ mol $C_{glucose}$. This means a decrease of 37.5% in comparison to the parental strain MS-1 (4 mM homocitrate). Since MS-1-pHCS had strong growth retardation, the additional pulse of glucose and acetate was added after 54 h, yielding in increased biomass formation of about 22%.

After 72 h approximately 45% (92 mM) of the added acetate and 44% (98 mM) of the added glucose were still present in the cell culture supernatant of MS-1-pHCS. In consequence of minor glucose and acetate uptake rate the strain *C glutamicum* MS-1-pHCS showed a decreased homocitrate accumulation (15.4 mM) and a slightly decreased yield of 0.058 mol C_{HC}/ mol $C_{glucose+acetate}$. Strain *C. glutamicum* MS-2, harbouring a plasmid encoded copy of the *pyc*^{P458S} gene, showed an enhanced growth rate (μ = of $0.22 \pm 0.008\ h^{-1}$). This indicates that the expression of the pyruvate carboxylase variant positively effects the growth of this strain compared to *C. glutamicum* MS-1. Under standard conditions the glucose in the culture of MS-2 was completely consumed within 24 h. Similar to *C. glutamicum* MS-1-pHCS the plasmid encoded overexpression of Pyc^{P458S} in the strain MS-2 was not beneficial for homocitrate production: After 72 h a maximal concentration of 2.5 mM, corresponding to a yield of 0.009 mol C_{HC}/ mol $C_{glucose}$, was measured.

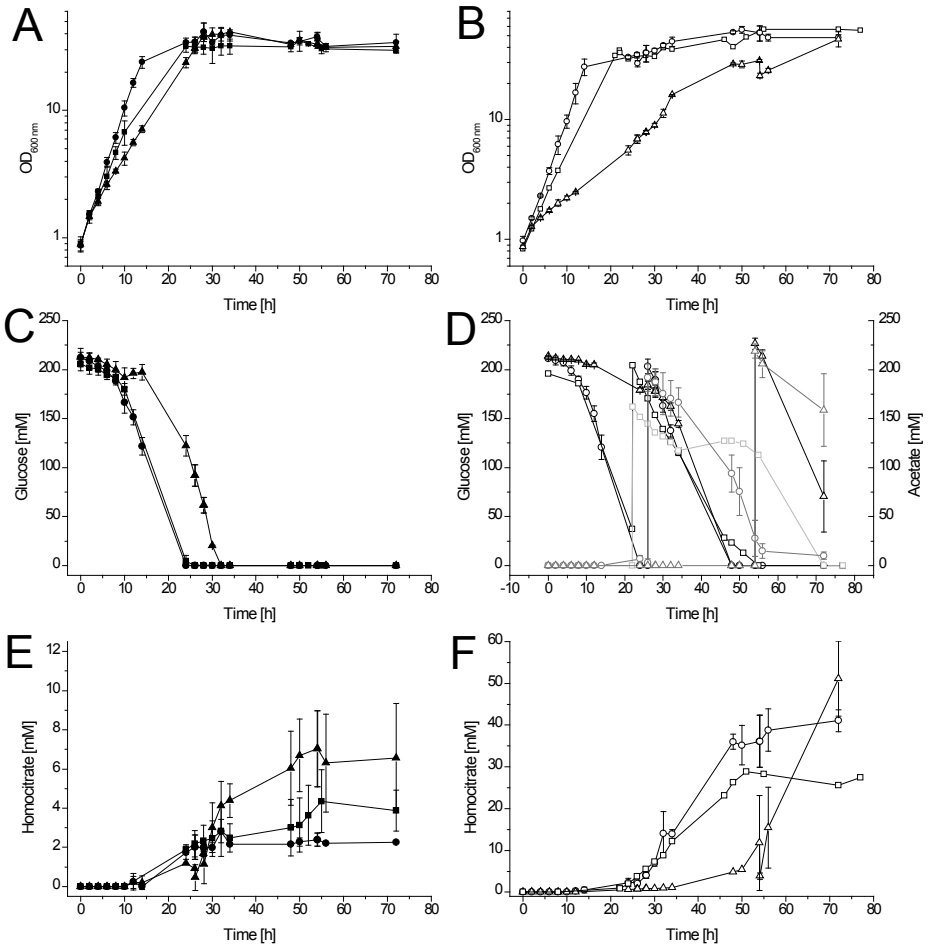

Fig. 13: Effect of various genetic modifications in *C. glutamicum* on homocitrate formation. Growth (A, B), glucose (C, D) and acetate consumption (D, grey) as well as homocitrate production (E, F) of the strains *C. glutamicum* MS-1 (–■–/–□–), *C. glutamicum* MS-3 (–●–/–○–) and *C. glutamicum* MS-3-pHCS (–▲–/–△–) was analysed in standard CGXII minimal medium with 4% (w/v) glucose (A, C, E) and under "fed-batch" conditions with addition of 222 mM glucose and 204 mM acetate at the beginning of the stationary growth phase (B, D, F) for 72 h. Data represent mean values with standard deviation from three independent experiments, except for the "fed-batch" cultivation of *C. glutamicum* MS-1, which was performed in a single experiment.

In the second experiment glucose and acetate were added after 28 h to the culture of MS-2, which led to an increased biomass formation of about 30% compared to standard conditions. Glucose was completely consumed within 56 h, whereas 10 mM acetate was present at the end of the cultivation. The strain, containing the plasmid-based pyruvate carboxylase gene *pyc*^{P458S} accumulated up to 31 mM homocitrate in 72 h, which corresponds to a yield of 0.069 mol C_{HC}/ mol $C_{glucose+acetate}$. Compared to the parental strain *C. glutamicum* MS-1, homocitrate production with MS-2 is increased by 11%.

In comparison to the parental strain, *C. glutamicum* MS-3 exhibited also an increased growth rate ($\mu = 0.23 \pm 0.03$ h^{-1}, Fig. 13A). Similar to *C. glutamicum* MS-2, MS-3 fully consumed the glucose within 24 h (Fig. 13C) and reached a decreased homocitrate titer (2.5 mM) under standard conditions (Fig. 13E). At the beginning of the stationary growth phase (26 h) of *C. glutamicum* MS-3, a 222 mM glucose plus 204 mM pulse was added (Fig. 13D), which led to a maximal OD of 56, representing a 30% increase in comparison to standard conditions. Analyses of the supernatant revealed that glucose was depleted within 56 h, whereas a remaining concentration of 10 mM acetate was measured after 72 h. Cultivation of *C. glutamicum* MS-3 under "fed-batch" conditions yielded in a maximal homocitrate concentration of 41.1 mM with a corresponding yield of 0.092 mol C_{HC}/ mol $C_{glucose+acetate}$ (Fig. 13F). This result indicates that deletion of *pta-ackA* and/or chromosomal expression of pyc^{P458S} are beneficial for homocitrate production.

Strain MS-3-pHCS ($\mu = 0.13 \pm 0.002$ h^{-1}) harbouring the additional plasmid encoded copy of the HCS gene exhibited strong growth retardation of about 44% in comparison to the strain without plasmid (MS-3) (Fig. 13A). Glucose was more slowly consumed by MS-3-pHCS and depleted within 48 h (Fig. 13C). Interestingly, increased homocitrate titers were observed with the strain *C. glutamicum* MS-3-pHCS (Fig. 13E). At the end of the cultivation homocitrate was accumulated up to 6.6 mM with a corresponding yield of 0.023 mol C_{HC}/mol $C_{glucose}$. To test this strain under "fed-batch" conditions glucose and acetate was added after 54 h, which led to a 34% increase of biomass after 72 h (Fig. 13B). HPLC measurements of the cell culture supernatant showed that 70 mM glucose and 158 mM were not metabolised within 72 h (Fig. 13D). An accumulation of up to 52.1 mM homocitrate was measured after 72 h, representing a yield of 0.21 mol C_{HC}/ mol $C_{glucose+acetate}$ (Fig. 13F).

Taken together, homocitrate production could be increased from 4 mM with *C. glutamicum* MS-1 under standard conditions to 52 mM with *C. glutamicum* MS-3-pHCS under "fed-batch" conditions by metabolic engineering and modification of the cultivation conditions.

The strain *C. glutamicum* MS-4, containing the deletion of the *pknG* gene encoding serine/threonine protein kinase, was tested independently of the other experiments under standard and "fed-batch" conditions in single experiments (data not shown). Cultivation under standard conditions revealed a diminished growth rate of $\mu = 0.11$ h^{-1} and slowed glucose consumption (within 48 h), compared to the parental strain MS-1. Addition of glucose and acetate at the beginning of the stationary growth phase led to increased biomass formation by about 28%. Both, glucose and acetate were completely consumed within 120 h. Analyses of

the cell culture supernatant resulted in homocitrate titers similar to that of the parental strain *C. glutamicum* MS-1 under standard (4.1 mM) or "additional feeding" conditions (27.1 mM).

Tab. 12: Summarised results of the genetically modified strains cultivated under "fed-batch" conditions. Cultivation of the strains *C. glutamicum* MS-1, MS-1-pHCS, MS-2, MS-3, MS-3-pHCS and MS-4 (Fig. 12) were performed in standard CGXII minimal medium with 4% (w/v) glucose as growth substrate. At the beginning of the stationary growth phase 4% (w/v) glucose (glu) and 2% (w/v) acetate (ac) dissolved in CGXII stock solution were added to the culture. Final product titers of homocitrate (HC) were determined via HPLC analyses after 72 h. Average data are calculated from three independent experiments, except for MS-1 and MS-4, where data from single experiments were obtained.

Strains	Genetic background	Growth rate [h^{-1}]	Final product titer HC [mM]	Consumed carbon source [mM]	HC yield [mol C_{HC}/ mol $C_{glucose+acetate}$]
MS-1	Δ*gdh*::P_{tuf}-*lys20*	0.18	27.5	222 glu 194 ac	0.06
MS-1-pHCS	Δ*gdh*::P_{tuf}-*lys20*/ pEKEx2-*lys20*	0.07 ± 0.006	15.4 ± 6.6	124 glu 112 ac	0.058
MS-2	Δ*gdh*::P_{tuf}-*lys20*/ pAN6-*pyc*^{P458S}	0.22 ± 0.008	31.0 ± 3.9	222 glu 194 ac	0.069
MS-3	Δ*gdh*::P_{tuf}-*lys20* Δ*pta-ackA*::P_{tuf}-*pyc*^{P458S}	0.24 ± 0.01	41.1 ± 2.6	222 glu 194 ac	0.092
MS-3-pHCS	Δ*gdh*::P_{tuf}-*lys20* Δ*pta-ackA*::P_{tuf}-*pyc*^{P458S}/ pEKEx2-*lys20*	0.13 ± 0.002	52.1 ± 12.5	152 glu 46 ac	0.21
MS-4	Δ*gdh*::P_{tuf}-*lys20* Δ*pknG*	0.11	27.1	222 glu 204 ac	0.052

Besides the main product homocitrate, several by-products were accumulated by the genetically engineered strains during cultivation. To identify the by-products as well as to verify the formation of homocitrate, GC-ToF-MS measurements of the cell culture supernatants were performed. Therefore, samples of the supernatant of the homocitrate producer strain MS-3 cultivated under standard conditions and with additional feeding of glucose and acetate, respectively, were taken after 48 h of cultivation. The GC-ToF-MS analysis confirmed homocitrate formation under both tested conditions. Furthermore, accumulation of 2-oxoglutarate, 2-hydroxyglutarate, malate and succinate were detected under both growth conditions. In addition lactate, citrate, 2-oxoisocaproate, 2-hydroxyisocaproate and glycerol were identified in samples of the "fed-batch" approach. None of these substances was detected in samples of the strains *C. glutamicum* wild type and

C. glutamicum/pAN6-*pyc*^{P458S} which were used as negative controls. Those metabolites which were detectable via HPLC measurements were quantified in samples after 72 h of cultivation of the genetically modified strains (Tab. 13). In general, it was observed that the concentration of each metabolite was higher if the respective strain was cultivated under the condition of additional glucose and acetate feeding.

The citrate cycle intermediates citrate, fumarate and malate were accumulated in the low mill molar range, whereas succinate was produced up to 21.7 mM with the strain *C. glutamicum* MS-3-pHCS. The accumulation of succinate might be an effect of the chromosomally encoded pyruvate carboxylase and the deletion of the *pta-ackA* genes, which have been described to be beneficial for succinate production in *C. glutamicum* (Litsanov *et al.*, 2012a, Litsanov *et al.*, 2012b).

Tab. 13: Comparison of the by-product formation of the plasmid-free homocitrate and 2-oxoadipate producer strains. Cell culture supernatants of the strains *C. glutamicum* MS-1-pHCS, MS-2, MS-3, MS-3-pHCS and MS-4 grown under standard conditions (-) and grown under "fed-batch" with additional feeding of glucose and acetate (+) were analysed via HPLC to determine formation of malate, fumarate, succinate and citrate. For 2-hydroxyglutarate (2-HG) and 2-oxoglutarate (2-OG) the integrated area of the HPLC peaks were taken.

	MS-1-pHCS		MS-2		MS-3		MS-3-pHCS		MS-4	
Carbon supply	-	+	-	+	-	+	-	+	-	+
Malate [mM]	0	2.2	0.6	3.5	0.3	3.3	0.3	5.4	0	0
Fumarate [mM]	0	0.1	0.1	0.2	0.1	0	0.1	0.3	0	0.01
Succinate [mM]	1.8	10.4	1.1	13.1	2.2	10.9	4.5	21.7	0	6.7
Citrate [mM]	0	0.1	0.5	1.1	0.3	0.6	0.8	0	1.0	2.1
2-OG/ 2-HG [mAU*s]	2701	13957	3049	30100	2951	44283	9488	52085	4880	19617

The concentration of 2-oxoglutarate, which represents the direct precursor of homocitrate, could not be determined quantitatively for the homocitrate producer strains. The accumulation of 2-oxoglutarate and 2-hydroxyglutarate caused an extensive overlap of the respective peaks in the HPLC measurements. Manual reintegration of peak areas for the sample of *C. glutamicum* MS-3-pHCS after 72 h would indicate concentrations of 27 mM and 484 mM

for 2-oxoglutarate and 2-hydroxyglutarate, respectively. Based on the supplied amount of carbon, a concentration of 484 mM 2-hydroxyglutarate is theoretically not possible, demonstrating that even the manual reintegration of partly separated signals could not be used to get reliable data. For this reason, only the summed up peak areas of 2-hydroxyglutarate and 2-oxoglutarate were analysed. For all homocitrate producer strains tested under “fed-batch” conditions a drastically increased peak area of 2-oxoglutarate and 2-hydroxyglutarate was observed (Tab. 13). The largest peak areas for 2-oxoglutarate and 2-hydroxyglutarate were detected in samples of the most promising homocitrate producer MS-3-pHCS under standard (9488 mAU*s) and much higher under “fed-batch” conditions (52085 mAU*s). The other tested strains obtained peak areas from 2700 to 4800 mAU*s under standard conditions and showed increased 2-oxoglutarate/2-hydroxyglutarate accumulation of 5-15-fold when cultivated under “fed-batch” conditions. However these results indicate that homocitrate production under “fed-batch” conditions is rather limited by acetyl-CoA than by 2-oxoglutarate supply. Since the highest homocitrate titers under “fed-batch” conditions were reached at different time points (Fig. 13F), e.g. MS-3 after 48 h and MS-3-pHCS after 72 h, loss of HCS activity can likely be excluded. This observation gives further evidence of a limitation of acetyl-CoA supply.

4.7 Establishment of 2-oxoadipate production with *C. glutamicum*

In the previous experiments of this thesis the establishment and enhancement of homocitrate production with *C. glutamicum* were demonstrated. These results form the basis for the development of a 2-oxoadipate producer strain. For the conversion of homocitrate to 2-oxoadipate enzyme activities for homoaconitase (HA) and homoisocitrate dehydrogenase (HICDH) are necessary. Similar to the strain development of the homocitrate producers, the genes encoding HA (*lys4*) and HICDH (*lys12*) of *S. cerevisiae* were introduced chromosomally and plasmid-encoded into the homocitrate producer strains. To provide the enzymes for the plasmid-based 2-oxoadipate production, the homocitrate producer strains *C. glutamicum*/pEKEx2-*ttc1550* and *C. glutamicum*/pEKEx2-*lys20* were transformed with the plasmid pVWEx2-*lys4*-*lys12*, encoding HA and HICDH, respectively.

For plasmid-free production of 2-oxoadipate the most promising strain MS-1 (*C. glutamicum* Δ*gdh*::P_{tuf}-*lys20*) of the first generation of homocitrate producers was selected as parental strain. The gene *aceA* was chosen as integration locus in strain MS-1 for the *S. cerevisiae* genes *lys4* and *lys12* controlled by P_{tuf}. The resulting strain containing all three genes (MS-1 Δ*aceA*::P_{tuf}-*lys4*-*lys12*) relevant for 2-oxoadipate production was named *C. glutamicum* MS-5 (Fig. 14).

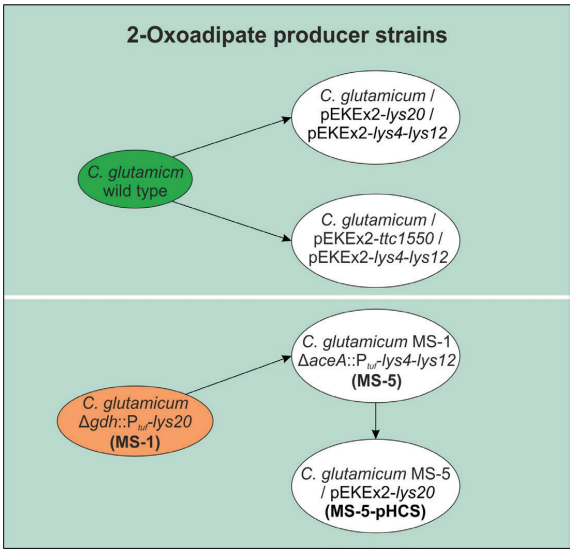

Fig. 14: Establishment of the 2-oxoadipate production in *C. glutamicum*. For plasmid-based expression of the AAA pathway genes, relevant for 2-oxoadipate production, the *C. glutamicum* wild type was transformed with the plasmids pEKEx2-*lys20* and pEKEx2-*ttc1550* encoding homocitrate synthases as well as with the plasmid pVWEx2-*lys4*-*lys12* encoding homoaconitase and homoisocitrate dehydrogenase. Gene deletion of *aceA* and simultaneous integration of *lys4*-*lys12*, controlled by the P_{tuf} promoter in *C. glutamicum* MS-1 leads to the plasmid-free 2-oxoadipate producer *C. glutamicum* MS-5. *C. glutamicum* MS-5 was transformed with the plasmid pEKEx2-*lys20*, resulting in the strain *C. glutamicum* MS-5-pHCS.

To test the effect of the gene dosage for the rate-limiting step in the AAA pathway catalysed by homocitrate synthase, the strain *C. glutamicum* MS-5 was transformed with the plasmid pEKEx2-*lys20*, resulting in the strain *C. glutamicum* MS-5-pHCS (Fig. 14).

To test the plasmid-based 2-oxoadipate production (Tab. 14), the strains *C. glutamicum*/ pEKEx2-*lys20*/pVWEx2-*lys4-lys12* (Fig. 15) and *C. glutamicum*/pEKEx2-*ttc1550*/pVWEx2-*lys4-lys12* (data not shown), were cultivated in standard CGXII medium (892 mM nitrogen) and under nitrogen limitation (59.6 mM nitrogen) with 4% (w/v)) glucose as sole carbon source. *C. glutamicum*/pEKEx2/pVWEx2 was used as a control. Evaluation of the growth behaviour under nitrogen excess (Fig. 15A) revealed growth rates of $\mu = 0.18 \pm 0.02$ h^{-1} (*C. glutamicum*/pEKEx2-*ttc1550*/pVWEx2-*lys4-lys12*), $\mu = 0.16 \pm 0.02$ h^{-1} (*C. glutamicum*/ pEKEx2-*lys20*/pVWEx2-*lys4-lys12*) and $\mu = 0.16 \pm 0.01$ h^{-1} (control). This strong growth retardation in comparison to the wild-type strain ($\mu = 0.41$ h^{-1}) is a result of the two plasmid-borne selections and expression stress.

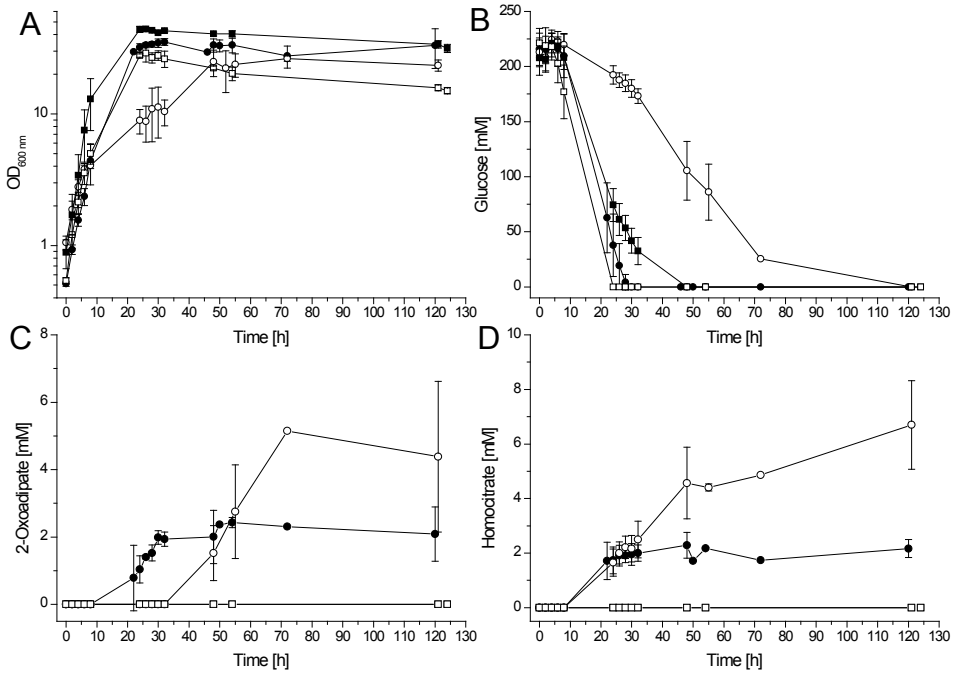

Fig. 15: Comparison of plasmid based 2-oxoadipate production with *C. glutamicum* producer strains under standard conditions and nitrogen limitation. Growth (A), glucose consumption (B) and formation of 2-oxoadipate (C) and homocitrate (D) in CGXII minimal medium with 4% glucose under nitrogen excess (892 mM N, black symbols) and nitrogen limitation (59.6 mM N, white symbols) of the strains *C. glutamicum*/ pEKEx2-*lys20*/ pVWEx2-*lys4-lys12* (–●–/–○–) and the control strain *C. glutamicum*/pEKEx2/pVWEx2 (–■–/–□–) were tested. Mean values and standard deviation of three independent experiments are shown

As shown before for the homocitrate producer strains, cultivation of 2-oxoadipate strains under nitrogen limitation led to a strong decrease of the growth rates of about 56%, resulting in growth rates of 0.07 ± 0.005 h^{-1} and 0.08 ± 0.01 h^{-1} for *C. glutamicum*/pEKEx2-*lys20*/pVWEx2-*lys4*-*lys12* (Fig. 15A) and *C. glutamicum*/pEKEx2-*ttc1550*/pVWEx2-*lys4*-*lys12* (data not shown), respectively. In contrast, the growth rate of the control culture was not significantly affected under nitrogen limitation ($\mu = 0.15\ h^{-1}$).

Under nitrogen excess the 2-oxoadipate producer strains completely consumed glucose within 28 h, whereas glucose was consumed within 24 h by the control strain (Fig. 15B). Cultivation of the 2-oxoadipate strains under nitrogen limitation led to retarded glucose consumption: *C. glutamicum*/pEKEx2-*lys20*/pVWEx2-*lys4*-*lys12* completely consumed the glucose within 72 h, whereas the glucose was still not fully consumed within 130 h by the strain *C. glutamicum*/pEKEx2-*ttc1550*/pVWEx2-*lys4*-*lys12*. Interestingly, the control strain did not fully consumed the glucose within 48 h under conditions of nitrogen limitation, although no difference in growth behaviour was observed compared to nitrogen excess (Fig. 15B).

Analyses of the cell culture supernatant revealed, that 2-oxoadipate was produced by both strains under standard conditions and under nitrogen limitation (Fig. 15C). Under standard conditions both strains accumulated up to approximately 2.2 mM 2-oxoadipate after 130 h, corresponding to a yield of 0.013 mol $C_{2\text{-}OA}$/mol $C_{glucose}$. As shown for homocitrate production, nitrogen limitation also positively influenced 2-oxoadipate formation: Product titer increased up to 5 mM (0.03 mol $C_{2\text{-}OA}$/mol $C_{glucose}$) for *C. glutamicum*/pEKEx2-*lys20*/pVWEx2-*lys4*-*lys12* and up to 9 mM (0.05 mol $C_{2\text{-}OA}$/mol $C_{glucose}$) for *C. glutamicum*/pEKEx2-*ttc1550*/pVWEx2-*lys4*-*lys12*, respectively. Further, analyses of the cell culture supernatant revealed a homocitrate accumulation for both strains of about 2 mM and 6.5 mM under standard and nitrogen limitation conditions, respectively (Fig. 15D, Tab. 14). Besides homocitrate, 2-oxoglutarate was also detected in the cell culture supernatant (Tab. 16), which leads to the assumption that neither homocitrate nor 2-oxoglutarate is limiting the 2-oxoadipate production.

It is worthwhile to notice that 2-oxoadipate and homocitrate were first detectable in the cell culture supernatant between 12 h and 22 h under standard conditions (Fig. 15C, D). In comparison, under nitrogen limitation homocitrate is present at the same time point, whereas 2-oxoadipate is first detectable between 32 h and 48 h. This observation further indicates that 2-oxoadipate production is limited by enzyme activity of homoaconitase or homoisocitrate dehydrogenase. Since the intermediates homoaconitate and homoisocitrate were not available

commercially, quantification of these substances in the cell culture supernatant by HPLC analyses was not possible.

In summary, the feasibility of heterologous, plasmid-based 2-oxoadipate production in *C. glutamicum*, using the enzymes HCS, HA and HICDH of the AAA pathway of *S. cerevisiae* and *T. thermophilus*, was demonstrated.

Tab. 14: Growth parameters and product formation of plasmid-based 2-oxoadipate production with *C. glutamicum* under nitrogen excess and nitrogen limitation conditions. The *C. glutamicum* strains were cultivated in standard CGXII minimal medium with 4% (w/v) glucose under nitrogen excess (892 mM N) and nitrogen limitation (59.6 mM N). The final titers of the products were determined after 130 h via HPLC measurements of the cell free supernatant. Product titers of 2-oxoglutarate and 2-hydroxyglutarate could not be determined from the HPLC measurements and are given as peak area.

C. glutamicum strains	Nitrogen supply	Growth rate [h^{-1}]	Biomass [g_{cdw}^{-1} h^{-1}]	Glucose uptake rate [mmol g_{cdw}^{-1} h^{-1}]	Final homo-citrate titer [mM]	Final 2-oxo-adipate titer [mM]	2-OG/ 2-HG [mAU*s]
pEKEx2-*lys20*/ pVWEx2-*lys4-lys12*	892 mM	0.16 ± 0.02	8.6 ± 2.6	4.6 ± 1.9	2.2 ± 0.3	2.1 ± 0.8	293
pEKEx2-*lys20*/ pVWEx2-*lys4-lys12*	59.6 mM	0.07 ± 0.005	5.8 ± 0.6	2.5 ± 0.5	6.7 ± 1.6	5.6 ± 0.4	1516
pEKEx2-*ttc1550*/ pVWEx2-*lys4-lys12*	892 mM	0.18 ± 0.02	7.9 ± 0.7	4.9 ± 0.9	1.9 ± 0.3	2.3 ± 0.6	489
pEKEx2-*ttc1550*/ pVWEx2-*lys4-lys12*	59.6 mM	0.08 ± 0.01	5.9 ± 0.4	2.4 ± 0.5	6.6 ± 0.9	9.1 ± 1.7	3032

In addition to the plasmid-based 2-oxoadipate production, the strains *C. glutamicum* MS-5 and MS-5-pHCS having the genes for HA and HICDH chromosomally integrated were also analysed. These strains were cultivated in CGXII minimal medium under standard conditions with 4% (w/v) glucose as starting carbon source and under "fed-batch" conditions with addition of 4% (w/v) glucose and 2% (w/v) acetate at the beginning of the stationary growth phase. Analyses of the growth behaviour of *C. glutamicum* MS-5 (Fig. 16A) under standard conditions showed a slightly increased growth rate ($\mu = 0.22 \pm 0.003$ h^{-1}) in comparison to the parental strain MS-1 ($\mu = 0.18 \pm 0.02$ h^{-1}), and exhibited a 23% increased biomass formation. On the contrary, a stronger growth retardation was observed for the strain *C. glutamicum* MS-5-pHCS ($\mu = 0.1 \pm 0.003$ h^{-1}), likely induced by the expression stress of the plasmid encoded HCS gene. In correlation with the results obtained for growth behaviour, the glucose consumption rate of MS-5-pHCS (2.4 ± 0.04 mmol g_{cdw}^{-1} h^{-1}) was significantly lower compared to MS-5 (3.6 ± 0.3 mmol g_{cdw}^{-1} h^{-1}) (Fig. 16B). Determination of 2-oxoadipate in

the cell culture supernatant of *C. glutamicum* MS-5 under standard conditions revealed a maximal production titer of up to 3.6 mM after 72 h, corresponding to a yield of 0.018 mol $C_{2\text{-}OA}$/mol $C_{glucose}$ (Fig. 16C). The second *lys20* copy had a positive effect on 2-oxoadipate production (Fig. 16C): The strain *C. glutamicum* MS-5-pHCS accumulated up to 7.2 mM 2-oxoadipate after 72 h, which represents a yield of 0.037 mol $C_{2\text{-}OA}$/mol $C_{glucose}$ and an increase of 100% compared to the strain *C. glutamicum* MS-5. Surprisingly, extracellular accumulation of 2-oxoadipate was detected after 8 h for both strains. This might be an indication that the chromosomally encoded genes were earlier expressed than the plasmid-encoded genes or deletion of *gdh* with integrated *lys20* has an effect on the time-course of product formation by influencing the precursor supply.

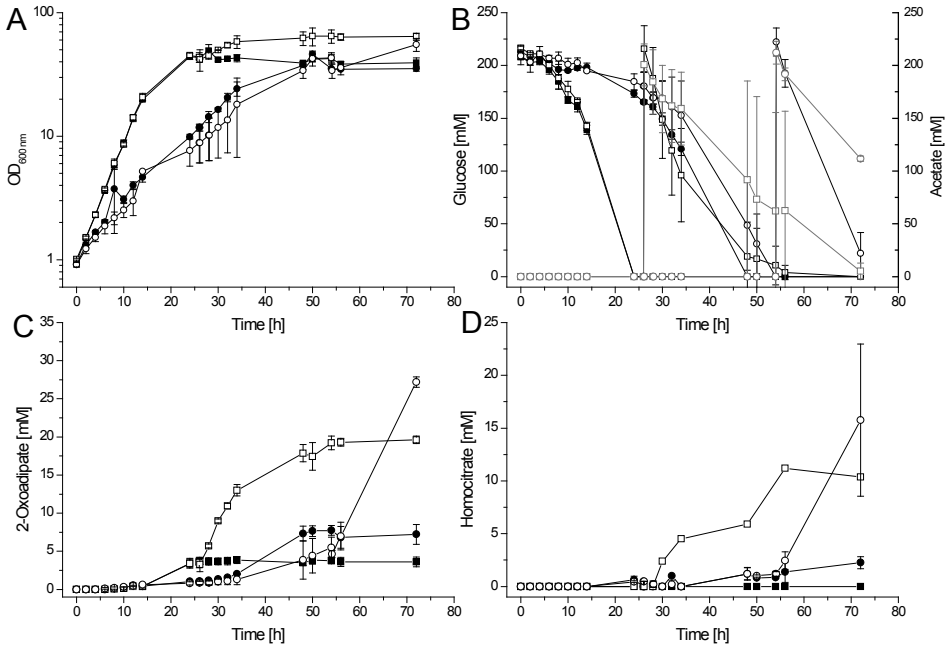

Fig. 16: Parameters of 2-oxoadipate production with *C. glutamicum* producer strains under standard and "fed-batch" conditions. Growth (A), glucose (B, black) and acetate (B, grey) consumption and product formation of 2-oxoadipate (C) and homocitrate (D) was analysed in standard CGXII minimal medium with 4% (w/v) glucose (black symbols) and under "fed-batch" conditions with addition of 222 mM glucose and 204 mM acetate at the beginning of the stationary growth phase (white symbols) for 72 h. The strains *C. glutamicum* MS-5 (–■–/–□–) and *C. glutamicum* MS-5-pHCS (–●–/–○–) were tested in this experiment. Mean values and standard deviation of three independent experiments are shown.

Further analyses revealed that the precursor homocitrate was not present in the supernatant of the strain *C. glutamicum* MS-5 and was accumulated up to 2.3 mM by the strain *C. glutamicum* MS-5-pHCS after 72 h. Increased carbon availability in consequence of the reduced growth of MS-5-pHCS might explain the homocitrate accumulation. Alternatively,

the second HCS gene copy increases formation of homocitrate and the further conversion to homoaconitate is limited.

For cultivation under "fed-batch" conditions, 222 mM glucose and 204 mM acetate were added after 26 h to the culture of the strain *C. glutamicum* MS-5, and in consequence of retarded growth after 54 h to the strain *C. glutamicum* MS-5-pHCS (Fig. 16B). An increased biomass formation of 30% and 22% for MS-5 and MS-5-pHCS, respectively, after additional carbon supply was observed (Fig. 16A). The additionally added glucose was completely consumed within 56 h by the *C. glutamicum* strain MS-5, whereas 10 mM acetate was present after 72h. In comparison, remaining concentrations of 20 mM glucose and of 92 mM acetate were measured in the supernatant of the strain MS-5-pHCS after 72 h.

Similar to the results obtained for homocitrate production, 2-oxoadipate accumulation was significantly enhanced by adding the additional carbon sources (Fig. 16C, Tab. 15). The strain *C. glutamicum* MS-5 accumulated up to 19.6 mM after 72 h cultivation, representing a carbon yield of 0.065 mol $C_{2\text{-}OA}$/mol $C_{glucose+acetate}$. Additionally, 10.4 mM (Fig. 16D) of the precursor homocitrate was present in the supernatant at the end of the cultivation. 2-Oxoadipate production was further enhanced by the strain MS-5-pHCS, yielding a final product titer of 29.3 mM 2-oxoadipate with a yield of 0.13 mol $C_{2\text{-}OA}$/mol $C_{glucose+acetate}$. Quantification of the precursor homocitrate revealed an accumulation of 15.7 mM after 72 h. Similar to the results of the plasmid based 2-oxoadipate production, the accumulation of the precursor homocitrate indicates that 2-oxoadipate production is limited either by the conversion of homocitrate to homoisocitrate or by the conversion of homoisocitrate to 2-oxoadipate.

Tab. 15: Summarised results of the plasmid free 2-oxoadipate strains cultivated under standard and "fed-batch" conditions. Cultivation of the strains *C. glutamicum* MS-5 and MS-5-pHCS were performed in standard CGXII minimal medium with 4% (w/v) glucose as growth substrate. At the beginning of the stationary growth phase 4% (w/v) glucose (glu) and 2% (w/v) acetate (ac) dissolved in CGXII stock solution were added to the culture. Final product titers of homocitrate (HC) and 2-oxoadipate (2-OA) were determined via HPLC analyses after 72 h. Mean values are calculated from three independent experiments.

Strains	Cultivation condition	Biomass [g_{cdw}^{-1} h^{-1}]	Growth rate [h^{-1}]	Final product titer 2-OA [mM]	Titer HC [mM]	Consumed carbon source [mM]	Carbon yield [mol $C_{product}$/ mol C_{glu+ac}]
MS-5	Standard (222 mM glucose)	10.7 ± 0.8	0.16 ± 0.004	3.6 ± 0.6	0.0	222 glu	0.018 (2-OA)
MS-5	"fed-batch" (222 mM glucose, 204 mM acetate)	16.0 ± 1.1	0.16 ± 0.004	19.6 ± 0.5	10.4 ± 0.2	222 glu 194 ac	0.065 (2-OA) 0.023 (HC)
MS-5-pHCS	Standard (222 mM glucose)	8.8 ± 0.4	0.1 ± 0.003	7.2 ± 1.3	2.6 ± 0.6	222 glu	0.037 (2-OA) 0.009 (HC)
MS-5-pHCS	"fed-batch" (222 mM glucose, 204 mM acetate)	13.8 ± 1.7	0.1 ± 0.003	27.2 ± 0.7	15.7 ± 7.2	202 glu 112 ac	0.13 (2-OA) 0.048 (HC)

Furthermore, 2-oxoglutarate and 2-hydroxyglutarate were identified in the cell culture supernatants of MS-5 and MS-5-pHCS under “fed-batch” conditions and in low quantity in the supernatant of the strain MS-5-pHCS under standard conditions. Based on the HPLC peak areas of 2-oxoglutarate and 2-hydroxyglutarate (1411 mAU*s for MS-5, 7292 mAU*s for MS-5-pHCS) drastically decreased amounts under “fed-batch” conditions can be assumed in comparison to the homocitrate producer strains. That indicates that more of the carbon source was used for 2-oxoadipate formation.

Additionally, the cell culture supernatants of the strain *C. glutamicum* MS-5 cultivated under standard as well as “fed-batch” conditions were analysed via GC-ToF-MS measurements after 48 h. Surprisingly, formation of 2-hydroxyadipate was observed under both tested conditions. 2-Hydroxyadipate is the product of the conversion of 2-oxoadipate in the proposed synthetic part of the pathway towards adipate (Fig. 3). Similar to the reduction of 2-oxoglutarate to 2-hydroxyglutarate, no enzyme activity in *C. glutamicum* is described, which naturally catalyse the reaction of 2-oxoadipate to 2-hydroxyadipate. However, it is likely that side-activities of enzymes are present which are capable of catalysing the described reductions. Furthermore, 2-oxoglutarate (under “fed-batch” conditions only), 2-hydroxyglutarate and glutarate were present in the supernatants. Glutarate formation was observed under “fed-batch” conditions up to 3 mM. The citrate cycle intermediates malate and fumarate were detected in the low milli-molar range for both strains under “fed-batch” conditions, whereas succinate was accumulated up to 12.5 mM by the strain MS-5-pHCS.

The most promising 2-oxoadipate producer strain *C. glutamicum* MS-5-pHCS was also tested under nitrogen-limited conditions. The experiment was performed in CGXII minimal medium, containing 59.6 mM nitrogen and 222 mM glucose as sole carbon source with and without “fed-batch” by additional feeding of glucose (222 mM) and acetate (204 mM) at the beginning of the stationary growth phase. Similar to the results of the homocitrate producer *C. glutamicum* MS-1, nitrogen limitation did not enhance the 2-oxoadipate titer (data not shown). Cultivation under standard conditions led to a final product titer of up to 5.2 mM 2-oxoadipate, whereas the addition of extra carbon supply slightly increased the production to a value of 8.5 mM.

In summary 2-oxoadipate production with *C. glutamicum* was demonstrated for the first time. The results obtained for 2-oxoadipate production further provide an excellent starting point for the development of an adipate producer strain.

4.8 2-Oxoadipate production under controlled conditions in a bioreactor

In the previous experiments it was shown that homocitrate and 2-oxoadipate product titers were enhanced by genetic modifications, modified cultivation conditions, and combinations of both. All these experiments were performed in 500-ml shake flasks containing 60 ml medium. As a further step to test for improved production, the most promising 2-oxoadipate producer strain *C. glutamicum* MS-5-pHCS was cultivated in 700 ml-scale under controlled conditions in a Sixfors multi fermenter system (Infors), which allows simultaneous cultivation in six independent bioreactors. Since it has been demonstrated that additional carbon supply at the beginning of the stationary growth phase enhanced product formation, three different feeding strategies were tested in duplicates:

The first strategy was the automatic feeding of glucose and acetate in dependency of the oxygen saturation. In previous experiments it was observed, that the oxygen saturation raised above 80% when glucose was completely depleted in the bioreactor. In accordance with this condition the threshold for addition of carbon supply was set to 80% oxygen saturation. When the threshold was exceeded, 20 mM glucose and 10 mM acetate were automatically added. In the second strategy, 222 mM glucose and 204 mM acetate were added by continuous feeding of a 25% glucose/12.5% acetate solution over 24 h. The third strategy was to add a single pulse of 4% (w/v) glucose and 2% (w/v) potassium acetate at the beginning of the stationary growth phase when glucose was depleted.

Since in one experiment the strain MS-5-pHCS showed significantly slower growth, the results obtained from the performed duplicates with the third strategy exhibited considerable differences. Thus, only one experiment was considered for analyses (Fig. 17). In comparison to the shake flask experiments ($\mu = 0.1 \pm 0.003$ h^{-1}) the growth rates under controlled conditions in the bioreactor were increased to values of 0.14 – 0.15 h^{-1}. Furthermore, differences in biomass formation of the various conditions and of the duplicates were observed (Fig. 17A). The starting point of the three different feeding strategies was after 24 h, when the glucose, which was applied at the beginning of the experiment was completely consumed (Fig. 17B).

After starting the feed in dependency of oxygen saturation, glucose was present during the whole cultivation and was accumulated at the end of cultivation (after 50 h) to 138 ± 24 mM. In contrast, acetate was only temporary detectable in dependency on the sample time point in relation to the time point of the feed (Fig. 17D). In case of the continuous feeding strategy, glucose accumulation in the medium started 13 h after the feed and ended up at a concentration of 51 ± 2 mM. Acetate accumulation was not observed during the whole

cultivation time. The approach of adding a single pulse revealed glucose consumption within 13 h. In comparison acetate uptake occurred faster, resulting in complete uptake within 7 h.

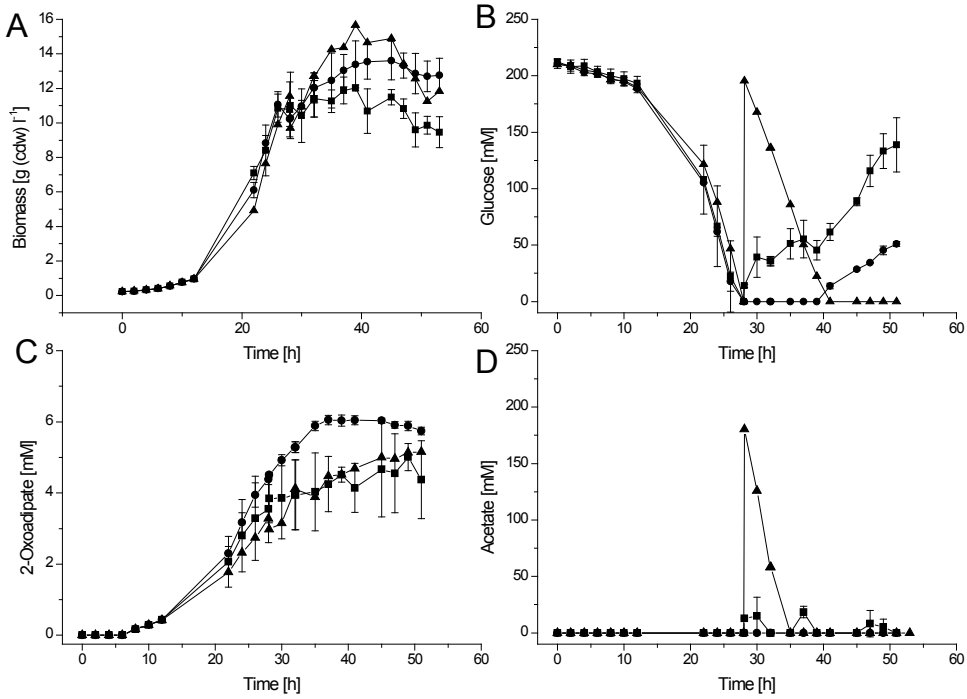

Fig. 17: Parameters of bioreactor cultivations of the 2-oxoadipate producer strain *C. glutamicum* MS-5-pHCS. Three different feeding strategies were tested and performed as duplicates in modified CGXII minimal medium with 4% (w/v) glucose omitting the buffer substance MOPS, except of the third strategy, for which only a single experiment is shown. Biomass formation (A), glucose (B) and acetate (D) consumption as well as 2-oxoadipate production (C) were analysed for each strategy: (1) Addition of 20 mM glucose and 10 mM acetate in dependency of the oxygen saturation (–■–), (2) continuous feed of 222 mM glucose and 204 mM acetate over 24 h (–●–) and (3) addition of 222 mM glucose and 204 mM acetate by a single pulse (–▲–). Average data with standard deviation are presented.

Determination of 2-oxoadipate in the cell culture supernatant revealed a maximal final product titer of up to 6 mM after 50 h of cultivation (Fig. 17C), whereas the strain accumulated up to 29.3 mM 2-oxoadipate in the shake flask experiments (Fig. 16C). Compared to the shake flask experiments none of the feeding strategies resulted in an improvement of 2-oxoadipate production. Before starting the different feedings, up to 4 mM 2-oxoadipate were accumulated, indicating that the additional carbon supply was mainly not converted to 2-oxoadipate. In contrast to the lowered 2-oxoadipate production, a high homocitrate concentration of up to 28 mM was obtained in the experiments with oxygen-dependent feeding. In shake flask experiments with 2-oxoadipate producers the highest titer of the intermediate homocitrate was about 16 mM (Tab. 15). The analyses of homocitrate

accumulation of the other two bioreactor-approaches yielded in approximately 10 mM (Tab. 16).

Tab. 16: Overview of biomass and product formation during bioreactor cultivation of the strain *C. glutamicum* MS-5-pHCS. 2-Oxoadipate**,** homocitrate, 2-oxoglutarate/2-hydroxyglutarate and glutarate concentrations were determined in the cell culture supernatants of the samples after 50 h of cultivation. Bioreactor cultivation experiments were performed with three different feeding strategies: Addition of 20 mM glucose and 10 mM acetate in dependency of the oxygen saturation (1), continuous feed of 222 mM glucose and 204 mM acetate over 24 h (2) and addition of 222 mM glucose and 204 mM acetate by a single pulse (3).

	Feeding strategy		
	1	2	3
Biomass [g_{cdw}^{-1} h^{-1}]	9.8 ± 0.5	12.8 ± 0.9	11.25
2-Oxoadipate [mM]	5.0 ± 0.4	6.0 ± 0.1	4.5
Homocitrate [mM]	28.3 ± 2.2	8.6 ± 2.5	9.5
2-Oxoglutarate/ 2-Hydroxyglutarate [mAU*s]	9496	4506	9093
Glutarate [mM]	1.8 ± 0.8	4.9 ± 0.7	3.8

In case of feeding strategy 1 and 3 by-product formation of 2-oxoglutarate and 2-hydroxyglutarate were similar compared to the shake flask cultivations of the strain *C. glutamicum* MS-5-pHCS. In contrast, only one half of 2-oxoglutarate and 2-hydroxyglutarate were produced under feeding strategy 2. Glutarate was accumulated in low millimolar levels similar to the results of the shake flask cultivations. By-product formation of homocitrate and 2-oxoglutarate leads to the suggestion that 2-oxoadipate is limited by HA or HICDH.

In summary, all tested conditions in the Bioreactor revealed drastically decreased 2-oxoadipate yields in comparison to the shake flask experiments. Besides the proposed limitation by HA and HICDH, the controlled conditions, in particular oxygen saturation, in the bioreactor might be unfavourable for 2-oxoadipate production, since 2-oxoadipate in shake flasks is mainly produced in the stationary growth phase under oxygen deprivation conditions.

5 Discussion

The overall goal of this project is the generation of a new synthetic pathway for the complete bio-based production of adipate within a microbial cell. Adipate is the most important commercial aliphatic dicarboxylic acid in the chemical industry with an estimated production of 2.6 million tons in 2010 (Merchant Research & Consulting Ltd., 2011). The chemical production process of adipate is coupled to the oil price and is linked to environmental damage and harmful substances (Galbraith *et al.*, 2010, Alini *et al.*, 2007). Confronted with these points and with the exhaustion of the earth´s fossil energy resources, the bio-based production of bulk chemicals such as adipate from renewable sources is of growing interest.

To this end, the primary aim of the studies presented here was the establishment of the production of the adipate precursor 2-oxoadipate in the biotechnologically relevant bacterium *Corynebacterium glutamicum* by heterologously expressed enzymes of the α-aminoadipate (AAA) pathway. Further aspects of this study were the analyses of growth parameters and the transcriptional response of *C. glutamicum* in the presence of adipate and 2-oxoadipate.

5.1 Influence of 2-oxoadipate and adipate on growth and global gene expression of *C. glutamicum*.

With respect to the desired production of 2-oxoadipate and finally adipate with *C. glutamicum,* their influence on growth and global gene expression of wild-type cells was analysed. The growth experiments in the presence of 50 mM (7.3 g l^{-1}), 150 mM (21.9 g l^{-1}) (data not shown), 250 mM (36.5 g l^{-1}) and 500 mM (73 g l^{-1}) adipate revealed increasing growth retardation at concentrations higher than 50 mM (Fig. 4). Similar to these results, no significant growth inhibition was obtained in the presence of 50 mM (8 g l^{-1}) 2-oxoadipate and 50 mM trisodium homocitrate (13.6 g l^{-1}). Experiments with using KOH instead of NaOH to adjust the adipate stock solution, revealed similar final biomass formation like the control, but did not completely restore the growth rate (Fig. 6). These results indicate an inhibitory effect on growth which is specifically linked to adipate and to some extent to osmotic stress in dependency of using sodium or potassium ions. In contrast to a low sodium concentration, *C. glutamicum* contains up to 800 mM potassium in the cytoplasm (Krämer *et al.*, 1990). Thus, in comparison to potassium ions the influx of sodium ions to emerge a steady state between intra- and extracellular concentrations is higher and caused osmotic stress. Additionally, it was shown that high concentrations of sodium ions are harmful for proteins and membranes by disrupting their hydration shell (Liu & Bolen, 1995). In contrast,

accumulation of intracellular potassium is described as a first response of bacterial cells toward hyperosmotic stress and contributes to the global transcriptional regulation, which is activated under osmotic stress conditions (Follmann *et al.*, 2009). In addition to potassium-mediated mechanisms, the accumulation of compatible solutes is a general defense mechanism of *C. glutamicum* to overcome hyperosmotic stress conditions. For uptake of compatible solutes such as glycine, betaine, proline and ectoine five secondary uptake systems, named BetP, PutP, ProP, EctP and LcoP have been characterised in *C. glutamicum* so far (Steger *et al.*, 2004, Peter *et al.*, 1996, Peter *et al.*, 1998). Since *betP* and *proP* showed elevated mRNA levels in the presence of 150 mM adipate (Tab. 5), cultivation experiments of *C. glutamicum* in the presence of 500 mM adipate supplemented with 5 mM proline and 5 mM glutamate were performed. Glutamate was added to supplement a possible adipate-mediated inhibition of the citrate synthase, which might be occurring due to some structural similarity of citrate and adipate. The growth rate in the presence of proline and glutamate was enhanced by 44% (μ = 0.16 h^{-1}) and the lag-phase was strongly reduced compared to the experiment without supplementation, indicating the positive effect which is likely primarily mediated by the compatible solute proline. In summary, adipate-mediated growth retardation was to some extent caused by osmotic stress, which could be compensated by both, the adjusting the pH of the adipate stock solution with potassium instead of sodium as counter ion and the addition of the compatible solute proline. Nevertheless, the growth rate of *C. glutamicum* wild-type cells was not completely restored, suggesting further inhibitory effects mediated by adipate itself.

To elucidate a possible adipate-mediated growth retardation on the transcriptional level, global gene expression experiments in the presence of 50 mM and 150 mM adipate (Tab. 5, Tab. 6) were performed. Interestingly, in the presence of 50 mM adipate, the genes *dccT* and *dctA* coding for the two dicarboxylate uptake systems in *C. glutamicum* were slightly down-regulated. These transporters were classified as an anion/sodium-dependent symporter (DccT) and a dicarboxylate amino acid-cation symporter (DctA), catalysing the uptake of the C_4-dicarboxylates succinate, fumarate and L-malate (Youn *et al.*, 2008, Youn *et al.*, 2009). Since it was shown that cultivation of the wild type in the presence of adipate caused growth retardation the strain *C. glutamicum* Δ*dccT*Δ*dctA* was cultivated in the presence of 500 mM adipate to test whether one or both of the transporters could be involved also in the uptake of adipate (Fig. 6B). The deletion of both dicarboxylate uptake systems was not beneficial for growth in the presence of 500 mM adipate, indicating that both uptake systems were not involved in transport of adipate into the cell under the conditions tested. Analyses of the data

of the global gene expression in the presence of 50 mM adipate exhibited no further obvious target genes, whose function could be linked to the growth retardation observed at higher adipate concentrations. In contrast, exposure to 150 mM adipate which clearly leads to some growth retardation, resulted in the down-regulation of further genes. Among these, several genes were identified whose corresponding proteins are participating in the central metabolism or are involved in its regulation (Tab. 6). For example, the genes *ldh* and cg3218 encoding the L-lactate dehydrogenase and a pyruvate kinase-like protein, respectively, showed the strongest decrease in mRNA levels. Further, the gene coding for transcriptional regulator RamA, announced to have global regulatory functions and primary being a regulator of the acetate metabolism (Auchter *et al.*, 2011), was slightly down-regulated under these conditions. RamA functions also as an activator of *adhA* (Zn-dependent alcohol dehydrogenase), which is down-regulated, too. This result is in agreement with the fact, that the second regulator of acetate metabolism RamB, which acts as repressor of *adhA* in the presence of glucose or acetate (Arndt & Eikmanns, 2007), is up-regulated under these conditions. The effectors of RamA and RamB were not identified so far and it seems unlikely that adipate acts as an effector of these regulators, since no further target genes of RamA and RamB were regulated in the presence of adipate. The genes which exhibited decreased mRNA levels in the presence of adipate were distributed among the central metabolism, which complicates the identification of direct target genes involved in adipate-mediated growth retardation from these data. In conclusion, the observed down-regulation of genes in response to adipate seems to be rather caused by secondary effects of the adipate-mediated growth retardation than to a direct effect of adipate.

Analyses of the genes which are up-regulated in the presence of adipate revealed the regulation of whole operons or gene clusters. Most of the genes, which showed highly elevated mRNA levels in the presence of adipate, belong to the degradation pathway of aromatic compounds, especially to the β-ketoadipate pathway in *C. glutamicum* (Fig. 18). Almost all genes of the operons/clusters *pca*, *ben* and *cat* were up-regulated at both, 50 mM and 150 mM adipate. The *pca* gene cluster, which consists of 10 genes (Fig. 18B) and one transporter gene located upstream of the *pca* operon (not shown in Fig. 18), encode the enzymes of the protocatechuate (PCA) branch of the β-ketoadipate pathway. The regulation of the PCA branch has been intensively studied in several organisms, e.g. *Pseudomonas putida* and *Acinetobacter baylyi* (Zhao *et al.*, 2010).

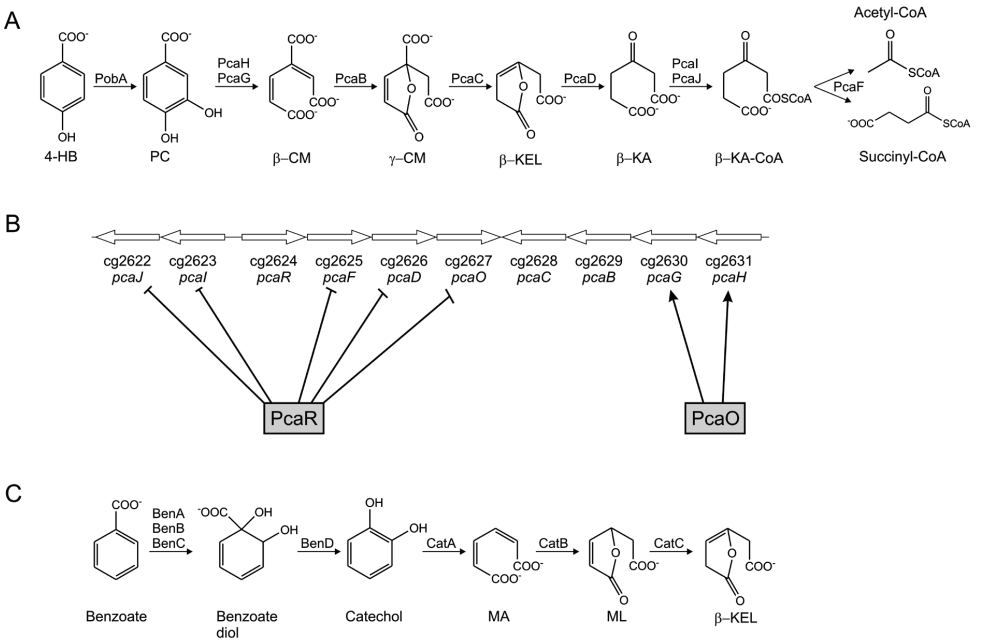

Fig. 18: Schematic overview of the β-ketoadipate pathway in *C. glutamicum* (Brinkrolf et al., 2006). (A) Metabolic pathway of the protocatechuate branch catalysing the conversion of 4-hydroxybenzoate to succinyl-CoA and acetyl-CoA. Abbreviations of the involved enzymes and metabolites: 4-HB, 4-hydroxybenzoate; PC, protocatechuate; β-CM, β-carboxy-*cis* ,*cis*-muconate; γ-CM, γ-carboxy-muconolactone; β-KEL, β-ketoadipate enol-lactone; β-KA, β-ketoadipate; β-KA-CoA, β-ketoadipyl-CoA; PobA, 4-hydroxybenzoate hydroxylase; PcaGH, protocatechuate-3,4-dioxygenase; PcaB, β-carboxy-*cis*, *cis*-muconate cycloisomerase; PcaC, γ-carboxy-muconolactone decarboxylase; PcaD, β-ketoadipate enol-lactone hydrolase; PcaIJ, β-ketoadipate succinyl-CoA transferase; PcaF, β-ketoadipyl-CoA thiolase. (B) Genetic organisation of the *pca* gene cluster in *C. glutamicum*. Boxed proteins show the two transcriptional regulators PcaR and PcaO and their respective target genes. (C) Metabolic pathway of the catechol branch of the β-ketoadipate pathway converting benzoate to β-ketoadipate enol-lactone. Abbreviations of the involved enzymes and metabolites: MA, *cis*,*cis*-muconate; ML, muconolactone; β-KEL, β-ketoadipate enol-lactone; BenAB, benzoate dioxygenase, BenC, benzoate dioxygenase reductase; BenD, 2-hydro-1,2-dihydroxybenzoate dehydrogenase; CatA, catechol-1,2-dioxygenase; CatB, *cis,cis*-muconate cycloisomerase; CatC, muconolactone isomerase.

In *C. glutamicum* the two regulators PcaR and PcaO were identified to regulate the PCA branch of the β-ketoadipate pathway. PcaR is a member of the IclR family of transcriptional regulators and is described to act as repressor of the genes *pcaIJ* and *pcaFDO* by binding to the DNA sequence motif GTTCGCATTGCGAAC (Molina-Henares *et al.*, 2006, Brinkrolf *et al.*, 2006). The second transcriptional regulator PcaO belongs to an ATP-binding LuxR (LAL)-type regulator and functions as an activator of the genes *pcaG* and *pcaH*. Transcription of *pcaO* is repressed by PcaR (Zhao *et al.*, 2010). In *P. putida* PcaR and CatR show specific affinities to adipate, which is not metabolised and seems to be a gratuitous inducer molecule of both transcriptional regulators (Romero-Steiner *et al.*, 1994). The transcriptome analyses of

C. glutamicum in the presence of adipate revealed high up-regulation of the genes *pcaIJ* and *pcaFDO* suggesting that the gene expression is no longer repressed under these conditions. Comparison of PcaR protein sequences of *C. glutamicum* and *P. putida* revealed 35.3% identity and 54.5% similarity. This result strongly indicates that adipate might also be an effector molecule for PcaR in *C. glutamicum*. In case of the second regulator PcaO it was reported, that PcaO binds only in response to protocatechuate and increased ADP level to its target sequence (Zhao *et al.*, 2010). In the presence of adipate unchanged expression level of *pcaH* and *pcaG* was observed, indicating that PcaO did not function as a transcriptional activator of *pcaH* and *pcaG* under the tested conditions in *C. glutamicum*.

Furthermore, up-regulation was observed for the genes *benA* and *benB* belonging to the *ben* operon and for the *catCBA* operon (Fig. 18C). The encoded proteins catalyse the reactions of benzoate to β-ketoadipate enol-lactone. This part of the β-ketoadipate pathway is named catechol branch (Brinkrolf *et al.*, 2006). In case of *C. glutamicum* it was postulated that the putative transcriptional regulator BenR, which belongs to the LuxR-type family, positively regulates the expression of the *ben* and *cat* operons (Brinkrolf *et al.*, 2006). BenR was described to be induced by benzoate in *P. putida* (Cowles *et al.*, 2000) and it can be assumed that adipate activates BenR-mediated transcription of *benAB* and possibly of *catCBA* in *C. glutamicum*. In addition to that, the embedding of a second, currently unknown regulator of the catechol branch is conceivable. In conclusion, an influence of adipate on the regulatory network of aromatic compound degradation in *C. glutamicum* is obvious and was revealed for the first time by these experiments.

Among the regulated operons, the genes *fabG1*, cg0345, *fadE* and *hdtZ* belonging to the predicted operon OP_cg0344 and the genes *fadD1* and cg0340 were highly up-regulated (10-38-fold) in the presence of adipate. The corresponding proteins are involved in fatty acid biosynthesis and metabolism. Furthermore it was predicted that the genes of the OP_cg0344 operon were repressed by GlxR (Schröder & Tauch, 2010). Since no further genes, which were described to be regulated by GlxR, are (highly) regulated in the presence of adipate, it seems very unlikely that adipate acts as effector of GlxR. The results rather suggest that besides GlxR, at least one other regulator is involved in the transcriptional regulation of the OP_cg0344 operon as well as the divergently orientated genes *fadD1* and cg0340 in the presence of adipate.

Furthermore, exposure of *C. glutamicum* to adipate also resulted in slightly increased mRNA levels of the *prpD2B2C2* cluster, which encodes proteins (2-methylcitrate dehydratase, 2-methylcitrate lyase, 2-methylcitrate synthase) of the 2-methylcitrate cycle and

enables *C. glutamicum* to grow on propionate as sole carbon source (Claes *et al.*, 2002). In the presence of propionate as additional carbon source, the expression of the genes *prpD2B2C2* is strongly induced (Claes *et al.*, 2002). In case of *Salmonella enterica* it was shown, that PrpR acts as transcriptional regulator of the 2-methylcitrate cycle genes (Palacios & Escalante-Semerena, 2004). Eventually, adipate functions as an effector molecule of PrpR in *C. glutamicum* leading to increased mRNA levels of the *prpD2B2C2* gene cluster. Since adipate presumably acts as effector molecule for PcaR and maybe also for further transcriptional regulators (BenR, PrpR), the application of these regulators in a biosensor system for screening adipate producers should be tested. Recently, the design and application of metabolite sensors based on transcription factors was described for *C. glutamicum* (Binder *et al.*, 2012): The transcriptional regulator LysG, which senses elevated concentrations of the basic amino acids L-lysine of L-arginine leading to the transcription of the LysG target gene *lysE*, was used for the design of an intracellular L-lysine detection system. For detection of increased intracellular L-lysine levels the *lysG* promoter was fused to a reporter gene (*eyfp*) (Binder *et al.*, 2012).

5.2 First generation of homocitrate and 2-oxoadipate producer strains

In this work the chosen strategy for establishing the 2-oxoadipate production in *C. glutamicum* was the implementation of three heterologous genes coding for homocitrate synthase, homoaconitase and homoisocitrate dehydrogenase. These enzymes naturally catalyse reactions in the α-aminoadipate (AAA) pathway, which represents one of two distinct pathways for the L-lysine biosynthesis (Xu *et al.*, 2006).

The presence of the AAA pathway in the baker´s yeast *S. cerevisiae* has been demonstrated several decades ago (Bhattacharjee & Strassman, 1967). Therefore one might speculate the easiest way to produce 2-oxoadipate could be the use of *S. cerevisiae* as production organism. In the course of this thesis, the potential of *S. cerevisiae* as natural 2-oxoadipate producer was tested by analysing two commercially available strains (data not shown). These strains are defective either in the 2-oxoadipate converting enzyme 2-aminoadipate transferase (Yer152c) or in the aromatic amino acid transferase (Ygl202w). Cultivation of these strains in SD minimal medium with and without L-lysine supplementation revealed no accumulation of 2-oxoadipate. The next step would be the construction and analyses of the double deletion strain *S. cerevisiae* Δ*yer152c*Δ*ygl202w* expected to be L-lysine auxotrophic, which was not done in this study.

The microorganism *C. glutamicum* is firmly established as host organism in industrial biotechnological applications and is intensively studied regarding the metabolism and its regulation. For this reason it was selected as host organism for 2-oxoadipate production. Two different approaches for the establishment of homocitrate and 2-oxoadipate production have been performed in this thesis: Firstly, the plasmid-based establishment by expression and testing of homocitrate synthases. The respective genes were chosen from the organisms *S. cerevisiae* (*lys20*), *T. thermophilus* (*ttc1550*) and *A. vinelandii* (*nifV*). A second plasmid, which harbours the genes *lys4* and *lys12* of *S. cerevisiae* encoding homoaconitase and homoisocitrate dehydrogenase were used for 2-oxoadipate production. Secondly, the three relevant genes of *S. cerevisiae* (*lys20*, *lys4*, *lys12*) were integrated into the genome of *C. glutamicum* to test plasmid-free production. Thereby the genes *gdh* and *aceA*, coding for glutamate dehydrogenase and isocitrate lyase, respectively, were simultaneously deleted.

Jo and co-workers (2012) reported that the deletion of *gdh* and *aceA* was beneficial for production of 2-oxoglutarate. The blocking of the glyoxylate shunt and biosynthesis of L-glutamate revealed a strong enhancement of 2-oxoglutarate production in a *C. glutamicum* strain engineered for L-glutamate production. Furthermore, the glutamate dehydrogenase was shown to be the key enzyme for converting 2-oxoglutarate to L-glutamate, whereas the production of 2-oxoglutarate was not influenced by the deletion of *gltB*, whose corresponding protein (glutamate synthase) is also participating in L-glutamate production (Jo *et al.*, 2012).

Based on glucose the maximal theoretical yield of homocitrate/2-oxoadipate is calculated to be 0.66 (66%) without considering the carbon consumed for biomass formation. Cultivation of the plasmid-based homocitrate producer strains under standard conditions revealed product formation up to 2.7 mM homocitrate (using Lys20) within 72 h, which corresponds to a yield of 0.009 mol C_{HC}/mol $C_{glucose}$. In comparison the Ttc1550-mediated homocitrate production was slightly lower (1.8 mM homocitrate, 0.006 mol C_{HC}/mol $C_{glucose}$). No homocitrate accumulation was detected when the homocitrate synthase of *A. vinelandii* (*nifV*) was tested. This was almost expected since HCS from the nitrogen-fixing *A. vinelandii* forms tiny amounts of homocitrate as cofactor for the nitrogenase. Heterologous expression of the *nifV* gene in *E. coli* showed in a proof of principle approach the extracellular accumulation of homocitrate, indicating that expression of *nifV* in *C. glutamicum* might be the limiting factor (Zheng *et al.*, 1997). In case of *E. coli* it is reported that overexpression of a heterologous protein is often connected to problems dealing with toxicity of the protein, different codon usage, inclusion bodies or missfolded protein structures (Terpe, 2006). Thus,

the adaption of the *nifV* DNA sequence to the codon usage of *C. glutamicum* might result in better expression and homocitrate formation.

As mentioned above, the plasmid-free establishment of the relevant AAA genes illustrates an important alternative in strain development for homocitrate and 2-oxoadipate production. Under standard conditions the strain MS-1 containing a single gene copy of *lys20* under control of the P_{tuf} promoter revealed an increased homocitrate production titer of up to 4.1 mM (0.014 mol C_{HC}/ mol $C_{glucose}$), compared to the plasmid-based variants. An explanation for this increase might be the enhanced intracellular 2-oxoglutarate pool, which was shown to be a result of the *gdh* deletion (Müller *et al.*, 2006). In consequence of the *gdh* deletion, a partially deregulated nitrogen starvation response was observed (Müller *et al.*, 2006), which might explain the decreased growth rate of *C. glutamicum* MS-1. This results in ammonium assimilation by the glutamate synthase instead of GDH. The glutamate synthase is not able to satisfy the glutamate demand of the cells completely (Rehm & Burkovski, 2011). Thus, the decreased growth rate is to some extent induced by a diminished L-glutamate pool and increased energy demand necessary for ammonium assimilation (Rehm & Burkovski, 2011). On the contrary, in the strain MS-5 the deletion of *aceA*, coding for isocitrate lyase did not affect the growth behaviour. This is consistent with previous results which demonstrated an unaltered growth rate of a Δ*aceA* mutant on glucose, whereas isocitrate lyase (ICL) was essential for growth on acetate (Reinscheid *et al.*, 1994).

Nevertheless, the yield of homocitrate under standard conditions was quite low, indicating that the production process is somehow limited: Comparison of the affinities of the enzymes competing for 2-oxoglutarate showed especially for the enzyme of *T. thermophilus* a high affinity with a K_M value between 5 and 24 µM, compared to the 2-oxoglutarate dehydrogenase complex (ODHC) of *C. glutamicum*, exhibiting a K_M of 80 µM (Wulandari *et al.*, 2002, Okada *et al.*, 2010, Shiio & Ujigawa-Takeda, 1980). In contrast, a significantly lower affinity with a K_M of 1.3 mM was determined for the HCS of *S. cerevisiae* (Andi *et al.*, 2004). The affinities of Lys20 and Ttc1550 toward the second substrate acetyl-CoA were almost identical (K_M values of 2.4 µM and 3.2 µM, respectively). Furthermore, a specific activity of 730 mU (mg protein)$^{-1}$ was measured for Lys20, compared to 41 mU (mg protein)$^{-1}$ for Ttc1550 (Okada *et al.*, 2010, Andi *et al.*, 2004). Since the temperature optimum of Ttc1550 is 60°C, cultivation at 30°C contributes to a loss of enzyme activity (Wulandari *et al.*, 2002). Despite the differences in substrate affinity and specific activity similar amounts of homocitrate were produced, suggesting that the production process is not limited by HCS enzyme activity itself but e.g. by a low expression level of the HCS genes, by somehow

partially inactivated enzyme or by limited precursor supply. To test whether gene expression of homocitrate synthase genes is a limiting factor, quantification of transcriptional levels by using real-time PCR could be performed in the future. Increase of the HCS gene dosage and the adaption of the HCS genes to the codon usage of *C. glutamicum* could be a further strategy to enhance the level of HCS mRNA and HCS protein in the producer strains.

Furthermore, it was shown that the homocitrate synthases are subject to complex regulation mechanisms. In organisms which contain an AAA (like) pathway almost all homocitrate synthases exhibit strong (feedback) inhibition by L-lysine, the end product of the AAA pathway (Xu *et al.*, 2006). The enzymes of *T. thermophilus* and *S. cerevisiae* are inhibited at L-lysine concentrations of 70 µM and 0.5 to 1 mM, respectively (Okada *et al.*, 2010, Feller *et al.*, 1999, Quezada *et al.*, 2011). In the past, several approaches have been performed to decrease the sensitivity toward L-lysine: Based on crystal structure information single amino acids were identified as being essential for competitive inhibition of 2-oxoglutarate binding by L-lysine. The exchange of those amino acids in *T. thermophilus*, *S. cerevisiae* and *Schizosaccharomyces pombe* HCS genes has been described to dramatically decrease the sensitivity toward L-lysine. In case of *T. thermophilus* the L-lysine insensitive variant showed comparable activity like the wild-type enzyme, whereas activity of the enzyme of *S. pombe* was strongly reduced (Okada *et al.*, 2010, Bulfer *et al.*, 2010). For the Lys20 of *S. cerevisiae* an impact of amino acids exchanges on activity was not directly tested, but a positive effect of the mutein ($Lys20^{R276K}$) was shown by an increased intracellular concentration of L-lysine (Feller *et al.*, 1999). Since the intracellular concentration of L-lysine at the mid-exponential phase of *C. glutamicum* was determined to be approximately 5 mM (Binder *et al.*, 2012), a possible inhibition of Lys20 and Ttc1550 could result in a bottleneck for homocitrate production. Thus, the L-lysine-insensitive variant $Lys20^{R276K}$, which was described to tolerate L-lysine concentrations up to 100 mM (Feller *et al.*, 1999), was tested in *C. glutamicum*. Determination of HCS enzyme activities of Lys20 and $Lys20^{R276K}$ expressed in *C. glutamicum* (Tab. 11) revealed similar values for both compared to those measured for the native Lys20 (10 mU (mg protein)$^{-1}$) in the mid-exponential phase of *S. cerevisiae* (Quezada *et al.*, 2011). Further, the decreased enzyme activity in the presence of L-lysine of both, the native Lys20 variant and the $Lys20^{R276K}$ mutein confirms the inhibitory effect of L-lysine towards the native HCS (Feller *et al.*, 1999). These results demonstrate that the mutation R276K did not decrease the sensitivity of *S. cerevisiae* HCS towards L-lysine. However, it is likely that the low homocitrate product titer was caused by L-lysine-mediated

HCS inhibition. To circumvent this "bottleneck" other L-lysine insensitive HCS variants (of *S. pombe* or *T. thermophilus*) could be tested.

Similar to the results obtained for the homocitrate producer strains, 2-oxoadipate accumulation of the plasmid-free producer strain MS-5 was slightly enhanced (3.5 mM, 0.018 mol $C_{2\text{-}OA}$/ mol $C_{glucose}$) compared to the plasmid-based producer strains *C. glutamicum*/ pEKEx2-*lys20*/pVWEx2-*lys4*-*lys12* and *C. glutamicum*/pEKEx2-*ttc1550*/pVWEx2-*lys4*-*lys12* which accumulated about 2 mM (0.013 mol $C_{2\text{-}OA}$/ mol $C_{glucose}$).

Accumulation of homocitrate by the plasmid-based 2-oxoadipate producer strains indicates a limitation of homoaconitase or homoisocitrate dehydrogenase enzyme activity. Very recently it was described that the homoaconitase Lys4 of *S. cerevisiae*, which were used in this work for the conversion of homocitrate to homoisocitrate, only catalyses the hydration of homoaconitate to homoisocitrate, but does not dehydrate homocitrate to homoaconitate. In case of *S. cerevisiae* aconitase Aco2p is not active on the citrate cycle intermediates, but specifically contributes to the dehydration of homocitrate to *cis*-homoaconitate (Fazius *et al.*, 2012). Since 2-oxoadipate production in *C. glutamicum* was proven by HPLC- and GC-ToF measurements it is suggested that the aconitase of *C. glutamicum* can also catalyse to some extent the formation of *cis*-homoaconitate from homocitrate. This has to be analysed and tested by in vitro enzyme assays and overexpression of *acn* in a 2-oxoadipate producer. Therefore, the dehydration of homocitrate is most likely a limiting factor for 2-oxoadipate production in the *C. glutamicum* strains constructed for 2-oxoadipate production. To overcome this, Aco2p from *S. cerevisiae* or other homoaconitase enzymes, e.g. of *Methanocaldococcus jannaschii* or of pig heart, should be tested. The enzyme of pig heart is described to complete the reaction of homocitrate to homoisocitrate by catalysing the dehydration of homocitrate to *cis*-homoaconitate (Jia *et al.*, 2006). Only recently, the homoaconitase of *M. jannaschii* was the first one which has been characterised in detail and which can catalyse both reactions from homocitrate to homoisocitrate (Jeyakanthan *et al.*, 2010). In comparison, homoisocitrate dehydrogenase of *S. cerevisiae* and also of *T. thermophilus* are very well characterised (Yamamoto *et al.*, 2007, Miyazaki *et al.*, 2003). However, to test whether homoaconitase or homoisocitrate dehydrogenase is a bottleneck in the production process of 2-oxoadipate, enzyme activities have to be determined, which is hampered by the fact that the substrates homoaconitate and homoisocitrate are not easily available.

Besides the selected strategy, conversion (degradation) of the end product of the AAA pathway, i.e. L-lysine, to 2-oxoadipate would provide a further opportunity for the production

of the adipate precursor. Therefore, the establishment of four enzymes, namely saccharopine dehydrogenase, saccharopine reductase, α-aminoadipate reductase and α-aminoadipate aminotransferase would be required (Xu *et al.*, 2006).

5.3 Improvement of production titers

On the assumption that a major portion of the glucose is consumed for biomass production, resulting in low availability of acetyl-CoA and 2-oxoglutarate for homocitrate and 2-oxoadipate production, modified cultivation conditions were tested. Recently, it has been shown that nitrogen limitation (59.6 mM) was beneficial for succinate production with *C. glutamicum* by redirecting the carbon used for biomass formation to product formation (Litsanov *et al.*, 2012a). Compared to nitrogen excess conditions (892 mM N), production of homocitrate and 2-oxoadipate was 3-fold and 2.5-4 fold increased under N-limiting conditions, respectively, using the plasmid-based strains (Tab. 14, Fig. 19). The highest 2-oxoadipate titer under nitrogen limitation was reached with the strain *C. glutamicum*/pEKEx2-*ttc1550*/pVWEx2-*lys4*-*lys12*, expressing the HCS gene of *T. thermophilus*. This indicates that chromosomal integration of *ttc1550* (instead of *lys20* of *S. cerevisiae*) could be tested for increased production. Surprisingly, a decreased product yield of homocitrate and 2-oxoadipate was observed under nitrogen limitation with the strains MS-1 and MS-5-pHCS harbouring the chromosomal integrations (section 4.7). It was reported that *C. glutamicum* strains lacking the *gdh* gene or cultivated under nitrogen limitation showed a somehow deregulated nitrogen response (Tesch *et al.*, 1998, Müller *et al.*, 2006). A *gdh*-defective strain has not been characterised under nitrogen limiting conditions, but the observed effects of lowered production titers indicate that the reported deregulated nitrogen response might cause a down-regulation of the "*gdh*"-locus at transcriptional level. To prove this assumption a *gdh*-defective strain has to be characterised under nitrogen limitation towards the nitrogen response. A further approach would be the analysis of the transcriptional level of the HCS gene under nitrogen surplus and limitation.

Cultivation under "fed-batch" conditions with addition of extra carbon sources (glucose, acetate, glucose + acetate, glucose + 2-oxoglutarate) at the beginning of the stationary growth phase revealed strongly increased production titers of homocitrate and 2-oxoadipate. The highest yield was achieved by adding a combination of glucose and acetate, which resulted in a 7-fold increase up to 27 mM homocitrate (0.05 mol C_{HC}/ mol $C_{glucose+acetate}$, Fig. 19). These results suggest that the production process is indeed limited by precursor supply. Most likely

acetyl-CoA is limiting, since additional glucose + 2-oxoglutarate did not further stimulate homocitrate accumulation compared to additional glucose alone.

Interestingly, the increased titers obtained in shake flasks were not reached in bioreactor cultivations under controlled conditions (Fig. 17). Here, 2-oxoadipate accumulation was about 80% decreased from 27 mM to 6 mM, independent of the applied feeding strategy. In comparison to shake flask experiments, cultivation in the bioreactor provides optimal controllable growth conditions. The conditions in shake flasks in which the cells have to cope with oxygen limitation seem to be more favourable for homocitrate/2-oxoadipate production than oxygen excess conditions in the bioreactor. This indicates that oxygen availability could be a crucial parameter for the production of homocitrate and 2-oxoadipate. It has been demonstrated that *C. glutamicum* wild type produces high amounts of organic acids, especially lactate, succinate and acetate, under oxygen deprivation (Inui *et al.*, 2004, Okino *et al.*, 2005). In the past years, *C. glutamicum* was also engineered to produce isobutanol, xylitol or D-alanine under oxygen deprivation (Blombach *et al.*, 2011, Sasaki *et al.*, 2010, Jojima *et al.*, 2010). D-alanine production from pyruvate for example was engineered by deletion of *ldhA* and *ppc* genes to prevent formation of organic acids and by overexpressing a heterologous alanine dehydrogenase (Jojima *et al.*, 2010). Further it was shown, that bioreactor cultivation of *C. glutamicum* with reduced oxygen content led to enhanced production of itaconate, whereas oxygen excess diminished the production (Otten, 2013). Thus, bioreactor cultivation under reduced oxygen availability to prevent loss of carbon for biomass formation but maintain the carbon flux via the citrate cycle could also be a promising strategy to enhance homocitrate and 2-oxoadipate production in the future.

The second strategy to enhance production titers was metabolic engineering of the central carbon metabolism of the production strains. Cultivation under standard conditions revealed that only the combination of all three modifications (deletion of *pta-ackA*, chromosomally-expressed pyc^{P458S}, and plasmid-based overexpression of *lys20*) introduced in strain MS-3-pHCS led to enhanced homocitrate accumulation. In contrast, under conditions of additional carbon supply (222 mM glucose + 204 mM acetate) all tested strains (MS-1-pHCS, MS-2, MS-3, MS-3-pHCS, MS-4) obtained a higher product yield (Fig. 19), demonstrating that homocitrate production was significantly affected by the genetic modifications only under this condition. Compared to MS-2 harbouring a plasmid-based copy of pyc^{P458S}, the chromosomally integrated pyc^{P458S} of MS-3 led to a higher accumulation of homocitrate suggesting an improved availability of acetyl-CoA or underlining general advantages of plasmid-free strains. In consequence of the deletion of acetate forming genes *pta* and *ackA*,

C. glutamicum is unable to grow on acetate as sole carbon source (Reinscheid *et al.*, 1999). Nevertheless, acetyl CoA:CoA transferase, encoded by *catA*, also catalyses CoA transfer to activate acetate to acetyl-CoA (Yasuda *et al.*, 2007, Veit *et al.*, 2009). The highest homocitrate production of up to 52 mM was achieved by using the strain MS-3-pHCS. This result corresponds to a yield of 0.21 mol C_{HC}/ mol $C_{glucose+acetate}$, representing 32% of the theoretical yield (Fig. 19).

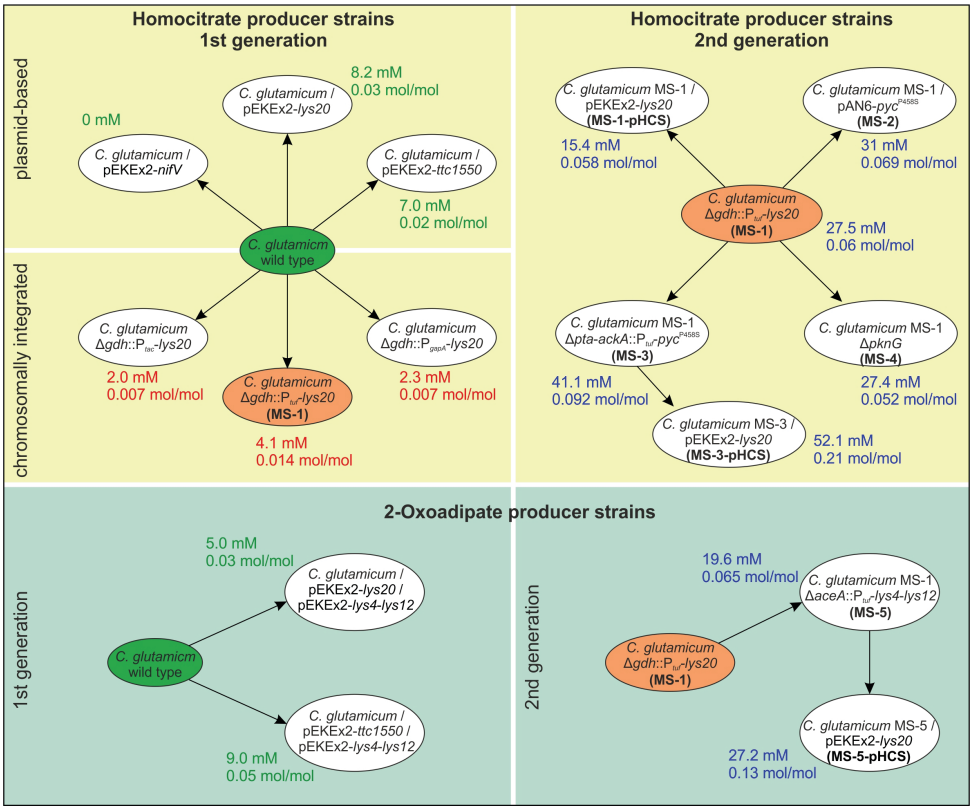

Fig. 19: Overview about homocitrate and 2-oxoadipate production by the *C. glutamicum* strains constructed in this study. Values represent the highest concentration (mM) and the highest yield ($mol_{product}$/ $mol_{carbon\ source}$) of homocitrate or 2-oxoadipate produced by the respective strain cultivated in CGXII minimal medium with 222 mM glucose as sole carbon source under standard conditions (red values), under nitrogen limitation (59.6 mM N, green values), and under "fed-batch" condition with addition of 222 mM glucose and 204 mM acetate at the beginning of the stationary growth phase (blue values).

2-Oxoadipate production was also improved by the addition of glucose and acetate. The parental strain MS-5 accumulated up to 20 mM, whereas the advanced strain MS-5-pHCS produced up to 27 mM, corresponding to yields of 0.065 mol $C_{2\text{-}OA}$/mol $C_{glucose+acetate}$ and 0.13 mol $C_{2\text{-}OA}$/mol $C_{glucose+acetate}$, respectively. In summary, the most promising 2-oxoadipate producer MS-5-pHCS achieved 20% of the maximal theoretical yield. Further, the by-product

accumulation of homocitrate showed that homocitrate was not fully converted to 2-oxoadipate under these conditions (Tab. 15). As mentioned above the aconitase/homoaconitase activity specific for the dehydration of homocitrate to form *cis*-homoaconitate is very likely the major limiting factor for 2-oxoadipate production. Therefore, additional expression von Aco2p from yeast or replacement of the homoaconitase by an enzyme variant catalysing both reactions from homocitrate to homoisocitrate should be beneficial for efficient conversion of homocitrate to 2-oxoadipate.

In addition, by-product accumulation of 2-hydroxyglutarate and 2-hydroxyadipate in the supernatant of the 2-oxoadipate producer strains was verified by GC-ToF-MS measurements. In contrast to 2-hydroxyglutarate, formation of 2-hydroxyadipate is beneficial for the desired biosynthetic pathway towards adipate (Fig. 3), since conversion of 2-oxoadipate to 2-hydroxyadipate represents the subsequent step in the pathway. In other organisms 2-hydroxyglutarate dehydrogenase, which is involved in the butanoate metabolism, is described to convert 2-oxoglutarate to 2-hydroxyglutarate. Furthermore, it has been shown that the enzymes phosphoglycerate dehydrogenase and hydroxyacid-oxoacid transhydrogenase catalyse the reduction of the C5 compound (http://www.genome.jp/kegg/kegg2.html). Enzyme activity for the reduction of 2-oxoadipate to 2-hydroxyadipate was found in the human placenta and in the heart muscle of rats, however the reductase has not been identified yet (Suda *et al.*, 1976, Suda *et al.*, 1977). In the case of isocitrate dehydrogenase, it has been demonstrated for the enzyme in human brain cancer cells that a single amino acid exchange in the protein sequence leads to loss of the natural decarboxylation activity. This cancer-associated mutation results in a completely new ability of dehydrogenase activity, catalysing the reduction of 2-oxoglutarate to 2-hydroxyglutarate (Dang *et al.*, 2009). Recently, Reitman and co-workers transferred the enzyme redesign, by homology comparisons, to the homoisocitrate dehydrogenase of *S. cerevisiae*. According to the cancer-derived mutations in the isocitrate dehydrogenase, the redesigned HICDH catalyses specifically the NADH-dependent reduction of 2-oxoadipate to 2-hydroxyadipate (Reitman *et al.*, 2012). Since 2-hydroxyglutarate and 2-hydroxyadipate were not present in the wild-type control and no enzyme activity in *C. glutamicum* is described to catalyse the formation of 2-hydroxyglutarate or 2-hydroxyadipate, sequencing of isocitrate dehydrogenase (of *C. glutamicum*) and homoisocitrate dehydrogenase (of *S. cerevisiae*) of the production strains is an option to analyse whether spontaneous mutations within these sequences emerged. However, the occurrence of side-activities of enzymes, catalysing the reactions

mentioned above, seems to be more likely and should be tested in a NADH- or NADPH-dependent enzyme assay.

In conclusion, it has been shown that the production process of homocitrate and 2-oxoadipate is limited by various bottlenecks at different stages: i) the production process is coupled to the metabolic status of growth-limited cells; ii) the enhanced 2-oxoglutarate/ 2-hydroxyglutarate accumulation of the second generation homocitrate producers reveals a limitation of either HCS activity or of acetyl-CoA supply; iii) homocitrate accumulation during 2-oxoadipate production indicated limitation by homoaconitase and/or homoisocitrate dehydrogenase.

To improve the production of 2-oxoadipate the discussed obstacles have to be addressed in further strain development. Also, the influence of oxygen availability should be tested. In addition, further metabolic engineering could improve the production: Additional gene copies coding for all three enzymes (HCS, HA, HICDH) should be chromosomally integrated. For this purpose the application of alternative enzymes (especially for the homoaconitase) of other organisms, for example of *S. pombe*, *T. thermophilus* or *M. jannaschii* can be tested. Besides different copy numbers, codon-optimised genes can be used to increase the protein level. Another option is to improve the protein translation efficiency by modulating the strength of the ribosomal binding site (Peralta-Yahya *et al.*, 2012). Additionally, the assembly of the relevant enzymes to a synthetic protein scaffold could help to improve the efficiency of multistep reactions. It was shown, that this strategy resulted in 77-fold improved mevalonate production, an intermediate in the biosynthesis of the antimalarial drug artemisinin (Dueber *et al.*, 2009). Furthermore, the metabolism has to be engineered toward an improved acetyl-CoA supply. This could be realised by overexpression of an acetyl-CoA synthetase (ACS) of *Bacillus subtilis*, which converts acetate via acetyl-AMP to acetyl-CoA. It was shown that overexpression of this enzyme led to an increased intracellular acetyl-CoA level in a *C. glutamicum* strain engineered for the aerobic succinate production (Zhu *et al.*, 2013). Moreover, promoter exchange in front of the *gltA* transcript in *C. glutamicum* for attenuated expression down to 10% residual citrate synthase activity, led to an increase of acetyl-CoA without affecting flux to citrate and consequently to 2-oxoglutarate (van Ooyen *et al.*, 2012). A further approach to improve the precursor supply could be to enhance the anaplerotic reactions by overexpression of the phosphoenolpyruvate carboxylase, which was shown to have the strongest effect on aerobic succinate production in *C. glutamicum* (Litsanov *et al.*, 2012a). Furthermore, several approaches have demonstrated that the efflux of the desired metabolite of the cell is a crucial challenge for an efficient production process. For example,

the amino acid exporter LysE was identified to be required for efficient L-lysine production (Bellmann *et al.*, 2001, Vrljic *et al.*, 1996). Similarly, the membrane protein SucE participates in the export of the dicarboxylic acid succinate (Huhn *et al.*, 2011). In case of homocitrate and 2-oxoadipate, the export is not characterised so far, but could be tested by determination of intracellular and extracellular concentrations using deletion mutants of candidate transporters. If export limitation is obvious, subsequent overexpression of the relevant exporter system seems to be a promising strategy to further enhance product formation.

5.4 On the route toward adipate

In the past years several approaches were performed using the organisms *P. putida* and *E. coli* to produce the adipate precursor *cis*, *cis*-muconate resulting in titers of up to 18.5 g l^{-1} with 96% molar product yield and 36.8 g l^{-1} with 22% molar product yield, respectively (van Duuren *et al.*, 2012, Niu *et al.*, 2002). Very recently, formation of *cis*, *cis*-muconate has also been demonstrated with *S. cerevisiae* (Curran *et al.*, 2013). However, since the resulting maximal titer of up to 0.2 g l^{-1} was very low, it was discussed that metabolic engineering of *S. cerevisiae* for *cis*, *cis*-muconate production seems to be much more difficult than with *E. coli* as the metabolic network in yeast is more rigid against modifications (Curran *et al.*, 2013). The precursor *cis*, *cis*-muconate has to be purified sufficiently from the cultivation broth and can be reduced in a hydrogenation process using platinum on carbon as catalyst to form adipate (Niu *et al.*, 2002). However, hitherto no enzyme was found or described catalysing the reduction of *cis, cis*-muconate to adipate directly in the cell.

Besides the approaches of engineering organisms for the production of *cis*, *cis*-muconate, the pathway to adipate via 2-oxoadipate as illustrated here, provides a new biosynthetic alternative toward the biotechnological production of adipate directly in the cell. In this work *C. glutamicum* was tested and engineered for the production of the adipate precursors homocitrate and 2-oxoadipate for the first time. The feasibility to produce homocitrate and 2-oxoadipate with *C. glutamicum* was demonstrated by plasmid-based implementation as well as by chromosomal integration of the genes coding for enzymes of the α-aminoadipate pathway. The most promising strain MS-5-pHCS produced up to 4.4 g l^{-1} 2-oxoadipate with a product yield of 20% in shake flasks. Furthermore, 3.2 g l^{-1} of the intermediate homocitrate was accumulated.

The establishment of the aspired biosynthetic route from 2-oxoadipate to adipate requires five further enzymatic reactions via the intermediates, 2-hydroxyadipate and 2-hexendioate (Fig. 3). Since 2-hydroxyadipate has been identified in this work, an enzyme activity

catalysing this reaction appears to be already present in *C. glutamicum* and the enzyme has to be identified. To establish the first biosynthetic pathway by reduction of 2-oxoadipate to adipate, a feasible strategy seems to be evolving enzymes of the reductive citrate cycle, catalysing naturally the reduction of oxaloacetate to succinate via malate and fumarate. As described by Buckel and co-workers the direct dehydration of 2-hydroxyadipate to 2-hexendioate is chemically not feasible and therefore CoA-activated intermediates has to be considered (Parthasarathy *et al.*, 2011). Also, no enzyme activity for the final oxidation of 2-hexendioate to adipate has been described. The development of an enzyme activity catalysing this step remains an open question to finalise the pathway for bio-based production of adipate via α-reduction of the AAA pathway intermediate 2-oxoadipate.

6 References

Abe, S., Takayama, K. & Kinoshita, S., (1967) Taxonomical studies on glutamic acid producing bacteria. *J Gen Appl Microbiol* **13**: 279-301.

Ajinomoto Co. Inc., (2010a) Feed-use amino acids business. *http://www.ajinomoto.com/ir/pdf/Food-Oct2010.pdf*.

Ajinomoto Co. Inc., (2010b) Food products business. *http://www.ajinomoto.com/ir/pdf/Food-Oct2010.pdf*.

Alini, S., Basile, F., Blasioli, S., Rinaldi, C. & Vaccari, A., (2007) Development of new catalysts for N2O-decomposition from adipic acid plant. *Applied Catalysis B: Environmental* **70**: 323-329.

Andi, B., West, A. H. & Cook, P. F., (2004) Stabilization and characterization of histidine-tagged homocitrate synthase from *Saccharomyces cerevisiae*. *Arch Biochem Biophys* **421**: 243-254.

Andi, B., West, A. H. & Cook, P. F., (2005) Regulatory mechanism of histidine-tagged homocitrate synthase from *Saccharomyces cerevisiae*. *J Biol Chem* **280**: 31624-31632.

Armstrong, J. M., (1964) The molar extinction coefficient of 2,6-dichlorphenol indophenol. *Biochimica et biophysica acta* **86**: 194-197.

Arndt, A. & Eikmanns, B. J., (2007) The alcohol dehydrogenase gene *adhA* in *Corynebacterium glutamicum* is subject to carbon catabolite repression. *J Bacteriol* **189**: 7408-7416.

Auchter, M., Cramer, A., Hüser, A., Rückert, C., Emer, D., Schwarz, P.*, et al.*, (2011) RamA and RamB are global transcriptional regulators in *Corynebacterium glutamicum* and control genes for enzymes of the central metabolism. *J Biotechnol* **154**: 126-139.

Bailey, J., (1991) Toward a science of metabolic engineering. *Science* **252**: 1668-1675.

Bang, S. G. & Choi, C. Y., (1995) DO-stat fed-batch production of *cis*, *cis*-muconic acid from benzoic acid by *Pseudomonas putida* BM014. *Journal of Fermentation and Bioengineering* **79**: 381-383.

Bellmann, A., Vrljic, M., Patek, M., Sahm, H., Kramer, R. & Eggeling, L., (2001) Expression control and specificity of the basic amino acid exporter LysE of *Corynebacterium glutamicum*. *Microbiology* **147**: 1765-1774.

Bhattacharjee, J. K. & Strassman, M., (1967) Accumulation of Tricarboxylic Acids Related to Lysine Biosynthesis in a Yeast Mutant. *Journal of Biological Chemistry* **242**: 2542-2546.

Bimboim, H. C. & Doly, J., (1979) A rapid alkaline extraction procedure for screening recombinant plasmid DNA. *Nucleic Acids Res* **7**: 1513-1523.

Binder, S., Schendzielorz, G., Stabler, N., Krumbach, K., Hoffmann, K., Bott, M.*, et al.*, (2012) A high-throughput approach to identify genomic variants of bacterial metabolite producers at the single-cell level. *Genome Biology* **13**: R40.

Blach, P., Böstrom, Z., Franceschi-Messant, S., Lattes, A., Perez, E. & Rico-Lattes, I., (2010) Recyclable process for sustainable adipic acid production in microemulsions. *Tetrahedron* **66**: 7124-7128.

Blombach, B., Riester, T., Wieschalka, S., Ziert, C., Youn, J. W., Wendisch, V. F.*, et al.*, (2011) *Corynebacterium glutamicum* tailored for efficient isobutanol production. *Appl Environ Microbiol* **77**: 3300-3310.

Bott, M., (2007) Offering surprises: TCA cycle regulation in *Corynebacterium glutamicum*. *Trends in microbiology* **15**: 417-425.

Brinkrolf, K., Brune, I. & Tauch, A., (2006) Transcriptional regulation of catabolic pathways for aromatic compounds in *Corynebacterium glutamicum*. *Genetics and molecular research : GMR* **5**: 773-789.

Brzostowicz, P. C., Walters, D. M., Thomas, S. M., Nagarajan, V. & Rouviere, P. E., (2003) mRNA differential display in a microbial enrichment culture: simultaneous identification of three cyclohexanone monooxygenases from three species. *Appl Environ Microbiol* **69**: 334-342.

Bulfer, S. L., Scott, E. M., Pillus, L. & Trievel, R. C., (2010) Structural basis for L-lysine feedback inhibition of homocitrate synthase. *J Biol Chem* **285**: 10446-10453.

Busche, T., Silar, R., Picmanova, M., Patek, M. & Kalinowski, J., (2012) Transcriptional regulation of the operon encoding stress-responsive ECF sigma factor SigH and its anti-sigma factor RshA, and control of its regulatory network in *Corynebacterium glutamicum*. *BMC Genomics* **13**: 445.

Cheng, Q., Thomas, S. M. & Rouviere, P., (2002) Biological conversion of cyclic alkanes and cyclic alcohols into dicarboxylic acids: biochemical and molecular basis. *Appl Microbiol Biotechnol* **58**: 704-711.

Choi, W. J., Lee, E. Y., Cho, M. H. & Choi, C. Y., (1997) Enhanced production of *cis*,*cis*-muconate in a cell-recycle bioreactor. *Journal of Fermentation and Bioengineering* **84**: 70-76.

Claes, W. A., Pühler, A. & Kalinowski, J., (2002) Identification of Two *prpDBC* Gene Clusters in *Corynebacterium glutamicum* and Their Involvement in Propionate Degradation via the 2-Methylcitrate Cycle. *J Bacteriol* **184**: 2728-2739.

Collier, L. S., Gaines, G. L., 3rd & Neidle, E. L., (1998) Regulation of benzoate degradation in *Acinetobacter* sp. strain ADP1 by BenM, a LysR-type transcriptional activator. *J Bacteriol* **180**: 2493-2501.

Cooke, P., (2008) Cleantech and an Analysis of the Platform Nature of Life Sciences: Further Reflections upon Platform Policies. *European Planning Studies* **16**.

Cowles, C. E., Nichols, N. N. & Harwood, C. S., (2000) BenR, a XylS homologue, regulates three different pathways of aromatic acid degradation in *Pseudomonas putida*. *J Bacteriol* **182**: 6339-6346.

Curran, K. A., Leavitt, J. M., Karim, A. S. & Alper, H. S., (2013) Metabolic engineering of muconic acid production in *Saccharomyces cerevisiae*. *Metab Eng* **15**: 55-66.

Dang, L., White, D. W., Gross, S., Bennett, B. D., Bittinger, M. A., Driggers, E. M.*, et al.*, (2009) Cancer-associated IDH1 mutations produce 2-hydroxyglutarate. *Nature* **462**: 739-744.

Davis, D. D., (1985) Adipic acid. In: Ullman's Encyclopedia of Industrial Chemistry. Gerhartz, W. (ed). New York: John Wiley and Sons, pp. 270-272.

de Boer, H. A., Comstock, L. J. & Vasser, M., (1983) The tac promoter: a functional hybrid derived from the trp and lac promoters. *Proceedings of the National Academy of Sciences* **80**: 21-25.

Djurdjevic, I., Zelder, O. & Buckel, W., (2011) Production of glutaconic acid in a recombinant *Escherichia coli* strain. *Appl Environ Microbiol* **77**: 320-322.

Draths, K. M. & Frost, J. W., (1994) Environmentally compatible synthesis of adipic acid from D-glucose. *Journal of the American Chemical Society* **116**: 399-400.

Dueber, J. E., Wu, G. C., Malmirchegini, G. R., Moon, T. S., Petzold, C. J., Ullal, A. V.*, et al.*, (2009) Synthetic protein scaffolds provide modular control over metabolic flux. *Nat Biotechnol* **27**: 753-759.

Durrant, M. C., Francis, A., Lowe, D. J., Newton, W. E. & Fisher, K., (2006) Evidence for a dynamic role for homocitrate during nitrogen fixation: the effect of substitution at the α-Lys426 position in MoFe-protein of *Azotobacter vinelandii*. *Biochem J* **397**: 261-270.

Eggeling, L. & Bott, M., (2005) *Handbook Of Corynebacterium glutamicum*. CRC Press.

Eikmanns, B. J., Kleinertz, E., Liebl, W. & Sahm, H., (1991) A family of *Corynebacterium glutamicum*/*Escherichia coli* shuttle vectors for cloning, controlled gene expression, and promoter probing. *Gene* **102**: 93-98.

Fazius, F., Shelest, E., Gebhardt, P. & Brock, M., (2012) The fungal α-aminoadipate pathway for lysine biosynthesis requires two enzymes of the aconitase family for the isomerization of homocitrate to homoisocitrate. *Molecular Microbiology* **86**: 1508-1530.

Feller, A., Ramos, F., Pierard, A. & Dubois, E., (1999) In *Saccharomyces cerevisae*, feedback inhibition of homocitrate synthase isoenzymes by lysine modulates the activation of LYS gene expression by Lys14p. *Eur J Biochem* **261**: 163-170.

Follmann, M., Becker, M., Ochrombel, I., Ott, V., Krämer, R. & Marin, K., (2009) Potassium Transport in *Corynebacterium glutamicum* Is Facilitated by the Putative Channel Protein CglK, Which Is Essential for pH Homeostasis and Growth at Acidic pH. *J Bacteriol* **191**: 2944-2952.

Frunzke, J., Engels, V., Hasenbein, S., Gätgens, C. & Bott, M., (2008) Co-ordinated regulation of gluconate catabolism and glucose uptake in *Corynebacterium glutamicum* by two functionally equivalent transcriptional regulators, GntR1 and GntR2. *Molecular Microbiology* **67**: 305-322.

Galbraith, D., Gross, S. A. & Paustenbach, D., (2010) Benzene and human health: A historical review and appraisal of associations with various diseases. *Crit Rev Toxicol* **40 Suppl 2**: 1-46.

Global Industry Analysts Inc., (2012) Adipic Acid: A Global Strategic Business Report. In. San Jose, California, USA: PRWEB.

Graham, D. E., (2011) Chapter fifteen - 2-Oxoacid Metabolism in Methanogenic CoM and CoB Biosynthesis. In: Methods in Enzymology. Amy, C. R. & Stephen, W. R. (eds). Academic Press, pp. 301-326.

Gregersen, N., Mortensen, P. B. & Kolvraa, S., (1983) On the biologic origin of C6-C10-dicarboxylic and C6-C10-omega-1-hydroxy monocarboxylic acids in human and rat with acyl-CoA dehydrogenation deficiencies: in vitro studies on the omega- and omega-1-oxidation of medium-chain (C6-C12) fatty acids in human and rat liver. *Pediatr Res* **17**: 828-834.

Grodsky, N. B., Soundar, S. & Colman, R. F., (2000) Evaluation by Site-Directed Mutagenesis of Aspartic Acid Residues in the Metal Site of Pig Heart NADP-Dependent Isocitrate Dehydrogenase. *Biochemistry* **39**: 2193-2200.

Hamilton, T. L., Ludwig, M., Dixon, R., Boyd, E. S., Dos Santos, P. C., Setubal, J. C., *et al.*, (2011) Transcriptional Profiling of Nitrogen Fixation in *Azotobacter vinelandii*. *J Bacteriol* **193**: 4477-4486.

Hanahan, D., (1985) Techniques for transformation of *E. coli*. *In DNA-cloning, Vol.1 Glover, D.M. (ed.). Oxford: IRL-Press, pp. 109–135*.

Howell, D. M., Harich, K., Xu, H. & White, R. H., (1998) Alpha-keto acid chain elongation reactions involved in the biosynthesis of coenzyme B (7-mercaptoheptanoyl threonine phosphate) in methanogenic Archaea. *Biochemistry* **37**: 10108-10117.

Huhn, S., Jolkver, E., Kramer, R. & Marin, K., (2011) Identification of the membrane protein SucE and its role in succinate transport in *Corynebacterium glutamicum*. *Appl Microbiol Biotechnol* **89**: 327-335.

Ikeda, M., Ohnishi, J., Hayashi, M. & Mitsuhashi, S., (2006) A genome-based approach to create a minimally mutated *Corynebacterium glutamicum* strain for efficient l-lysine production. *J IND MICROBIOL BIOTECHNOL* **33**: 610-615.

Inui, M., Murakami, S., Okino, S., Kawaguchi, H., Vertes, A. A. & Yukawa, H., (2004) Metabolic analysis of *Corynebacterium glutamicum* during lactate and succinate productions under oxygen deprivation conditions. *J Mol Microbiol Biotechnol* **7**: 182-196.

Jeyakanthan, J., Drevland, R. M., Gayathri, D. R., Velmurugan, D., Shinkai, A., Kuramitsu, S., *et al.*, (2010) Substrate Specificity Determinants of the Methanogen Homoaconitase Enzyme: Structure and Function of the Small Subunit. *Biochemistry* **49**: 2687-2696.

Jia, Y., Tomita, T., Yamauchi, K., Nishiyama, M. & Palmer, D. R. J., (2006) Kinetics and product analysis of the reaction catalysed by recombinant homoaconitase from *Thermus thermophilus*. *Biochem J* **396**: 479-485.

Jo, J. H., Seol, H. Y., Lee, Y. B., Kim, M. H., Hyun, H. H. & Lee, H. H., (2012) Disruption of genes for the enhanced biosynthesis of alpha-ketoglutarate in *Corynebacterium glutamicum*. *Can J Microbiol* **58**: 278-286.

Jojima, T., Fujii, M., Mori, E., Inui, M. & Yukawa, H., (2010) Engineering of sugar metabolism of *Corynebacterium glutamicum* for production of amino acid L-alanine under oxygen deprivation. *Appl Microbiol Biotechnol* **87**: 159-165.

Kabus, A., Niebisch, A. & Bott, M., (2007) Role of Cytochrome bd Oxidase from *Corynebacterium glutamicum* in Growth and Lysine Production. *Appl Environ Microbiol* **73**: 861-868.

Kalinowski, J., Bathe, B., Bartels, D., Bischoff, N., Bott, M., Burkovski, A., *et al.*, (2003) The complete *Corynebacterium glutamicum* ATCC 13032 genome sequence and its impact on the production of l-aspartate-derived amino acids and vitamins. *J Biotechnol* **104**: 5-25.

Keasling, J. D., (2008) Synthetic biology for synthetic chemistry. *ACS Chem Biol* **3**: 64-76.

Keasling, J. D., (2012) Synthetic biology and the development of tools for metabolic engineering. *Metab Eng* **14**: 189-195.

Kinoshita, S., Udaka, S. & Shimono, M., (1957) Studies on the amino acid fermentation. Part 1. Production of L-glutamic acid by various microorganisms. *J Gen Appl Microbiol* **3**: 193-205.

Koch-Koerfges, A., Kabus, A., Ochrombel, I., Marin, K. & Bott, M., (2012) Physiology and global gene expression of a *Corynebacterium glutamicum* ΔF1FO-ATP synthase mutant devoid of oxidative phosphorylation. *Biochimica et Biophysica Acta (BBA) - Bioenergetics* **1817**: 370-380.

Kosuge, T. & Hoshino, T., (1998) Lysine is synthesized through the alpha-aminoadipate pathway in *Thermus thermophilus*. *FEMS Microbiol Lett* **169**: 361-367.

Krämer, R., Lambert, C., Hoischen, C. & Ebbighausen, H., (1990) Uptake of glutamate in *Corynebacterium glutamicum*. *European Journal of Biochemistry* **194**: 929-935.

Litsanov, B., Brocker, M. & Bott, M., (2012b) Toward Homosuccinate Fermentation: Metabolic Engineering of *Corynebacterium glutamicum* for Anaerobic Production of Succinate from Glucose and Formate. *Appl Environ Microbiol* **78**: 3325-3337.

Litsanov, B., Brocker, M. & Bott, M., (2013) Glycerol as a substrate for aerobic succinate production in minimal medium with *Corynebacterium glutamicum*. *Microb Biotechnol* **6**: 189-195.

Litsanov, B., Kabus, A., Brocker, M. & Bott, M., (2012a) Efficient aerobic succinate production from glucose in minimal medium with *Corynebacterium glutamicum*. *Microb Biotechnol* **5**: 116-128.

Liu, Y. & Bolen, D. W., (1995) The Peptide Backbone Plays a Dominant Role in Protein Stabilization by Naturally Occurring Osmolytes. *Biochemistry* **34**: 12884-12891.

Luedeke, V., (1977) In: McKetta J., Cunningham W. (Eds.). In: Encyclopedia of Chemical Processing and Design. Marcel Dekker Inc. New York, pp. 128-146.

Matsuoka, M., Ju, W.-S., Takahashi, K., Yamashita, H. & Anpo, M., (2000) Photocatalytic Decomposition of N2O into N2 and O2 at 298 K on Cu(I) Ion Catalysts Anchored onto Various Oxides. The Effect of the Coordination State of the Cu(I) Ions on the Photocatalytic Reactivity. *The Journal of Physical Chemistry B* **104**: 4911-4915.

McFall, S. M., Chugani, S. A. & Chakrabarty, A. M., (1998) Transcriptional activation of the catechol and chlorocatechol operons: variations on a theme. *Gene* **223**: 257-267.

Merchant Research & Consulting Ltd., (2011) Adipic acid 2011 World Market Outlook and Forecast. In., pp.

Miyazaki, J., Kobashi, N., Nishiyama, M. & Yamane, H., (2003) Characterization of Homoisocitrate Dehydrogenase Involved in Lysine Biosynthesis of an Extremely Thermophilic Bacterium,*Thermus thermophilus* HB27, and Evolutionary Implication of β-Decarboxylating Dehydrogenase. *Journal of Biological Chemistry* **278**: 1864-1871.

Mizuno, S., Yoshikawa, N., Seki, M., Mikawa, T. & Imada, Y., (1988) Microbial production of *cis*, *cis*-muconic acid from benzoic acid. *Appl Microbiol Biotechnol* **28**: 20-25.

Molina-Henares, A. J., Krell, T., Eugenia Guazzaroni, M., Segura, A. & Ramos, J. L., (2006) Members of the IclR family of bacterial transcriptional regulators function as activators and/or repressors. *FEMS Microbiology Reviews* **30**: 157-186.

Moon, T. S., Dueber, J. E., Shiue, E. & Prather, K. L., (2010) Use of modular, synthetic scaffolds for improved production of glucaric acid in engineered *E. coli*. *Metab Eng* **12**: 298-305.

Moon, T. S., Yoon, S. H., Lanza, A. M., Roy-Mayhew, J. D. & Prather, K. L., (2009) Production of glucaric acid from a synthetic pathway in recombinant *Escherichia coli*. *Appl Environ Microbiol* **75**: 589-595.

Mortensen, P. B., (1980) The possible antiketogenic and gluconeogenic effect of the ω-oxidation of fatty acids in rats. *Biochimica et Biophysica Acta (BBA) - Lipids and Lipid Metabolism* **620**: 177-185.

Müller, T., Strösser, J., Buchinger, S., Nolden, L., Wirtz, A., Krämer, R.*, et al.*, (2006) Mutation-induced metabolite pool alterations in *Corynebacterium glutamicum*: Towards the identification of nitrogen control signals. *J Biotechnol* **126**: 440-453.

Mullis, K., Faloona, F., Scharf, S., Saiki, R., Horn, G. & Erlich, H., (1986) Specific Enzymatic Amplification of DNA In Vitro: The Polymerase Chain Reaction. *Cold Spring Harbor Symposia on Quantitative Biology* **51**: 263-273.

Musser, M. T., (2005) Adipic acid. In: ULLMANN´S Encyclopedia of Industrial Chemistry. Wiley-VCH Verlag GmbH & Co. KGaA, Weinheim, pp. 537-548.

Niebisch, A. & Bott, M., (2001) Molecular analysis of the cytochrome bc 1-aa 3 branch of the *Corynebacterium glutamicum* respiratory chain containing an unusual diheme cytochrome c 1. *Arch Microbiol* **175**: 282-294.

Niebisch, A., Kabus, A., Schultz, C., Weil, B. & Bott, M., (2006) Corynebacterial Protein Kinase G Controls 2-Oxoglutarate Dehydrogenase Activity via the Phosphorylation Status of the OdhI Protein. *Journal of Biological Chemistry* **281**: 12300-12307.

Nishida, H. & Nishiyama, M., (2000) What is characteristic of fungal lysine synthesis through the alpha-aminoadipate pathway? *Journal of molecular evolution* **51**: 299-302.

Niu, W., Draths, K. M. & Frost, J. W., (2002) Benzene-free synthesis of adipic acid. *Biotechnol Prog* **18**: 201-211.

Okada, T., Tomita, T., Wulandari, A. P., Kuzuyama, T. & Nishiyama, M., (2010) Mechanism of Substrate Recognition and Insight into Feedback Inhibition of Homocitrate Synthase from *Thermus thermophilus*. *Journal of Biological Chemistry* **285**: 4195-4205.

Okino, S., Inui, M. & Yukawa, H., (2005) Production of organic acids by *Corynebacterium glutamicum* under oxygen deprivation. *Appl Microbiol Biotechnol* **68**: 475-480.

Okino, S., Noburyu, R., Suda, M., Jojima, T., Inui, M. & Yukawa, H., (2008) An efficient succinic acid production process in a metabolically engineered *Corynebacterium glutamicum* strain. *Appl Microbiol Biotechnol* **81**: 459-464.

Otten, A., (2013) *Metabolic engineering von Corynebacterium glutamicum für die Produktion einer Dicarbonsäure,* p. 98 S. Forschungszentrum Jülich GmbH Zentralbibliothek, Verlag, Jülich.

Palacios, S. & Escalante-Semerena, J. C., (2004) 2-Methylcitrate-dependent activation of the propionate catabolic operon (prpBCDE) of *Salmonella enterica* by the PrpR protein. *Microbiology* **150**: 3877-3887.

Parthasarathy, A., Pierik, A. J., Kahnt, J., Zelder, O. & Buckel, W., (2011) Substrate specificity of 2-hydroxyglutaryl-CoA dehydratase from *Clostridium symbiosum*: toward a bio-based production of adipic acid. *Biochemistry* **50**: 3540-3550.

Peralta-Yahya, P. P., Zhang, F., del Cardayre, S. B. & Keasling, J. D., (2012) Microbial engineering for the production of advanced biofuels. *Nature* **488**: 320-328.

Peter, H., Burkovski, A. & Krämer, R., (1996) Isolation, characterization, and expression of the *Corynebacterium glutamicum betP* gene, encoding the transport system for the compatible solute glycine betaine. *J Bacteriol* **178**: 5229-5234.

Peter, H., Weil, B., Burkovski, A., Krämer, R. & Morbach, S., (1998) *Corynebacterium glutamicum* Is Equipped with Four Secondary Carriers for Compatible Solutes: Identification, Sequencing, and Characterization of the Proline/Ectoine Uptake System, ProP, and the Ectoine/Proline/Glycine Betaine Carrier, EctP. *J Bacteriol* **180**: 6005-6012.

Peters-Wendisch, P., Schiel, B., Wendisch, V., Katsoulidis, E., Möckel, B., Sahm, H*., et al.*, (2001) Pyruvate carboxylase is a major bottleneck for glutamate and lysine production by *Corynebacterium glutamicum*. *J Mol Microbiol Biotechnol* **2**: 295-300.

Quezada, H., Marín-Hernández, A., Aguilar, D., López, G., Gallardo-Pérez, J. C., Jasso-Chávez, R*., et al.*, (2011) The Lys20 homocitrate synthase isoform exerts most of the flux control over the lysine synthesis pathway in *Saccharomyces cerevisiae*. *Molecular Microbiology* **82**: 578-590.

Rehm, N. & Burkovski, A., (2011) Engineering of nitrogen metabolism and its regulation in *Corynebacterium glutamicum*: influence on amino acid pools and production. *Appl Microbiol Biotechnol* **89**: 239-248.

Reimer, R. A., Slaten, C. S., Seapan, M., Lower, M. W. & Tomlinson, P. E., (1994) Abatement of N2O emissions produced in the adipic acid industry. *Environmental Progress* **13**: 134-137.

Reinscheid, D. J., Eikmanns, B. J. & Sahm, H., (1994) Characterization of the isocitrate lyase gene from *Corynebacterium glutamicum* and biochemical analysis of the enzyme. *J Bacteriol* **176**: 3474-3483.

Reinscheid, D. J., Schnicke, S., Rittmann, D., Zahnow, U., Sahm, H. & Eikmanns, B. J., (1999) Cloning, sequence analysis, expression and inactivation of the *Corynebacterium glutamicum pta-ack* operon encoding phosphotransacetylase and acetate kinase. *Microbiology* **145**: 503-513.

Reitman, Z. J., Choi, B. D., Spasojevic, I., Bigner, D. D., Sampson, J. H. & Yan, H., (2012) Enzyme redesign guided by cancer-derived IDH1 mutations. *Nat Chem Biol* **8**: 887-889.

Romero-Steiner, S., Parales, R. E., Harwood, C. S. & Houghton, J. E., (1994) Characterization of the *pcaR* regulatory gene from *Pseudomonas putida*, which is required for the complete degradation of p-hydroxybenzoate. *J Bacteriol* **176**: 5771-5779.

Sambrook, J., MacCallum, P. & Russell, D., (2001) *Molecular Cloning. A Laboratory Manual*. 3rd ed. Ed., Cold Spring Harbor Laboratory Press, Cold Spring Harbor, New York.

Sasaki, M., Jojima, T., Inui, M. & Yukawa, H., (2010) Xylitol production by recombinant *Corynebacterium glutamicum* under oxygen deprivation. *Appl Microbiol Biotechnol* **86**: 1057-1066.

Sato, K., Aoki, M. & Noyori, R., (1998) A "Green" route to adipic acid: direct oxidation of cyclohexenes with 30 percent hydrogen peroxide. *Science* **281**: 1646-1647.

Sauer, M., Porro, D., Mattanovich, D. & Branduardi, P., (2008) Microbial production of organic acids: expanding the markets. *Trends Biotechnol* **26**: 100-108.

Schäfer, A., Tauch, A., Jäger, W., Kalinowski, J., Thierbach, G. & Pühler, A., (1994) Small mobilizable multi-purpose cloning vectors derived from the *Escherichia coli* plasmids pK18 and pK19: selection of defined deletions in the chromosome of *Corynebacterium glutamicum*. *Gene* **145**: 69-73.

Schmidt, E. & Knackmuss, H.-J., (1984) Production of *cis*,*cis*-muconate from benzoate and 2-fluoro-*cis*,*cis*-muconate from 3-fluorobenzoate by 3-chlorobenzoate degrading bacteria. *Appl Microbiol Biotechnol* **20**: 351-355.

Schöbel, F., Jacobsen, I. D. & Brock, M., (2010) Evaluation of Lysine Biosynthesis as an Antifungal Drug Target: Biochemical Characterization of *Aspergillus fumigatus* Homocitrate Synthase and Virulence Studies. *Eukaryotic Cell* **9**: 878-893.

Schröder, J. & Tauch, A., (2010) Transcriptional regulation of gene expression in *Corynebacterium glutamicum*: the role of global, master and local regulators in the modular and hierarchical gene regulatory network. *FEMS Microbiology Reviews* **34**: 685-737.

Schultz, C., Niebisch, A., Gebel, L. & Bott, M., (2007) Glutamate production by *Corynebacterium glutamicum*: dependence on the oxoglutarate dehydrogenase inhibitor protein OdhI and protein kinase PknG. *Appl Microbiol Biotechnol* **76**: 691-700.

Schwarzer, A. & Puhler, A., (1991) Manipuiation of *Corynebacterium glutamicum* by Gene Disruption and Replacement. *Nat Biotech* **9**: 84-87.

Shiio, I. & Ujigawa-Takeda, K., (1980) Presence and regulation of alpha-ketoglutarate dehydrogenase complex in a glutamate-producing bacterium, *Brevibacterium flavum*. *Agric. Biol. Chem.* **44**: 1897-1904.

Steffensen, W. S. & Alexander, M., (1995) Role of competition for inorganic nutrients in the biodegradation of mixtures of substrates. *Appl Environ Microbiol* **61**: 2859-2862.

Steger, R., Weinand, M., Krämer, R. & Morbach, S., (2004) LcoP, an osmoregulated betaine/ectoine uptake system from *Corynebacterium glutamicum*. *FEBS Letters* **573**: 155-160.

Suda, T., Robinson, J. C. & Fjellstedt, T. A., (1976) Purification and properties of alpha-ketoadipate reductase, a newly discovered enzyme from human placenta. *Arch Biochem Biophys* **176**: 610-620.

Suda, T., Robinson, J. C. & Fjellstedt, T. A., (1977) Subcellular localization and tissue distribution of alpha-ketoadipate reduction and oxidation in the rat. *Biochem Biophys Res Commun* **77**: 586-591.

Tauch, A., Kirchner, O., Löffler, B., Götker, S., Pühler, A. & Kalinowski, J., (2002) Efficient Electrotransformation of *Corynebacterium diphtheriae* with a Mini-Replicon Derived from the *Corynebacterium glutamicum* Plasmid pGA1. *Curr Microbiol* **45**: 362-367.

Terpe, K., (2006) Overview of bacterial expression systems for heterologous protein production: from molecular and biochemical fundamentals to commercial systems. *Appl Microbiol Biotechnol* **72**: 211-222.

Tesch, M., Eikmanns, B., de Graaf, A. & Sahm, H., (1998) Ammonia assimilation in *Corynebacterium glutamicum* and a glutamate dehydrogenase-deficient mutant. *Biotechnology Letters* **20**: 953-957.

van Duuren, J. B., Brehmer, B., Mars, A. E., Eggink, G., Dos Santos, V. A. & Sanders, J. P., (2011a) A limited LCA of bio-adipic acid: manufacturing the nylon-6,6 precursor adipic acid using the benzoic acid degradation pathway from different feedstocks. *Biotechnol Bioeng* **108**: 1298-1306.

van Duuren, J. B., Wijte, D., Karge, B., dos Santos, V. A., Yang, Y., Mars, A. E.*, et al.*, (2012) pH-stat fed-batch process to enhance the production of *cis*, *cis*-muconate from benzoate by *Pseudomonas putida* KT2440-JD1. *Biotechnol Prog* **28**: 85-92.

van Duuren, J. B., Wijte, D., Leprince, A., Karge, B., Puchalka, J., Wery, J.*, et al.*, (2011b) Generation of a *catR* deficient mutant of *P. putida* KT2440 that produces *cis*, *cis*-muconate from benzoate at high rate and yield. *J Biotechnol* **156**: 163-172.

van Kempen, T. A., van Heugten, E. & Trottier, N. L., (2001) Adipic acid increases plasma lysine but does not improve the efficiency of lysine utilization in swine. *J Anim Sci* **79**: 2406-2411.

Van Ooyen, J., (2011) *Systemische Analyse des Citratzyklus in Corynebacterium glutamicum / Jan van Ooyen,* p. 117 S. Forschungszentrum Jülich GmbH Zentralbibliothek, Verlag, Jülich.

van Ooyen, J., Noack, S., Bott, M., Reth, A. & Eggeling, L., (2012) Improved L-lysine production with *Corynebacterium glutamicum* and systemic insight into citrate synthase flux and activity. *Biotechnol Bioeng* **109**: 2070-2081.

Veit, A., Rittmann, D., Georgi, T., Youn, J.-W., Eikmanns, B. J. & Wendisch, V. F., (2009) Pathway identification combining metabolic flux and functional genomics analyses: Acetate and propionate activation by *Corynebacterium glutamicum*. *J Biotechnol* **140**: 75-83.

Vogel, H. J., (1964) Distribution of lysine pathways among fungi: evolutionary implications. *The American Naturalist* **98**: 435-446.

Vrljic, M., Sahm, H. & Eggeling, L., (1996) A new type of transporter with a new type of cellular function: L-lysine export from *Corynebacterium glutamicum*. *Molecular microbiology* **22**: 815-826.

Wendisch, V. F., Spies, M., Reinscheid, D. J., Schnicke, S., Sahm, H. & Eikmanns, B. J., (1997) Regulation of acetate metabolism in *Corynebacterium glutamicum*: transcriptional control of the isocitrate lyase and malate synthase genes. *Arch Microbiol* **168**: 262-269.

Werpy, T. & Petersen, G., (2004) Top Value Added Chemicals from Biomass: Volume I - Results of Screening for Potential Candidates from Sugars and Synthesis Gas. *U.S. Department of Energy*.

Wieschalka, S., Blombach, B. & Eikmanns, B. J., (2012) Engineering *Corynebacterium glutamicum* for the production of pyruvate. *Appl Microbiol Biotechnol* **94**: 449-459.

Wu, C.-M., Lee, T.-H., Lee, S.-N., Lee, Y.-A. & Wu, J.-Y., (2004) Microbial synthesis of *cis*,*cis*-muconic acid by *Sphingobacterium* sp. GCG generated from effluent of a styrene monomer (SM) production plant. *Enzyme and Microbial Technology* **35**: 598-604.

Wulandari, A. P., Miyazaki, J., Kobashi, N., Nishiyama, M., Hoshino, T. & Yamane, H., (2002) Characterization of bacterial homocitrate synthase involved in lysine biosynthesis. *FEBS Letters* **522**: 35-40.

Xu, H., Andi, B., Qian, J., West, A. H. & Cook, P. F., (2006) The alpha-aminoadipate pathway for lysine biosynthesis in fungi. *Cell Biochem Biophys* **46**: 43-64.

Yamamoto, T., Miyazaki, K. & Eguchi, T., (2007) Substrate specificity analysis and inhibitor design of homoisocitrate dehydrogenase. *Bioorganic & Medicinal Chemistry* **15**: 1346-1355.

Yasuda, K., Jojima, T., Suda, M., Okino, S., Inui, M. & Yukawa, H., (2007) Analyses of the acetate-producing pathways in *Corynebacterium glutamicum* under oxygen-deprived conditions. *Appl Microbiol Biotechnol* **77**: 853-860.

Youn, J.-W., Jolkver, E., Krämer, R., Marin, K. & Wendisch, V. F., (2008) Identification and Characterization of the Dicarboxylate Uptake System DccT in *Corynebacterium glutamicum*. *J Bacteriol* **190**: 6458-6466.

Youn, J.-W., Jolkver, E., Krämer, R., Marin, K. & Wendisch, V. F., (2009) Characterization of the Dicarboxylate Transporter DctA in *Corynebacterium glutamicum*. *J Bacteriol* **191**: 5480-5488.

Yukawa, H., Omumasaba, C. A., Nonaka, H., Kós, P., Okai, N., Suzuki, N*., et al.*, (2007) Comparative analysis of the *Corynebacterium glutamicum* group and complete genome sequence of strain R. *Microbiology* **153**: 1042-1058.

Zabriskie, T. M. & Jackson, M. D., (2000) Lysine biosynthesis and metabolism in fungi. *Nat Prod Rep* **17**: 85-97.

Zhao, K.-X., Huang, Y., Chen, X., Wang, N.-X. & Liu, S.-J., (2010) PcaO Positively Regulates *pcaHG* of the β-Ketoadipate Pathway in *Corynebacterium glutamicum*. *J Bacteriol* **192**: 1565-1572.

Zheng, L., White, R. H. & Dean, D. R., (1997) Purification of the *Azotobacter vinelandii nifV*-encoded homocitrate synthase. *J Bacteriol* **179**: 5963-5966.

Zhu, N., Xia, H., Wang, Z., Zhao, X. & Chen, T., (2013) Engineering of Acetate Recycling and Citrate Synthase to Improve Aerobic Succinate Production in *Corynebacterium glutamicum*. *PLoS ONE* **8**: e60659.

7 Appendix

7.1 Sequences of used enzymes

Homocitrate synthase of *Thermus thermophilus*

>*ttc1550*, gene sequence
ATGCGGGAGTGGAAGATTATTGACTCCACCTTACGGGAAGGGGAACAGTTTGAAAAGGCGAACTTCTCCACCCAG
GACAAGGTGGAGATCGCCAAGGCCCTGGACGAGTTCGGCATTGAGTACATTGAGGTCACCACCCCGGTGGCCTCC
CCCCAGTCCCGCAAGGACGCCGAGGTCCTCGCCTCCTTGGGCCTCAAGGCCAAGGTGGTGACCCACATCCAGTGC
CGCCTGGACGCGGCCAAGGTGGCGGTGGAGACGGGAGTCCAGGGGATTGACCTCCTCTTCGGCACGAGCAAGTAC
CTCCGGGCGCCCCATGGGCGTGACATCCCCAGGATCATTGAGGAGGCCAAAGAGGTGATCGCCTACATCCGCGAG
GCGGCCCCCCACGTGGAGGTGCGCTTCTCCGCCGAGGACACCTTCCGCTCCGAGGAGCAGGACCTCCTCGCCGTC
TACGAGGCCGTCGCCCCCTACGTGGACCGGGTGGGACTGGCGGACACCGTGGGCGTGGCCACGCCCCGGCAGGTC
TACGCCCTGGTGCGGGAGGTGCGGCGGGTGGTGGGGCCCAGGGTGGACATTGAGTTCCACGGCCACAACGACACC
GGGTGCGCCATCGCCAACGCGTATGAGGCCATTGAGGCCGGGGCCACCCACGTGGACACCACCATCCTGGGGATC
GGGGAGAGGAACGGGATCACGCCTTTGGGGGGGTTCCTCGCCCGCATGTACACCCTCCAGCCCGAGTACGTGCGC
AGGAAGTACAAGCTGGAGATGCTCCCCGAGCTGGACCGGATGGTGGCCCGGATGGTGGGGGTGGAGATCCCCTTC
AACAACTACATCACCGGGGAGACGGCCTTCAGCCACAAGGCGGGGATGCACCTCAAGGCCATCTACATCAACCCC
GAGGCCTACGAGCCCTACCCCCCGGAGGTCTTCGGGGTGAAGCGGAAGCTCATCATCGCCTCGAGGCTCACCGGG
CGGCACGCCATCAAGGCGCGGGCGGAGGAGCTCGGCCTCCACTACGGGGAGGAGGAGCTCCACCGGGTCACCCAG
CACATCAAGGCCCTGGCCGACCGGGGCCAGCTCACCCTGGAGGAGCTGGACCGGATCCTCCGGGAGTGGATCACG
GCGTGA

>Ttc1550, translated protein sequence
MREWKIIDSTLREGEQFEKANFSTQDKVEIAKALDEFGIEYIEVTTPVASPQSRKDAEVLASLGLKAKVVTHIQC
RLDAAKVAVETGVQGIDLLFGTSKYLRAAHGRDIPRIIEEAKEVIAYIREAAPHVEVRFSAEDTFRSEEQDLLAV
YEAVAPYVDRVGLADTVGVATPRQVYALVREVRRVVGPRVDIEFHGHNDTGCAIANAYEAIEAGATHVDTTILGI
GERNGITPLGGFLARMYTLQPEYVRRKYKLEMLPELDRMVARMVGVEIPFNNYITGETAFSHKAGMHLKAIYINP
EAYEPYPPEVFGVKRKLIIASRLTGRHAIKARAEELGLHYGEEELHRVTQHIKALADRGQLTLEELDRILREWIT
A

Homocitrate synthase of *Saccharomyces cerevisiae*

>*lys20*, gene sequence
ATGACTGCTGCTAAACCAAATCCATATGCTGCCAAACCGGGCGACTATCTTTCTAATGTAAATAATTTCCAGTTA
ATCGATTCGACGCTGAGAGAAGGTGAACAATTTGCCAACGCATTCTTCGATACTGAAAAAAAGATCGAAATTGCT
AGAGCCTTGGACGATTTCGGTGTGGACTACATCGAGTTAACCTCACCAGTAGCATCTGAACAATCAAGAAAGGAC
TGTGAAGCTATATGTAAACTAGGTTTAAAGGCCAAGATCCTTACACACATTCGTTGTCATATGGATGACGCCAAA
GTCGCCGTAGAGACTGGTGTCGACGGTGTCGATGTCGTTATCGGCACCTCCAAATTTTTAAGACAATATTCCCAC
GGTAAGGATATGAACTACATCGCCAAGAGTGCTGTTGAAGTCATTGAATTTGTCAAATCCAAAGGTATTGAAATC
AGATTTTCCTCTGAAGATTCCTTCAGAAGTGATCTCGTTGATCTTTTGAACATTTATAAAACCGTTGACAAGATC
GGTGTAAATAGAGTCGGTATTGCCGACACAGTTGGATGTGCCAACCCAAGACAAGTATATGAACTGATCAGAACT
TTGAAGAGTGTTGTTTCATGTGACATCGAATGCCATTTCCACAACGATACTGGTTGTGCCATTGCAAACGCCTAC
ACTGCTTTGGAAGGTGGTGCCAGATTGATTGACGTCAGTGTACTGGGTATTGGTGAAAGAAACGGTATCACTCCT
CTAGGTGGGCTCATGGCAAGAATGATTGTTGCCGCACCAGACTATGTCAAGTCCAAATACAAGTTGCACAAGATC
AGAGACATTGAAAACCTGGTCGCTGATGCTGTGGAAGTTAACATTCCATTCAACAACCCTATCACCGGGTTCTGT
GCATTCACACATAAAGCAGGTATCCATGCCAAGGCCATTTTGGCTAACCCATCTACCTACGAAATCTTGGACCCT
CACGATTTCGGTATGAAGAGGTATATCCACTTCGCCAACAGACTAACTGGCTGGAACGCCATCAAAGCCAGAGTC
GACCAGTTGAACTTGAACTTGACGGATGACCAAATCAAGGAAGTTACTGCTAAGATTAAGAAGCTGGGTGATGTC
AGATCGCTGAATATCGATGATGTTGACTCTATCATCAAGAACTTCCACGCAGAGGTCAGCACTCCTCAAGTACTA
TCTGCAAAAAAGAACAAGAAGAATGACAGCGATGTACCGGAACTGGCCACCATCCCCGCCGCCAAGCGGACTAAG
CCATCCGCCTAA

>Lys20, translated protein sequence
MTAAKPNPYAAKPGDYLSNVNNFQLIDSTLREGEQFANAFFDTEKKIEIARALDDFGVDYIELTSPVASEQSRKD
CEAICKLGLKAKILTHIRCHMDDAKVAVETGVDGVDVVIGTSKFLRQYSHGKDMNYIAKSAVEVIEFVKSKGIEI
RFSSEDSFRSDLVDLLNIYKTVDKIGVNRVGIADTVGCANPRQVYELIRTLKSVVSCDIECHFHNDTGCAIANAY
TALEGGARLIDVSVLGIGERNGITPLGGLMARMIVAAPDYVKSKYKLHKIRDIENLVADAVEVNIPFNNPITGFC
AFTHKAGIHAKAILANPSTYEILDPHDFGMKRYIHFANRLTGWNAIKARVDQLNLNLTDDQIKEVTAKIKKLGDV
RSLNIDDVDSIIKNFHAEVSTPQVLSAKKNKKNDSDVPELATIPAAKRTKPSA

L-lysine-insensitive homocitrate synthase from *Saccharomyces cerevisiae*

>*lys20*^{R276K}, gene sequence
ATGACTGCTGCTAAACCAAATCCATATGCTGCCAAACCGGGCGACTATCTTTCTAATGTAAATAATTTCCAGTTA
ATCGATTCGACGCTGAGAGAAGGTGAACAATTTGCCAACGCATTCTTCGATACTGAAAAAAAGATCGAAATTGCT
AGAGCCTTGGACGATTTCGGTGTGGACTACATCGAGTTAACCTCACCAGTAGCATCTGAACAATCAAGAAAGGAC
TGTGAAGCTATATGTAAACTAGGTTTAAAGGCCAAGATCCTTACACACATTCGTTGTCATATGGATGACGCCAAA
GTCGCCGTAGAGACTGGTGTCGACGGTGTCGATGTCGTTATCGGCACCTCCAAATTTTTAAGACAATATTCCCAC
GGTAAGGATATGAACTACATCGCCAAGAGTGCTGTTGAAGTCATTGAATTTGTCAAATCCAAAGGTATTGAAATC
AGATTTTCCTCTGAAGATTCCTTCAGAAGTGATCTCGTTGATCTTTTGAACATTTATAAAACCGTTGACAAGATC
GGTGTAAATAGAGTCGGTATTGCCGACACAGTTGGATGTGCCAACCCAAGACAAGTATATGAACTGATCAGAACT
TTGAAGAGTGTTGTTTCATGTGACATCGAATGCCATTTCCACAACGATACTGGTTGTGCCATTGCAAACGCCTAC
ACTGCTTTGGAAGGTGGTGCCAGATTGATTGACGTCAGTGTACTGGGTATTGGTGAAAGAAACGGTATCACTCCT
CTAGGTGGGCTCATGGCAAGAATGATTGTTGCCGCACCAGACTATGTCAAGTCCAAATACAAGTTGCACAAGATC
AAAGACATTGAAAACCTGGTCGCTGATGCTGTGGAAGTTAACATTCCATTCAACAACCCTATCACCGGGTTCTGT
GCATTCACACATAAAGCAGGTATCCATGCCAAGGCCATTTTGGCTAACCCATCTACCTACGAAATCTTGGACCCT
CACGATTTCGGTATGAAGAGGTATATCCACTTCGCCAACAGACTAACTGGCTGGAACGCCATCAAAGCCAGAGTC
GACCAGTTGAACTTGAACTTGACGGATGACCAAATCAAGGAAGTTACTGCTAAGATTAAGAAGCTGGGTGATGTC
AGATCGCTGAATATCGATGATGTTGACTCTATCATCAAGAACTTCCACGCAGAGGTCAGCACTCCTCAAGTACTA
TCTGCAAAAAAGAACAAGAAGAATGACAGCGATGTACCGGAACTGGCCACCATCCCCGCCGCCAAGCGGACTAAG
CCATCCGCCTAA

>Lys20^{R276K}, translated protein sequence
MTAAKPNPYAAKPGDYLSNVNNFQLIDSTLREGEQFANAFFDTEKKIEIARALDDFGVDYIELTSPVASEQSRKD
CEAICKLGLKAKILTHIRCHMDDAKVAVETGVDGVDVVIGTSKFLRQYSHGKDMNYIAKSAVEVIEFVKSKGIEI
RFSSEDSFRSDLVDLLNIYKTVDKIGVNRVGIADTVGCANPRQVYELIRTLKSVVSCDIECHFHNDTGCAIANAY
TALEGGARLIDVSVLGIGERNGITPLGGLMARMIVAAPDYVKSKYKLHKIKDIENLVADAVEVNIPFNNPITGFC
AFTHKAGIHAKAILANPSTYEILDPHDFGMKRYIHFANRLTGWNAIKARVDQLNLNLTDDQIKEVTAKIKKLGDV
RSLNIDDVDSIIKNFHAEVSTPQVLSAKKNKKNDSDVPELATIPAAKRTKPSA

Homocitrate synthase of *Azotobacter vinelandii*

>*nifV*, gene sequence
ATGGCTAGCGTGATCATCGACGACACTACCCTGCGTGACGGTGAACAGAGTGCCGGGGTCGCCTTCAATGCCGAC
GAGAAGATCGCTATCGCCCGCGCGCTCGCCGAACTGGGCGTGCCGGAGTTGGAGATCGGCATTCCCAGCATGGGC
GAGGAAGAGCGCGAGGTGATGCACGCCATCGCCGGTCTCGGCCTGTCGTCTCGCCTGCTGGCCTGGTGCCGGCTA
TGCGACGTCGATCTCGCGGCGGCGCGCTCCACCGGGGTGACCATGGTCGACCTTTCGCTGCCGGTCTCCGACCTG
ATGCTGCACCACAAGCTCAATCGCGATCGCGACTGGGCCTTGCGCGAAGTGGCCAGGCTGGTCGGCGAAGCGCGC
ATGGCCGGGCTCGAGGTGTGCCTGGGCTGCGAGGACGCCTCGCGGGCGGATCTGGAGTTCGTCGTGCAGGTGGGC
GAAGTGGCGCAGGCCGCCGGCGCCCGTCGGCTGCGCTTCGCCGACACCGTCGGGGTCATGGAGCCCTTCGGCATG
CTCGACCGCTTCCGTTTCCTCAGCCGGCGCCTGGACATGGAGCTGGAAGTGCACGCCCACGATGATTTCGGGCTG
GCCACGGCCAACACCCTGGCCGCGGTGATGGGCGGGGCGACTCATATCAACACCACGGTCAACGGGCTCGGCGAG
CGTGCCGGCAACGCCGCGCTGGAAGAGTGCGTGCTGGCGCTCAAGAACCTCCACGGTATCGACACCGGTATCGAT
ACCCGCGGCATCCCGGCCATCTCCGCGCTGGTCGAGCGGGCCTCGGGGCGCCAGGTGGCCTGGCAGAAGAGCGTG
GTCGGCGCCGGGGTGTTCACTCACGAGGCCGGTATCCACGTCGACGGACTGCTCAAGCATCGGCGCAACTACGAG
GGGCTGAATCCCGACGAACTCGGTCGCAGCCACAGTCTGGTGCTGGGCAAGCATTCCGGGGCGCACATGGTGCGC
AACACGTACCGCGATCTGGGTATCGAGCTGGCGGACTGGCAGAGCCAAGCGCTGCTCGGCCGCATCCGTGCCTTC
TCCACCAGGACCAAGCGCCGCAGCCCGCAGCCTGCCGAGCTGCAGGATTTCTATCGGCAGTTGTGCGAGCAAGGC
AATCCCGAACTGGCCGCAGGAGGAATGGCATGA

>NifV, translated protein sequence
MASVIIDDTTLRDGEQSAGVAFNADEKIAIARALAELGVPELEIGIPSMGEEEREVMHAIAGLGLSSRLLAWCRL
CDVDLAAARSTGVTMVDLSLPVSDLMLHHKLNRDRDWALREVARLVGEARMAGLEVCLGCEDASRADLEFVVQVG
EVAQAAGARRLRFADTVGVMEPFGMLDRFRFLSRRLDMELEVHAHDDFGLATANTLAAVMGGATHINTTVNGLGE
RAGNAALEECVLALKNLHGIDTGIDTRGIPAISALVERASGRQVAWQKSVVGAGVFTHEAGIHVDGLLKHRRNYE
GLNPDELGRSHSLVLGKHSGAHMVRNTYRDLGIELADWQSQALLGRIRAFSTRTKRRSPQPAELQDFYRQLCEQG
NPELAAGGMA

Homoaconitase of *Saccharomyces cerevisiae*

>*lys4*, gene sequence
ATGCTACGATCAACCACATTTACTCGTTCGTTCCACAGTTCTAGGGCCTGGTTGAAAGGTCAGAACCTAACTGAA
AAAATTGTTCAGTCGTATGCGGTCAACCTTCCCGAGGGTAAAGTTGTGCATTCTGGTGACTATGTATCGATCAAG
CCGGCACACTGTATGTCCCACGATAATTCGTGGCCTGTAGCTTTGAAATTCATGGGGCTTGGCGCTACCAAGATC
AAGAATCCTTCACAGATTGTGACCACTCTGGACCACGATATTCAGAACAAATCAGAGAAAAATTTGACCAAGTAC
AAGAACATCGAAAATTTTGCTAAGAAACACCATATAGACCACTACCCTGCCGGTAGAGGTATTGGTCATCAAATT
ATGATTGAGGAGGGCTATGCTTTCCCCTTGAACATGACTGTCGCATCTGACTCGCATTCAAACACCTACGGTGGT
CTGGGGTCGCTGGGCACTCCAATAGTGAGAACAGACGCTGCAGCCATATGGGCCACGGGACAGACGTGGTGGCAG
ATCCCACCAGTGGCTCAGGTTGAGTTGAAAGGTCAATTGCCTCAGGGTGTTTCCGGAAAAGATATCATTGTCGCA
TTATGTGGGCTTTTCAACAATGATCAAGTTCTAAATCACGCCATTGAATTCACGGGTGACTCTTTGAATGCATTG
CCTATCGATCACAGACTCACTATTGCTAACATGACCACCGAGTGGGGGGCTCTTTCTGGTTTGTTCCCCGTGGAC
AAAACTTTGATCGACTGGTATAAAAACCGTTTGCAAAAGCTGGGCACCAATAATCATCCAAGGATTAATCCAAAG
ACTATCCGCGCACTAGAAGAAAAGGCGAAGATTCCGAAAGCAGACAAGGATGCACATTATGCCAAGAAACTGATC
ATCGATCTAGCCACGCTAACTCACTACGTCTCAGGTCCAAATAGTGTTAAGGTCTCCAACACCGTGCAAGATCTA
TCTCAACAAGACATCAAGATAAATAAAGCTTATCTAGTGTCATGTACAAACTCCCGTCTATCTGATTTGCAATCT
GCAGCGGATGTGGTTTGTCCTACTGGAGACTTAAACAAAGTCAACAAGGTGGCTCCAGGTGTGGAGTTCTATGTC
GCTGCTGCCTCTTCAGAAATTGAGGCTGATGCCCGTAAATCAGGCGCTTGGGAAAAGCTGCTAAAGGCTGGCTGT
ATCCCACTGCCTTCTGGTTGTGGTCCATGCATCGGTCTAGGTGCGGGATTACTGGAACCAGGTGAAGTTGGTATC
AGTGCCACAAACAGAAACTTCAAAGGTAGAATGGGTTCCAAGGATGCATTGGCTTACTTAGCTTCCCCTGCTGTA
GTCGCCGCTTCTGCCGTGCTGGGTAAGATTAGTTCTCCTGCTGAGGTATTGTCCACAAGCGAAATTCCATTCAGC
GGCGTTAAGACTGAGATAATTGAGAATCCCGTGGTTGAAGAGGAAGTTAACGCTCAAACAGAGGCTCCAAAACAA
TCCGTTGAGATATTAGAAGGTTTCCCAAGAGAGTTTTCTGGTGAATTAGTTTTATGTGATGCCGATAACATCAAT
ACCGATGGTATATATCCTGGTAAGTACACTTATCAGGATGATGTGCCTAAAGAAAAGATGGCGCAAGTTTGTATG
GAAAATTATGATGCCGAGTTCAGAACCAAGGTTCATCCAGGTGATATAGTGGTCAGTGGGTTCAATTTCGGTACC
GGTTCCTCCAGGGAACAAGCGGCCACCGCCTTATTGGCTAAAGGTATCAACTTAGTTGTTTCAGGATCTTTTGGT
AATATTTTTTCAAGAAACTCCATTAACAATGCTCTTCTGACCTTGGAAATCCCAGCATTAATCAAAAAATTACGT
GAGAAATATCAAGGTGCTCCAAAAGAACTTACAAGAAGAACTGGTTGGTTTTTGAAATGGGATGTAGCTGATGCT
AAAGTGGTCGTTACCGAAGGTTCTTTGGACGGCCCTGTGATCTTGGAGCAAAAAGTGGGTGAGCTAGGTAAGAAC
CTACAAGAAATTATTGTAAAAGGAGGCTTGGAAGGTTGGGTCAAATCCCAACTATAA

>Lys4, translated protein sequence
MLRSTTFTRSFHSSRAWLKGQNLTEKIVQSYAVNLPEGKVVHSGDYVSIKPAHCMSHDNSWPVALKFMGLGATKI
KNPSQIVTTLDHDIQNKSEKNLTKYKNIENFAKKHHIDHYPAGRGIGHQIMIEEGYAFPLNMTVASDSHSNTYGG
LGSLGTPIVRTDAAAIWATGQTWWQIPPVAQVELKGQLPQGVSGKDIIVALCGLFNNDQVLNHAIEFTGDSLNAL
PIDHRLTIANMTTEWGALSGLFPVDKTLIDWYKNRLQKLGTNNHPRINPKTIRALEEKAKIPKADKDAHYAKKLI
IDLATLTHYVSGPNSVKVSNTVQDLSQQDIKINKAYLVSCTNSRLSDLQSAADVVCPTGDLNKVNKVAPGVEFYV
AAASSEIEADARKSGAWEKLLKAGCIPLPSGCGPCIGLGAGLLEPGEVGISATNRNFKGRMGSKDALAYLASPAV
VAASAVLGKISSPAEVLSTSEIPFSGVKTEIIENPVVEEEVNAQTEAPKQSVEILEGFPREFSGELVLCDADNIN
TDGIYPGKYTYQDDVPKEKMAQVCMENYDAEFRTKVHPGDIVVSGFNFGTGSSREQAATALLAKGINLVVSGSFG
NIFSRNSINNALLTLEIPALIKKLREKYQGAPKELTRRTGWFLKWDVADAKVVVTEGSLDGPVILEQKVGELGKN
LQEIIVKGGLEGWVKSQL

Homoisocitrate dehydrogenase of *Saccharomyces cerevisiae*

>*lys12*, gene sequence

```
ATGTTTAGATCTGTTGCTACTAGATTATCTGCCTGCCGTGGGTTAGCATCTAACGCTGCTCGCAAATCACTCACT
ATTGGTCTTATCCCCGGTGACGGTATCGGTAAGGAAGTCATTCCTGCTGGTAAGCAAGTTTTGGAAAACCTTAAC
TCCAAGCACGGCCTAAGCTTCAACTTTATTGATCTCTACGCCGGTTTCCAAACATTCCAAGAAACAGGAAAGGCG
TTGCCTGATGAGACTGTTAAAGTGTTGAAGGAACAATGTCAAGGTGCTCTTTTCGGTGCAGTTCAGTCTCCAACT
ACTAAGGTGGAAGGTTACTCCTCACCAATTGTTGCTCTAAGGAGGGAAATGGGCCTTTTCGCTAATGTTCGTCCT
GTTAAGTCTGTAGAGGGAGAAAAGGGTAAACCAATTGACATGGTTATCGTCAGAGAAAATACTGAGGACCTGTAC
ATTAAAATTGAAAAAACATACATTGACAAGGCCACAGGTACAAGAGTTGCTGATGCCACAAAGAGAATATCCGAA
ATTGCAACAAGAAGAATTGCAACCATTGCATTAGATATTGCCTTGAAAAGATTACAAACAAGAGGCCAAGCCACT
TTGACAGTGACTCATAAATCAAATGTTCTATCTCAAAGTGATGGTCTATTCAGAGAAATCTGTAAGGAAGTCTAC
GAATCTAACAAGGACAAGTACGGTCAAATCAAATATAACGAACAAATTGTGGATTCCATGGTTTATAGGCTGTTC
AGAGAACCACAATGTTTTGATGTGATAGTGGCACCAAACCTATACGGGGATATATTATCTGACGGTGCTGCTGCT
TTAGTCGGTTCATTAGGTGTTGTTCCAAGCGCCAACGTAGGTCCAGAAATTGTCATTGGTGAACCATGCCATGGT
TCTGCACCAGATATTGCTGGTAAAGGTATTGCTAACCCAATCGCCACTATAAGATCTACTGCTTTGATGTTGGAA
TTCTTGGGCCACAACGAAGCTGCCCAAGATATCTACAAGGCTGTTGATGCTAACTTAAGAGAGGGTTCTATCAAG
ACACCAGATTTAGGTGGTAAGGCTTCTACTCAACAAGTCGTTGACGACGTTTTGTCGAGATTATAG
```

>Lys12, translated protein sequence

```
MFRSVATRLSACRGLASNAARKSLTIGLIPGDGIGKEVIPAGKQVLENLNSKHGLSFNFIDLYAGFQTFQETGKA
LPDETVKVLKEQCQGALFGAVQSPTTKVEGYSSPIVALRREMGLFANVRPVKSVEGEKGKPIDMVIVRENTEDLY
IKIEKTYIDKATGTRVADATKRISEIATRRIATIALDIALKRLQTRGQATLTVTHKSNVLSQSDGLFREICKEVY
ESNKDKYGQIKYNEQIVDSMVYRLFREPQCFDVIVAPNLYGDILSDGAAALVGSLGVVPSANVGPEIVIGEPCHG
SAPDIAGKGIANPIATIRSTALMLEFLGHNEAAQDIYKAVDANLREGSIKTPDLGGKASTQQVVDDV
```

Danksagung

Mein ganz besonderer Dank gilt Herrn Prof. Dr. Michael Bott für die Überlassung dieses interessanten Arbeitsthemas, sein Interesse an dieser Arbeit und die tollen Arbeitsmöglichkeiten am IBG-1: Biotechnologie.

Bei PD Dr. Ulrich Schulte möchte ich mich ganz herzlich für die Übernahme des Zweitgutachtens bedanken.

Ein besonderer Dank gilt Dr. Tino Polen für seine großartige fachliche Unterstützung, Hilfs- und Diskussionsbereitschaft während dieser ganzen Arbeit, sowie für die Durchsicht dieser Arbeit.

Jan und Simon danke ich für die vielen produktiven fachlichen Diskussionen während dieser Arbeit, sowie für die vielen abwechslungsreichen und lustigen Gespräche während der Mittags- und Kaffeepausen.

Bei Ulli und Doris möchte ich mich für ihre Hilfsbereitschaft und für die Beantwortung aller meiner Fragen bedanken, die mir die Laborarbeit sehr vereinfacht haben.

Weiterhin möchte ich mich bei meinen Kollegen Jenni, Andi und Michael und allen ehemaligen Mitgliedern der Arbeitsgruppe für das nette Arbeitsklima, die fachlichen und nicht fachlichen Unterhaltungen, sowie die lustigen Kaffeepausen bedanken.

Bedanken möchte ich mich auch bei Sabrina, Simon, Celine und Steffi für die tollen und lustigen Unternehmungen abseits der Arbeit, die das Leben in Jülich deutlich aufregender gemacht haben.

Ich bedanke mich bei allen meinen Freunden, ganz besonders Christoph, Moritz und Frederick für die vielen ereignisreichen Momente abseits der Arbeit und vor allem, dass man sich immer auf euch verlassen kann!

Liebe Steffi, mein Dank an dich ist kaum in Worte zu fassen. Ich danke für Alles, deine Aufmunterungen, dein Vertrauen, deine Unterstützung und für deine Liebe. Du bist der großartigste Mensch den ich kenne!

Unendlicher Dank gebührt meinen großartigen Eltern und meiner Familie für das grenzenlose Vertrauen und die Unterstützung in jeder Lebenssituation, wodurch es mir erst möglich wurde, heute dazustehen wo ich bin!

Erklärung

Hiermit versichere ich, dass ich die hier vorgelegte Dissertation eigenständig und ohne unerlaubte Hilfe angefertigt habe. Die Dissertation wurde in der vorgelegten oder in ähnlicher Form noch bei keiner anderen Institution eingereicht. Ich habe bisher keine erfolglosen Promotionsversuche unternommen.

Jülich, März 2014

Band / Volume 56
Untersuchungen zur sekretorischen Proteingewinnung industriell relevanter Enzyme mit *Corynebacterium glutamicum*
S. Scheele (2012), vii, 127 pp
ISBN: 978-3-89336-815-0

Band / Volume 57
Novel insights into the energy metabolism of *Corynebacterium glutamicum* by comprehensive analysis of mutants defective in respiration or oxidative phosphorylation
A. Koch-Körfges (2012), III, 137 pp
ISBN: 978-3-89336-826-6

Band / Volume 58
Prozessnahe Hochdurchsatzoptimierung der heterologen Proteinproduktion in alternativen Wirtsorganismen
P. Rohe (2012), 165 pp
ISBN: 978-3-89336-834-1

Band / Volume 59
Validation and characterisation of novel cellular ligands of membrane-associated HIV-1 Nef
E.C.Kammula (2012), 151 pp
ISBN: 978-3-89336-839-6

Band / Volume 60
Untersuchungen zur Membranintegrität während der Tat-abhängigen Proteintranslokation in *Escherichia coli*
S. Fleckenstein (2013), VI, 160 pp
ISBN: 978-3-89336-841-9

Band / Volume 61
Characterization of Novel Amyloid-β Peptide (Aβ) Binding Ligands
S. Dornieden (2013), vii, 129 pp
ISBN: 978-3-89336-844-0

Band / Volume 62
Regulatorische Aspekte der Expression und Sekretion heterologer Proteine in *Corynebacterium glutamicum*
A. R. Chattopadhyay (2013), VIII, 195 pp
ISBN: 978-3-89336-845-7

Band / Volume 63
***Gluconobacter oxydans* strain development: Studies on central carbon metabolism and respiration**
J. Richhardt (2013), III, 181 pp
ISBN: 978-3-89336-851-8

Band / Volume 64
Metabolic Engineering von *Corynebacterium glutamicum* für die Produktion einer Dicarbonsäure
A. Otten (2013), 98 pp
ISBN: 978-3-89336-860-0

Band / Volume 65
Rapid Development of Small-Molecule producing Microorganisms based on Metabolite Sensors
S. Binder (2013), 138 pp
ISBN: 978-3-89336-872-3

Band / Volume 66
Increasing the NADPH supply for whole-cell biotransformation and development of a novel biosensor
S. Solvej (2013), 130 pp
ISBN: 978-3-89336-900-3

Band / Volume 67
Expression, purification and biophysical characterization of human Presenilin 2
G. Yang (2013), 159 pp
ISBN: 978-3-89336-928-7

Band / Volume 68
Modifikationen der Atmungskette in *Corynebacterium glutamicum* und Rolle des Flavohämoproteins Hmp
L. Platzen (2013), IV, 119 pp
ISBN: 978-3-89336-931-7

Band / Volume 69
L-Cystein-Bildung mit *Corynebacterium glutamicum* und optische Sensoren zur zellulären Metabolitanalyse
K. Hoffmann (2014),vi, 83 pp
ISBN: 978-3-89336-939-3

Band / Volume 70
Metabolic engineering of *Corynebacterium glutamicum* for production of the adipate precursor 2-oxoadipate
M. Spelberg (2014), 118 pp
ISBN: 978-3-89336-954-6

Weitere ***Schriften des Verlags im Forschungszentrum Jülich*** unter
http://wwwzb1.fz-juelich.de/verlagextern1/index.asp

Gesundheit / Health
Band / Volume 70
ISBN 978-3-89336-954-6

JÜLICH
FORSCHUNGSZENTRUM